

Determination of Gearing Life in Bending Fatigue
For a Multi Branched Linear Torsional System
Subjected to Random Loading Environment

Man Mohan Sharan.

A Thesis
in
The Department
of
Mechanical Engineering

Presented in Partial Fulfillment of the Requirements
for the degree of Master of Engineering
Concordia University
Montréal, Québec, Canada

December 1983

© Man Mohan Sharan, 1983

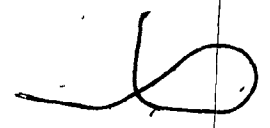
ABSTRACT

Determination of Gearing Life in Bending Fatigue
for a Multibranch Linear Torsional System
Subjected to Random Loading Environment

Man Mohan Sharan

A method for predicting the useful working life of gears in machinery is outlined.

The model investigated is a linear branched torsional system subjected to a dynamic loading environment which reflects the influence of manufacturing and assembly imperfections as well as, the fluctuation in the transmitted torque. The useful working life of gears has been evaluated at various speeds by the deterministic and random approaches. Also, the working life of gears has been estimated at varying loading conditions by changing the static angular transmission error at various operational speeds and at different loading conditions by assuming the angular transmission error to be an exponentially decaying function of the speed of operation.



ACKNOWLEDGEMENTS.

The author is deeply indebted to his supervisors, Dr. T.S. Sankar and Dr. G.D. Xistris for initiating the project and providing continued guidance throughout the course of this investigation.

The constructive criticism and cooperation of Dr. Rama Bhat is gratefully acknowledged.

Thanks are due to Mrs. Ijana Crawford for her sincere effort in typing this manuscript.

The financial support of the National Research Council Grant Numer A0792 is also acknowledged.

TABLE OF CONTENTS

	<u>Page</u>
ABSTRACT	i
ACKNOWLEDGEMENTS	ii
NOMENCLATURE	v
LIST OF FIGURES	viii
LIST OF TABLES	xi
CHAPTER 1: INTRODUCTION AND LITERATURE SURVEY	1
1.1 Introduction	1
1.2 Review of Past Work	6
1.3 Summary of "Errors" in Geared Systems	8
1.4 Reliability of Gears	15
1.5 Objective of Investigation	17
CHAPTER 2: DESCRIPTION OF MATHEMATICAL MODEL OF A LINEAR BRANCHED TORSIONAL SYSTEM	19
2.1 Generalized Coordinates	19
2.2 Principal Coordinates	19
2.3 Modal Analysis	21
2.4 Deterministic Model	25
2.4.1 Description of Analytical Model	25
2.4.2 Derivation Torque Equation	36
2.4.3 Force Analysis	41
2.4.4 Stress Analysis	41
2.4.5 Fatigue Loading	45
2.4.6 Fatigue Failure	49
2.4.7 Fatigue Life with Fluctuating Stress	50
2.4.8 Fatigue Life with Mean and Fluctuating Stress	53
2.4.9 Effect of Various Transmission Errors on the Fatigue Life of Gear Teeth	61
2.5 Stochastic Model	61
2.5.1 Introduction	61
2.5.2 Random Model	63
2.5.3 System Transfer Function	63
2.5.4 Narrow Band Random Process	64
2.5.5 Response of Gears to Random Vibration	66
2.5.6 Failure Mechanism in Gears	68
2.5.7 Fatigue Failure	69

	<u>Page</u>
CHAPTER 3: ANALYSIS OF RESULTS, COMBUSTION AND RECOMMENDATION FOR FUTURE WORK	72
3.1 Discussion of Results	72
3.1.1 Effect of Error on Torque	72
3.1.2 Effect of Error on Working Life of Gear	86
3.2 Conclusion	100
3.3 Recommendation for Future Work	102
REFERENCES	104
APPENDIX Computer Programme	106

NOMENCLATURE

a	inertia coefficient
b	width of gear tooth
c	material constant
f	input fluctuations
h	height of gear tooth
k	stiffness of system
e	length of gear tooth
n	number of cycles
{p}	principal coordinate
{q}	generalized coordinate
[A]	square matrix of inertia coefficients
[B]	square matrix of stiffness coefficients
C	coefficients
D	cumulative damage fraction
E	expected value
F	force
G	response fluctuation
H(ω)	system transfer function
I	moment of inertia
K _G	geometric shape factor
L	total number of cycles
N	number of cycles
N _p	number of peaks
Q	dynamic magnification at resonance
Q _Y	dynamic torque

R	reliability
S	stress in bending
S_a	stress amplitude
S_t	fracture stress
S_r	stress range
S_{max}	maximum stress
S_{min}	minimum stress
S_m	mean stress
S_{ut}	ultimate strength in tension
S_{yt}	yield strength in tension
S_e	endurance strength
$\{S_v\}$	state vector
$S(\omega)$	spectral density
$S_x(\omega)$	input spectral density
$S_s(\omega)$	spectral density of response
$[T_m]$	transfer matrix
T	kinetic energy
ΔT	time interval
V	strain energy
W_t	transmitted load
$[X]$	square matrix of displacement
α	pressure angle
γ	transmission error
$\{\psi\}$	displacement or amplitude vector
ϕ	torque
ω	speed
θ	negative reciprocal of slope

- σ root mean square value
- σ_s^2 variance of first derivative of stress with time
- $\sigma_{\ddot{s}}^2$ variance of second derivative of stress with time

LIST OF FIGURES

<u>Figure No.</u>	<u>Description</u>	<u>Page</u>
Fig. 1.1	Plot of Accumulated Pitch Error	10
Fig. 1.2	Profile Error Projected from Path of Contact	12
Fig. 2.1	Schematic Diagram of System Under Consideration	26
Fig. 2.2	Sign Convention	28
Fig. 2.3	Sign Convention	28
Fig. 2.4	Multidegree of freedom system	29
Fig. 2.5	Torque and Displacement in Isolated n^{th} Section	29
Fig. 2.6	Free Body Diagram of Forces Acting Upon Two Gears in a Simple Gear Train	42
Fig. 2.7	Free Body Diagram of Gear Tooth with Forces Acting on it	43
Fig. 2.8	Static Loading	46
Fig. 2.9	Fatigue Loading	47
Fig. 2.10	Stress Versus Time Relationship	48
Fig. 2.11	Fatigue Fracture of Gear Tooth	51
Fig. 2.12	S-N Curve	52
Fig. 2.13	Fatigue Life with Mean Stress	54
Fig. 2.14	Fatigue Life with Fluctuating and Mean Stress	56
Fig. 2.15	Modified Goodman Diagram	57
Fig. 2.16	Fatigue Life with Compressive and Tensile Mean Stress	59
Fig. 2.17	Effect of Mean Stress on Endurance Strength	60
Fig. 2.18	Narrow Band Record and its Spectral Density	65
Fig. 3.1	Variation of Torque Versus Speed for $\gamma_B = 0.00001$ and $\lambda = 0.0$	73
Fig. 3.2	Variation of Torque Versus Speed for $\gamma_B = 0.00001$ and $\lambda = 0.00008$	74

<u>Figure No.</u>	<u>Description</u>	<u>Page</u>
Fig. 3.3	Variation of Torque Versus-Speed for $\gamma_B = 0.00001$ and $\lambda = 0.0007$	75
Fig. 3.4	Variation of Torque Versus Speed for $\gamma_B = 0.0001$ and $\lambda = 0.0$	76
Fig. 3.5	Variation of Torque Versus Speed for $\gamma_B = 0.0001$ and $\lambda = 0.00008$	78
Fig. 3.6	Variation of Torque Versus Speed for $\gamma_B = 0.0001$ and $\lambda = 0.0007$	79
Fig. 3.7	Variation of Torque Versus Speed for $\gamma_B = 0.0005$ and $\lambda = 0.0$	80
Fig. 3.8	Variation of Torque Versus Speed for $\gamma_B = 0.0005$ and $\lambda = 0.00008$	81
Fig. 3.9	Variation of Torque Versus Speed for $\gamma_B = 0.0005$ and $\lambda = 0.0007$	82
Fig. 3.10	Variation of Torque Versus Speed for $\gamma_B = 0.0009$ and $\lambda = 0.0$	83
Fig. 3.11	Variation of Torque Versus Speed for $\gamma_B = 0.0009$ and $\lambda = 0.00008$	84
Fig. 3.12	Variation of Torque Versus Speed for $\gamma_B = 0.0009$ and $\lambda = 0.0007$	85
Fig. 3.13	Variation of Life Versus Speed for $\gamma_B = 0.00001$ and $\lambda = 0.0$	88
Fig. 3.14	Variation of Life Versus Speed for $\gamma_B = 0.00001$ and $\lambda = 0.00008$	89
Fig. 3.15	Variation of Life Versus Speed for $\gamma_B = 0.00001$ and $\lambda = 0.0007$	90
Fig. 3.16	Variation of Life Versus Speed for $\gamma_B = 0.0001$ and $\lambda = 0.0$	91
Fig. 3.17	Variation of Life Versus Speed for $\gamma_B = 0.0001$ and $\lambda = 0.00008$	92
Fig. 3.18	Variation of Life Versus Speed for $\gamma_B = 0.00001$ and $\lambda = 0.0007$	93
Fig. 3.19	Variation of Life Versus Speed for $\gamma_B = 0.0005$ and $\lambda = 0.0$	94

<u>Figure No.</u>	<u>Description</u>	<u>Page</u>
Fig. 3.20	Variation of Life Versus Speed for $\gamma_B = 0.0005$ and $\lambda = 0.00008$.	95
Fig. 3.21	Variation of Life Versus Speed for $\gamma_B = 0.0005$ and $\lambda = 0.0007$.	96
Fig. 3.22	Variation of Life Versus Speed for $\gamma_B = 0.0009$ and $\lambda = 0$.	97
Fig. 3.23	Variation of Life Versus Speed for $\gamma_B = 0.0009$ and $\lambda = 0.00008$.	98
Fig. 3.24	Variation of Life Versus Speed for $\gamma_B = 0.0009$ and $\lambda = 0.0007$.	101

LIST OF TABLES

<u>Table No.</u>	<u>Description</u>	<u>Page</u>
Table 1.1	Analysis and Development of Gear Work	3
Table 1.2	Gear Theories	5

CHAPTER 1

INTRODUCTION AND LITERATURE SURVEY

CHAPTER 1

INTRODUCTION AND LITERATURE SURVERY

1.1 Introduction

Gears and gear trains are used extensively throughout modern devices and equipment, to provide change in angular speed and to transmit torque. The applications may be simple, as in bicycle drives to quite complex such as gas turbine speed reduction arrangements and process machinery drive mechanisms.

Gears are one of man's oldest mechanical devices. The earliest known example of gearing is found in the "South Pointing Chariot" constructed circa 2600 B.C. This chariot incorporated a complicated differential gear train with the gears constructed in the form of wooden pins [1]. As early as 100 B.C., there are several examples of gears made from metallic materials and wood [2]. The gears were cut with triangular teeth, buttressed teeth and pin shaped teeth. Gear trains at this time consisted of spur gears, rack and pinion, and worm gears. For right angle drive applications, pin tooth drives were employed.

In 1000 A.D. there are examples of machines constructed in India in a form approximating closely 30° pressure angle involute. Several Islamic gear devices used for pumping water, which were constructed at about the same time, appear to have involute profiled gear elements as well. Willis [3] was the first person to recognize the advantages of the involute tooth profile and based his development on a $14\frac{1}{2}$ degree pressure angle system.

The first analytical works on involute profiles and general gear

technology began to appear in the seventeenth century [4]. The salient features of the published works of that time are:

1) James-Carmichaels investigated the load carrying capacity of gears which, he stated, to be proportional to the product of face width (breadth) and the square of the thickness and inversely proportional to the height (length) [5].

2) It was recognized that in order to transmit angular motion with minimum friction, the tooth profile should be an epicycloid. Such profiles were approximated by employing a series of circles with different radii so that the resulting tooth form approached an involute profile. The minimum number of teeth on a pinion was thought to be six [6].

3) The effect of friction and shape irregularities during engagement of gear teeth is much more severe than during disengagement. Because of this it was the general design approach to engage gear teeth as close as possible to the line joining the two gear centres [7].

4) The influence of wear in enhancing tooth shape irregularities and then by increasing frictional losses had been recognized [8].
The literature development of gearing manufacture and analysis up to the beginning of the nineteenth century is summarized in Tables 1.1 and 1.2 respectively.

The dynamic character of the gear meshing process began to surface in the early 20th century when it was observed that high speed gear trains failed prematurely when compared to the slow speed gearing under similar torque conditions [9]. This phenomenon was initially attributed to the fact that gear teeth are subjected to transient loads, the

TABLE 1.1: CHRONOLOGICAL CHART [1]

<u>Classical Europe</u>	
3rd C; B.C.	Archimedes Planetarium
2nd C; B.C.	Hipparachus stereographic projection
1st C; B.C.	Vitruvius hodometer and water clocks
65 B.C. (ca)	Antikythera machine
1st C; A.D.	Hero hodometer and water clocks
2nd C; A.D.	Salzburg and Vosges anaphoric clocks
<u>Europe</u>	
1000	Gerbert astronomical model
1187	Neckham on compass
1198	Jocelin on water clock
1245	Villard clocktower, "escapement" perpetual motion
1267	Villers Abbey clock
1269	Peregrinus, compass and perpetual motion
1271	Robertus Anglicus, animated models and "perpetual motion" clock
1285	Drover's water clock with wheel and weight drive
1300 (ca)	French geared astrolabe
1320	Richard of Wallingford astronomical clock and equatorium
1364	de Dondi's astronomical clock with mechanical escapement
<u>Islam</u>	
-807	Harun-al-Rashid
850 (ca)	Earliest extant astrolabes
1000	Geared astrolabe of al-Biruni
1025	Equatorium text
1050	Saladin clock
1200 (ca)	Ridwan water-clocks, perpetual motion and weight drive
1206	al-Jazari clocks
1221	Geared astrolabe
1232	Charlemagne clock
1243	al-Konpas (compass)
1272	Alfonsine corpus clock with memory drum, equatoria

TABLE 1.1 cont'd

<u>China</u>	
4th C; B.C. 2nd C; A.D.	Power gearing Chang Heng animated globe hodometer continuing tradition of animated astronomical models
725	Invention of Chinese escapement by I-Hsing and Liang Ling-tsan
1074	Shen Kua, clocks and magnetic compass
1080	Su Sung clock built
1101	Su Sung clock destroyed
<u>India</u>	
1100	Sūrya Siddhānta animated astronomical models and perpetual motion
1150	Siddhānta Siromani animated models and perpetual motion

TABLE 1.2: GEAR THEORISTS [1]

In this period theory of gear tooth action was first worked out.

APPROX. DATE	NAME	NATIONALITY	CONTRIBUTION
1451	Nicholas of Cusa	French	Studied cycloidal curve.
1525	Albert Dürer	German	Discovered epicycloids.
1557	Girolamo Cardano	Swiss	First mathematics of gear in print.
1694	Philip de la Hire	French	Full mathematical analysis of epicycloids. Recommended involute curve for gearing. (Involute not used in practice until 150 yrs. later).
1733	Charles Camus	French	Expanded on works of la Hire, developed theories of mechanism, studied lantern pinion and gear, crown gears and beveled gears.
1754	Leonard Euler	Swiss	Euler worked out design principles, worked out rules for conjugate action. Some consider him "the father of involute-gear gearing".
1781	Abraham Kaestner	German	Wrote up practical methods for computing tooth shapes of epicycloid and involute gear teeth. Considered 15° to be a minimum pressure angle.
1832	Robert Willis	English	Wrote and taught extensively in gear field: A pioneer in gear engineering.
1852	Edward Sang	Scotch	General theory of gear teeth. Provided theoretical basis on which all gear tooth generating machines are based.

magnitude of which depends directly on the rotational speed. In 1931, the first known attempt to define the actual nature of gear loads occurred when a research committee of the ASME under the chairmanship of Eamle Buckingham conducted experimental studies on different types of gear trains. This work culminated in a series of relationships for the estimation of dynamic loads and revised design criteria which included dynamic factors appropriate to the speed of the gear train.

1.2 Review of Past Work

Subsequent to the work of Buckingham, several investigators studied the dynamics of gears. The results directly relevant to this work are reviewed in the following paragraphs.

Tuplin [10] showed that gearing failures are primarily due to fatigue and consequently, for infinite life applications, he recommended that gears be designed on the basis of the material fatigue endurance limit. In his analysis, it was assumed that the time rate of stress application (frequency of stress history) does not affect the life of gears and that the governing parameter was the magnitude of the stress itself. Failure of high speed gear teeth at stress levels apparently below the endurance limit were attributed to pitch and profile errors which gave rise to actual stresses higher than those calculated on the basis of static considerations alone. Tuplin felt that these deviations were proportional to the rotational speed up to a certain limit. Beyond this critical speed, the magnitude of fluctuating load remained constant. These statements were made on the basis of a limited number of observations without any analytical justification. The potential occurrences of high stress in high speed installations operating close to the system

structural resonance was identified as a factor to be considered in any future dynamic analysis of gear trains.

A method of computing the dynamic load increment arising from profile and pitch errors has been reported in [11]. The profile and pitch errors were defined by modelling the meshing process as a one degree of freedom spring-mass system under the excitation provided by a reciprocating wedge inserted at the spring end. This has become known as the wedge analogy and has been used by other investigators [12].

Bishop [13] showed that gearing errors are of two types:

- 1) Errors in which the pitch point moves backwards and forwards along the common tangent of the pitch circles, and
- 2) Errors in which the pitch point moves radially.

Yates [14] showed that displacement excitation in gear meshing systems arises from errors in the gear cutting processes which cause periodic variations in the velocity ratio of the mating components.

Johnson and Bishop [15] analyzed the response of geared systems to the excitation of harmonic forces using the concept of receptance. The receptance or flexibility which is the inverse of stiffness is defined as the movement in a given direction per unit of applied force. It was found that the concept of receptance can be used successfully in such problems.

Johnson [16] treated dynamic loading as a set of harmonic vibrations, rather than as a number of isolated transients. Since troublesome resonances are likely to be restricted to a limited band of harmonics only, applications where vibrational modes involving shaft

flexure, having resonant frequencies within the narrow band, should be avoided.

Mahalingam and Bishop [17] have outlined a method for the calculation of the dynamic torque due to angular transmission errors. The angular transmission error is defined for any instantaneous position of one gear, as the departure of the mating gear from the position it would occupy if the system exhibited an unvarying velocity ratio and the teeth were rigid. The static transmission error encompasses all such effects as eccentric mounting, errors of manufacture, elastic deformation etc. This is discussed in detail in the next section.

1.3 Summary of "Errors" in Geared Systems

It is to be noted that due to production equipment limitations, the manufactured spur gear form is not a pure involute helicoid, but a somewhat modified version of the ideal involute shape. Consequently, all errors are determined with respect to the manufacturing model and not the theoretical one. Further, the magnitude of these errors is a function of tooth deterioration and hence, will vary with time of operation.

There are four types of errors which may vary from tooth to tooth such as pitch, profile, tooth alignment and tooth thickness. Radial run-out or lateral runout is independent of tooth spacing and is given for each individual gear. These errors are defined in detail below:

Pitch Error

The spacing of the teeth must be uniform along the circumference. Any departure from the ideal spacing represents a pitch error. This is also designated as division error.

In the measurement of pitch, a reference circle is implicit around which the points of intersection of the set of tooth-flanks ideally, are equally spaced; but the reference circle used in actual measurements rarely, coincides, with the pitch circle. Thus, measured pitch errors do not represent the absolute departure from the nominal pitch around the pitch circle, but the departure from equal spacing around whatever reference circle happens to have been used during the process of measurement. In the presence of variable profile errors, pitch errors are different on different reference circles.

Thus, the adjacent pitch error is the departure from ideal spacing of the corresponding flanks of two adjacent teeth. Considering all the teeth around a given reference circle, the sum of all the adjacent pitch errors on either set of flanks will be zero.

Between similar flanks of any two chosen teeth more than one pitch apart, the departure from the ideal spacing is the accumulated pitch error between those teeth. This is clearly the sum of the adjacent pitch errors of all the intervening pairs of teeth.

If a perfect gear is mounted about an axis eccentric to that on which it was cut, a curve of apparent accumulated pitch error will result (Fig. 1.1). This curve will be a sine curve having a half amplitude equal to the eccentricity; the peaks of the curve will be displaced around the periphery by 90° - pressure the angle relative to the radius along which the eccentricity is measured. Similarly, the effect of any error of eccentricity in its mounting is to superimpose a sine curve of apparent error on to the errors about its own axis.

Correspondingly, if a gear is mounted about its operating axis of

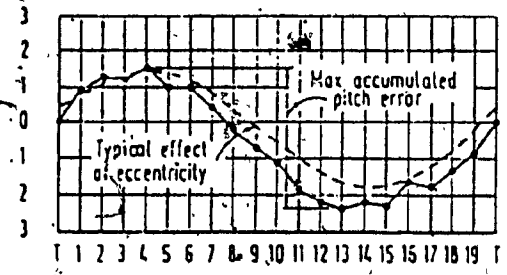


Fig. 1.1: Plot of Accumulated Pitch Error.

rotation after having been cut with an error of eccentricity, the curve of accumulated pitch error shows the effective error when the gear is running, embracing both the error due to eccentricity and the errors due to the gear cutting machine.

Minimum pitch error is important in precision instruments and mechanisms in which, particular angular positions as distinct from mean speed, must be transmitted. In a long train of gears used for such a purpose, the resultant position error reflects the sum of the pitch errors in all the gears.

In simple power transmission drives, pitch errors are only one factor in the kinematic error. These errors cause vibration and noise. The part played in this by a smooth curve of accumulated pitch error such as a characteristic sine curve due to eccentricity is comparatively small since the slow rate of change of position error will result only in very low angular acceleration. More severe irregularities in the curve of accumulated pitch error, i.e. rapid changes in tooth-to-tooth pitch errors, are clearly more detrimental, but the resultant changes in position error are then influenced by profile errors also.

Profile Error

All transverse tooth sections should be identical. Deviations of any transverse section chosen for measurement from the design form constitute a profile error.

A schematic diagram of profile error is shown in Fig. 1.2. It will be noted that in Fig. 1.2 the profile of tooth A is shown touching the true involute drawn to the base circle at point P only. The departure of the actual profile from the involute at any point is measured

normal to the involute. At the tooth tip, this deviation is denoted by e_1 .

If a gear having true involute profiles is set up for measurement with an error of eccentricity present, apparent profile errors will be recorded. Profile diagrams of different teeth indicate apparent error of base diameter alternating from plus to minus around the gear. The effect is not however, the same as that due to an abrupt change of profile because the base pitch remains unaffected and in the running of the gear eccentricity gives rise to a small cyclic speed or positional variation.

If there is an error e_0 on the nominal diameter D_0 of the basic disc, the effect of e_0 is to cause the tip of the tooth to deviate from the normal to the gear radius. The result is to produce an apparent involute error progressively giving minus metal towards the tip.

In case of hobbled gears, inaccurate mounting of the hob on its arbour leads to profile errors. Eccentric mounting of a gear shaper cutter produces corresponding accumulated pitch errors often with a local, more pronounced pitch error at the place where the cutting operation terminates. An error in the setting of a rack form cutter on a gear planning machine produces mainly profile errors:

Tooth Alignment Error

The tooth surface may be regarded as swept out by a designed traverse profile moved along the axis with linear motion. Departures from this relative motion are termed tooth alignment error.

Tooth Thickness Error

Departure from the designed relative position of the driving and

trailing flank of any tooth are referred to, as tooth thickness error.

Radial Runout or Lateral Runout

It is assumed that the axis of measurement, the axis of gear cutting and the axis of gear mounting all coincide. But any two of these axes may not be coincident, and an error in position of any one of them relative to any other will result in a real or apparent error of radial runout or lateral runout, singly or combined.

Periodic Errors

Deviations in the angular motion of the gear blank with respect to the motion of the generating cutter produce periodic errors which repeat with every revolution of the gear. In effect, these errors superimpose an oscillation of the nominally uniform rotation of the blank and the presence of this superimposed error is not detected by tooth profile measurements nor pitch error measurements.

In general, periodic error results in an undulating departure from the true profile. Small amplitude but high frequency periodic errors may be caused by the generating gear devices. Because of the many factors which may give rise to generating drive errors, these are manifested as random fluctuations of the accumulated pitch error.

Composite Errors

A composite error is one revealed by measurements of a dimension which is influenced by two or more of the errors of pitch profile, tooth alignment and radial and lateral runout.

The ultimate composite error is the kinematic error of a pair of mating gears, or the departure from the uniform motion of one gear shaft

relative to the other. If one of the gears is a perfect master gear, then the kinematic error is the single flank composite error of the last gear.

Kinematic and Transmission Errors

If a pair of gears is very slowly rotated under very light tooth load, the departure from the theoretical uniform velocity transmission is defined as the kinematic error. This error is the result of the pitch, profile and runout errors on both gears.

The static transmission error is defined, for any instantaneous position of one gear, as the departure of mating gear from the position it would occupy if the system were perfect, with an unvarying velocity ratio, and the teeth were rigid. The static transmission error thus encompasses all the effects such as eccentric mounting, errors of manufacturing and elastic deformation.

The static transmission error can be measured directly while one of the gears is rotated very slowly and this produces an oscillatory motion in addition to the steady rotation with constant velocity ratio.

When gears run under full operating load and speed, the errors induce dynamic loads between teeth, with resulting vibrations which change the deflection pattern of the teeth. Then the departure from the theoretical uniform velocity transmission is the dynamic transmission error.

1.4 Reliability of Gears

The parameter which is used to obtain an indication of the useful life of a gear is the reliability index. This index is based upon a

functional estimation of the difference between actual and acceptable performance. In the context of industrial gears, reliability may be interpreted as a measure of the remaining failure free life. Thus, reliability calculations require quantitative knowledge of satisfactory or acceptable performance.

The gears of a mechanical system considered in this investigation are subjected to a dynamic loading environment. These input conditions severely limit the useful life of gears. Therefore, determination of the reliability index requires knowledge of either the system properties and input forcing function or, the output time history.

For gears operating under constant loads, in an accurately controlled environment, the input is completely known at any instant of time. However, in most real cases, the input dynamic characteristics are not fully known. The operating conditions, loading intensity and environmental parameters all change gradually, or at times, abruptly over the life of gears.

For a given linear system, its behavior and properties such as fatigue resistance, damping, stiffness and natural frequency can always be established.

Regardless of the actual nature of forcing functions arising during operation, fluctuations in the input will affect the output to the extent predicted by the system transfer-function and thus influence its reliability. Therefore to assess the performance of a gear in a mechanical system, the input and output should be monitored.

If it is assumed that gear properties remain time invariant, then according to Xistris [18], reliability can be expressed as

$$R = f(\text{input fluctuations}) \quad (1.4.1)$$

But, this is an oversimplification of the real situation. Gears change their characteristics with increasing operating time. It is known that gears deteriorate in proportion to the length of service. Progressive cumulative deterioration is caused by overstressing of gears, an accumulation of set-in-deformation, reduction in elastic properties and heat dissipation capacities etc. Thus the system properties and functions change with operating time. So the reliability index should be expressed as

$$R_s = f(\text{input fluctuations \& system property fluctuation}) \quad (1.4.2)$$

In some cases, the response of a geared system is relatively easy to obtain and also, the response reflects both the input as well as the system properties. Therefore it is better to utilize response fluctuations to monitor the reliability of a geared system

$$R = G(\text{response fluctuations}) \quad (1.4.3)$$

However for any geared system vibration is a reliable performance dependent indicator [19,20,21]. Mechanical vibration is the response of the geared system to the forcing functions which arise within the system under operating conditions. Further, the level of the vibratory response is directly proportional to the severity of the defects present in the geared system.

1.5 Objective of the Investigation

Although considerable work has been done in the dynamic analysis of gear trains, the problem of predicting the expected useful life of gearing has not been fully addressed. In machinery where gears are the

primary elements, there is a definite requirement to develop reliable condition assessment mechanisms in order to predict the performance of gearing.

The purpose of this investigation is to outline a method for estimating the working life of gears in a linear branched torsional system subjected to dynamic loading conditions.

The loading environment reflects the influence of manufacturing and assembly imperfections as well as fluctuations in the transmitted torque which have established that the static transmission error approach employed in a two branched gear system indeed incorporate the necessary features to approximate closely the actual loading conditions.

This method has been used successfully in this thesis to evaluate the life of gears under varying dynamic loading conditions and at various speeds. The results obtained from this phase were employed to estimate the life of a gear at varying dynamic loading conditions. These conditions were obtained by changing the static angular transmission error, at various operational speeds. The dynamic loading conditions were also changed, by assuming the angular transmission error to be an exponentially decaying function of the speed of operation.

CHAPTER 2

DESCRIPTION OF MATHEMATICAL MODEL OF A
LINEAR BRANCHED TORSIONAL SYSTEM

CHAPTER 2

DESCRIPTION OF MATHEMATICAL MODEL OF A

LINEAR BRANCHED TORSIONAL SYSTEM

2.1 Generalized Coordinates

The configuration of any system can be expressed in terms of various sets of coordinates. No specific set of coordinates is uniquely suited to the analysis of a given mechanical system. In fact, there is an infinite number of coordinate systems, all of which can express the configuration of any given system. The number of coordinates used in any one system depends on the choice of axes employed. The number of equations describing the configuration for any system of coordinates is always equal to the number of degrees of freedom plus the number of constraints placed on the system configuration. The coordinates employed in such systems are called generalized coordinates.

In a given coordinate system, the number of coordinates depends on the actual choice of coordinate system. If a coordinate system is chosen in such a way that the minimum coordinates are required to specify the system completely, then these coordinates are called independent generalized coordinates. The number of independent generalized coordinates is equal to the number of degrees of freedom. In such a system, the configuration is completely described by a set of independent equations of motion, the number of which equals the degrees of freedom present in the system, i.e. there are no redundant equations.

2.2 Principal Coordinates

A linear system with n degrees of freedom has n natural

frequencies. It is possible for the system to oscillate by properly establishing a set of initial conditions.

A set of principal coordinates for a system is a set of coordinates chosen in such a way that when the system is vibrating in a principal mode, only one coordinate varies while the others remain zero. In other words principal coordinate is that coordinate system for which, when the system oscillates at any single natural frequency, only one of the coordinates varies, whereas all others remain invariant. For a linear system, with n degrees of freedom there are n principal coordinates. When the system is vibrating freely in the n th mode, the n th principal coordinate will vary harmonically with frequency ω_n while all other remaining $n-1$ principal coordinates will be zero. In terms of generalized coordinates, when the system oscillates in the n th mode, all general coordinates will be multiples of the n principal coordinate [22].

If $\{p\}$ and $\{q\}$ are the principal and generalized coordinates, $\{\omega\}$ are the natural frequencies and $\{\psi\}$ the amplitude vector corresponding to $\{\omega\}$, then assuming a value of the principal coordinate (p) equal to one for the first mode, the generalized coordinates (q) will be

$$q_1 = \psi_1^1$$

$$q_2 = \psi_2^1$$

$$- = -$$

$$- = -$$

$$q_n = \psi_n^1$$

For the s th mode with $p_s = 1$, where the subscripts identify the coordinate number and the superscripts designate the vibrating mode, one obtains,

$$q_1 = \psi_1^S$$

$$q_2 = \psi_2^S$$

$$- = -$$

$$- = -$$

$$q_n = \psi_n^S$$

When the system is vibrating in all its modes simultaneously, the generalized coordinate $\{q\}$ and the principal coordinate column vectors $\{p\}$ will be related as follows:

$$\{q\} = [X] \{p\} \tag{2.2.1}$$

where

$$[X] = \begin{bmatrix} \psi_1^1 & \psi_1^2 & \dots & \psi_1^n \\ \psi_2^1 & \psi_2^2 & \dots & \psi_2^n \\ \dots & \dots & \dots & \dots \\ \psi_n^1 & \psi_n^2 & \dots & \psi_n^n \end{bmatrix}$$

Since $\{q\}$ are the generalized coordinates, they are known. The principal coordinates $\{p\}$ may be determined from

$$\{p\} = [X]^{-1} \{q\} \tag{2.2.2}$$

2.3 Modal Analysis

The system shown in Fig. 2.1 has four degrees of freedom and consequently, four different natural frequencies. Corresponding to each natural frequency ω_i the angular displacements (mode shapes) are defined by the column matrix ψ^i .

If ω_r and ω_s are two of the natural frequencies of the system

and $\{\psi^r\}$ and $\{\psi^s\}$ are the corresponding displacement vectors, then ψ^r and ψ^s must satisfy the following conditions

$$[[k] - \omega_s^2[I]]\{\psi^s\} = 0 \quad (2.3.1)$$

$$[[k] - \omega_r^2[I]]\{\psi^r\} = 0 \quad (2.3.2)$$

where, $[k]$ and $[I]$ are the system stiffness and inertia matrices. Pre-multiplying Equation (2.3.1) by the transpose matrix $\{\psi^{T(r)}\}$ for the r th mode gives

$$\{\psi^{T(r)}\}[[k] - \omega_s^2[I]]\{\psi^s\} = 0 \quad (2.3.3)$$

Since $[k]$ and $[I]$ are symmetric matrices, the transpose of Equation (2.3.2) becomes

$$\{\psi^{T(r)}\}[[k] - \omega_r^2[I]] = 0 \quad (2.3.4)$$

Post multiplying Equation (2.3.4) by $\{\psi^s\}$ yields

$$\{\psi^{T(r)}\}[[k] - \omega_r^2[I]]\{\psi^s\} = 0 \quad (2.3.5)$$

Subtracting Equation (2.3.5) from Equation (2.3.3) results in

$$(\omega_r^2 - \omega_s^2)\{\psi^{T(r)}\}[I]\{\psi^s\} = 0 \quad (2.3.6)$$

Since $\omega_r \neq \omega_s$, it follows that

$$\{\psi^{T(r)}\}[I]\{\psi^s\} = 0 \quad (\text{for } r \neq s) \quad (2.3.7)$$

Combining Equations (2.3.7) and (2.3.5) results in

$$\{\psi^{T(r)}\}[k]\{\psi^s\} = 0 \quad (\text{for } r \neq s) \quad (2.3.8)$$

The system of equations defined by Equation (2.3.8) may be solved

independently only when static and dynamic coupling is eliminated. For an undamped system, the equations of motion may be uncoupled by a judicious selection of coordinate axes, namely the principal coordinates. For a four degree of freedom lumped mass system for which the normal oscillation modes are known, the equations of motion may be uncoupled in the following manner:

In the matrix product $[X^T][I][X]$ where $[X]$ is a square matrix of the mode shape column vectors

$$[X] = \begin{bmatrix} \psi_1^1 & \psi_1^2 & \dots & \psi_1^4 \\ \psi_2^1 & \psi_2^2 & \dots & \psi_2^4 \\ \dots & \dots & \dots & \dots \\ \psi_4^1 & \psi_4^2 & \dots & \psi_4^4 \end{bmatrix} \quad (2.3.9)$$

the elements in the r th row and s th column are found by multiplying the r th row of $[X^T]$ by the s th column of $[I][X]$. The r th row of $[X^T]$ is simply $\{\psi^{T(r)}\}$ and the s th column $[I][X]$ is

$$\begin{bmatrix} a_{11}\psi_1^s + a_{12}\psi_2^s + \dots + a_{14}\psi_4^s \\ a_{21}\psi_1^s + a_{22}\psi_2^s + \dots + a_{24}\psi_4^s \\ \dots \\ a_{41}\psi_1^s + a_{42}\psi_2^s + \dots + a_{44}\psi_4^s \end{bmatrix} \quad (2.3.10)$$

$$= [I]\{\psi^s\} \quad (2.3.11)$$

Therefore the element in the r th row and s th column of $[X^T][I][X]$ is $\{\psi^{T(r)}\}[I]\{\psi^s\}$. But

$$\{\psi^T(r)\}[I]\{\psi^s\} = 0 \quad (\text{for } r \neq s) \quad (2.3.12)$$

hence,

$$[X^T][I][X] = [A] \quad (2.3.13)$$

where [A] is a diagonal matrix of the form

$$[A] = \begin{bmatrix} a_1 & 0 & 0 & 0 \\ 0 & a_2 & 0 & 0 \\ 0 & 0 & a_3 & 0 \\ 0 & 0 & 0 & a_4 \end{bmatrix} \quad (2.3.14)$$

The elements of Equation (2.3.14) are always positive as can be inferred from Equation (2.3.11) and are given by

$$[a_r] = \{\psi^T(r)\}[I]\{\psi^r\} \quad (2.3.15)$$

Similarly,

$$[X^T][k][X] = [B] \quad (2.3.16)$$

$$[B] = \begin{bmatrix} c_1 & 0 & 0 & 0 \\ 0 & c_2 & 0 & 0 \\ 0 & 0 & c_3 & 0 \\ 0 & 0 & 0 & c_4 \end{bmatrix} \quad (2.3.17)$$

and the C_i terms are defined by

$$[c_r] = \{\psi^T(r)\}[C]\{\psi^r\} \quad (2.3.18)$$

Expanding Equation (2.3.3) yields

$$\{\psi^T(r)\}[k]\{\psi^s\} - \omega_s^2\{\psi^T(r)\}[I]\{\psi^s\} = 0 \quad (2.3.19)$$

Substituting Equation (2.3.17) for $\{\psi^T(r)\}[k]\{\psi^s\}$ and Equation (2.3.13) for $\omega_s^2\{\psi^T(r)\}[I]\{\psi^s\}$, gives the uncoupled form of the equation of motion

$$[B] - \omega^2[A] = 0$$

In view of the structure of [A] and [B] for $r = s$ we obtain

$$[C_r] = \omega_r^2[a_r] \quad (2.3.20)$$

The stiffness coefficients, $[C_r]$ and inertia coefficients $[a_r]$ will be employed to compute the principal modes and dynamic torque in the ensuing section.

2.4 Deterministic Model

2.4.1 Description of Analytical Model

The system under consideration is a 4-degree of freedom lumped parameter linear torsional system having two branches coupled by a pair of geared wheels. The displacement excitation is provided by the static transmission error which is periodic in nature and is applied at the internal point which links the two gear wheels. The model employed in this analysis is illustrated in Fig. 2.1.

The analysis of dynamic systems of several degrees of freedom is cumbersome due to the large number of equations required to define the system. The transfer matrix method is ideally suited to the manipulation of large arrays because of the concise and efficient manner in which the various equations are identified. It is mainly for this reason that this technique has been adopted in the present investigation.

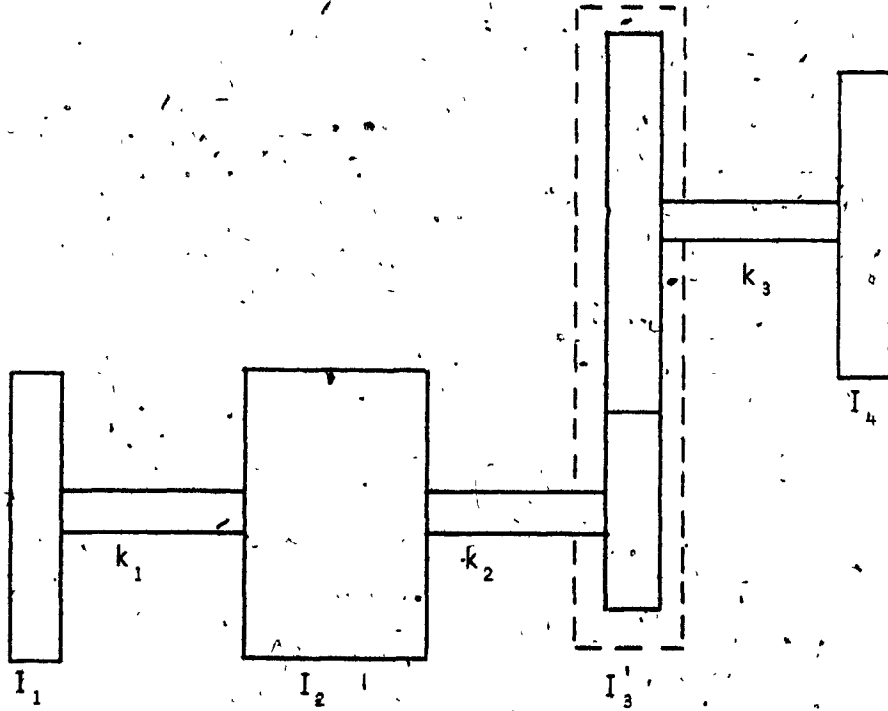


Fig. 2.1: Schematic Diagram of the Model.

In the transfer matrix method, a large system is broken down into sub-systems with distinct elastic and dynamic properties. The formulation of sub-systems is in terms of state vectors, which is the column matrix consisting of the rotations and the torque at each mass point; the point matrix, which contains the dynamic properties of the system; and the field matrix, which describes the elastic properties of the sub-system. In this formulation, the analysis proceeds from one end of the system to the other end. The natural frequencies are established by satisfying the appropriate boundary conditions.

For the four degrees of freedom system shown in Fig. 2.1, the coordinate along the axis of rotation is considered positive towards the right. If a cut is made across the shaft, the face with an outward normal towards the positive coordinate direction is defined as positive. Positive torques and positive angular displacements are indicated on the positive face by arrows pointing along the positive sense according to the righthand screw rule as illustrated in Figs. 2.2 and 2.3. A multi-degree of freedom system is shown in Fig. 2.4.

Figure 2.5 shows a typical subsection of the linear torsional system. The nth subsection consists of the inertia I_n with angular displacement ψ_n and the shaft with stiffness k_n whose ends have angular displacement ψ_n and ψ_{n-1} . The quantities to the left and to the right of the element are designated via the superscripts L and R respectively.

If the torque is denoted by ϕ_n , then for the rotor having inertia I_n , Newton's second law states that

$$I_n \ddot{\psi}_n = \phi_n^R - \phi_n^L \quad (2.4.1)$$

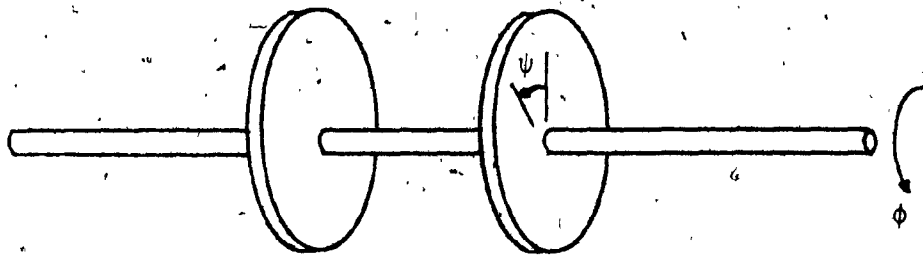


Fig. 2.2: Sign Convention

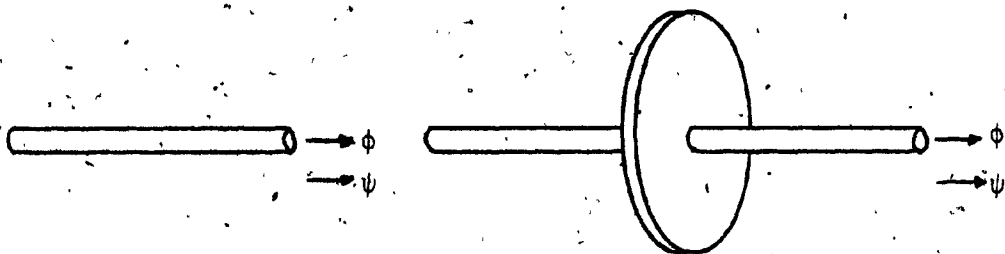


Fig. 2.3: Sign Convention

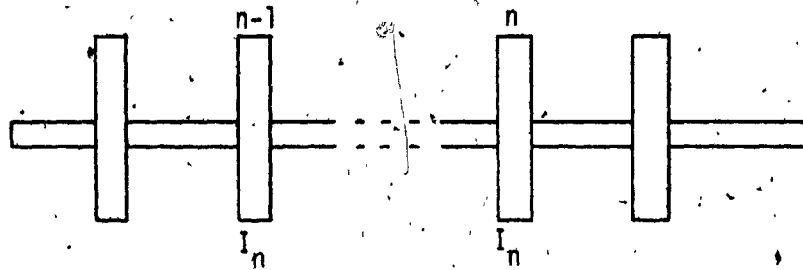


Fig. 2.4: Multidegree of Freedom System.

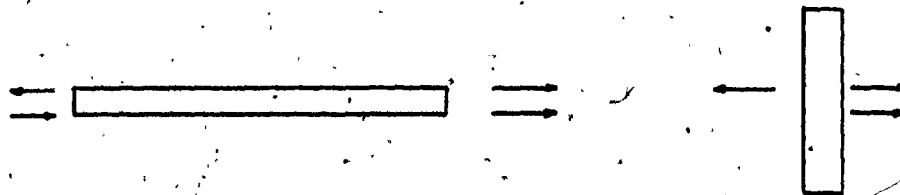


Fig. 2.5: Torque and Displacement in Isolated n^{th} Section.

For harmonic motion, the angular acceleration is

$$\ddot{\psi}_n = -\omega^2 \psi_n \quad (2.4.2)$$

where ω is the angular velocity. Thus Equation (2.4.1) becomes

$$-I_n \omega^2 \psi_n = \phi_n^R - \phi_n^L \quad (2.4.3)$$

or

$$\phi_n^R = -I_n \omega^2 \psi_n + \phi_n^L \quad (2.4.4)$$

The angular displacement on either side of \bar{I}_n is the same i.e.,

$$\psi_n = \psi_n^L = \psi_n^R \quad (2.4.5)$$

In matrix form Equations (2.4.4) and (2.4.5) become

$$\begin{Bmatrix} \psi \\ \phi \end{Bmatrix}_n^R = \begin{bmatrix} 1 & 0 \\ -\omega^2 I & 1 \end{bmatrix}_n \begin{Bmatrix} \psi \\ \phi \end{Bmatrix}_n^L \quad (2.4.6)$$

where

$$\begin{Bmatrix} \psi \\ \phi \end{Bmatrix}_n^R$$

is the state vector for the right face of section n . In this representation, the superscript identifies the side and the subscript the subsection of the linear torsional system. The square matrix on the right hand side of Equation (2.4.6) is the point matrix. Equation (2.4.6) defines the state vector relationship between the left and right hand-sides of a given subsection.

Under steady state, the stiffness and torques acting at the two

ends of a given shaft element remain unchanged. Thus,

$$\phi_{n-1}^R = \phi_n^L \quad (2.4.7)$$

The shaft torque is related to the stiffness k_n and displacement ψ_n by

$$\psi_n^L - \psi_{n-1}^R = \frac{\phi_{n-1}^R}{k_n}$$

or

$$\psi_n^L = \psi_{n-1}^R + \frac{\phi_{n-1}^R}{k_n} \quad (2.4.8)$$

Combining Equations (2.4.7) and (2.4.8) yields

$$\begin{Bmatrix} \psi \\ \phi \end{Bmatrix}_n^L = \begin{bmatrix} 1 & 1/k \\ 0 & 1 \end{bmatrix}_n \begin{Bmatrix} \psi \\ \phi \end{Bmatrix}_{n-1}^R \quad (2.4.9)$$

where the square matrix

$$\begin{bmatrix} 1 & 1/k \\ 0 & 1 \end{bmatrix}_n$$

is the field matrix at the nth subsection.

Using Equations (2.4.6) and (2.4.9), the matrices for the nth subsection may be expressed in terms of the parameters for the (n-1)th subsection as

$$\begin{Bmatrix} \psi \\ \phi \end{Bmatrix}_n^R = \begin{bmatrix} 1 & 0 \\ -\omega^2 I & 1 \end{bmatrix}_n \begin{bmatrix} 1 & 1/k \\ 0 & 1 \end{bmatrix}_n \begin{Bmatrix} \psi \\ \phi \end{Bmatrix}_{n-1}^R \quad (2.4.10)$$

$$= \begin{bmatrix} 1 & 1/k \\ -\omega^2 I & (1 - \frac{\omega^2 I}{k}) \end{bmatrix}_n \begin{Bmatrix} \psi \\ \phi \end{Bmatrix}_{n-1}^R \quad (2.4.11)$$

In Equation (2.4.11) the state vector at $n-1$ is transferred to the state vector at n through the transfer matrix for subsection n .

In short this can be written as

$$\{S_v\}_n = [T_m]_n \{S_v\}_{n-1} \quad (2.4.12)$$

where $\{S_v\}$ is the state vector containing ψ and ϕ and $[T_m]_n$ is the transfer matrix for the n th subsection. To evaluate the overall transfer matrix for branch A, this operation is repeated for each segment of the branch starting from segment 1 where the stations are numbered in increasing order from left to right with the transfer matrices also progressing to the right. The '0' section is taken at the free-end. The state vector for branch A which has 3 stations becomes

$$\begin{aligned} \{S_v\}_1 &= [T_m]_1 \{S_v\}_0 \\ \{S_v\}_2 &= [T_m]_2 \{S_v\}_1 \\ &= [T_m]_2 [T_m]_1 \{S_v\}_0 \\ \{S_v\}_3 &= [T_m]_3 \{S_v\}_2 \\ &= [T_m]_3 [T_m]_2 [T_m]_1 \{S_v\}_0 \end{aligned}$$

or

$$\{S_v\}_3 = [A] \{S_v\}_0 \quad (2.4.13)$$

where $[A]$ is the overall transfer matrix for branch A. This can also be

written as

$$[A] = [T_m]_3 [T_m]_2 [T_m]_1$$

In expanded form the overall transfer matrix is

$$\begin{bmatrix} A_{11} & A_{12} \\ A_{21} & A_{22} \end{bmatrix} = \begin{bmatrix} 1 & 1/k_2 \\ -\omega^2 I_3 & 1 - \frac{\omega^2 I_3}{k_2} \end{bmatrix} \begin{bmatrix} 1 & 1/k_1 \\ -\omega^2 I_2 & 1 - \frac{\omega^2 I_2}{k_1} \end{bmatrix} \begin{bmatrix} 1 & 0 \\ -\omega^2 I_1 & 1 \end{bmatrix}$$

where A_{11} , A_{12} , A_{21} and A_{22} are elements of $[A]$ defined in Equation (2.4.11).

Equation (2.4.13) for branch A, may be rewritten as

$$\{S_v\}_3^R = [A] \{S_v\}_1^L \tag{2.4.14}$$

$$\{S_v\}_3^R = \begin{bmatrix} A_{11} & A_{12} \\ A_{21} & A_{22} \end{bmatrix} \{S_v\}_1^L \tag{2.4.15}$$

where the superscripts R and L denote the right and left surface of the station.

The state vector at the left of section 1 under the boundary condition that the torque at the free-end ϕ_1^L is 0 and for an initial angular displacement ψ_1^L of 1 will be

$$\begin{Bmatrix} 1 \\ 0 \end{Bmatrix}$$

Consequently,

$$\begin{Bmatrix} \psi \\ \phi \end{Bmatrix}_3^R = \begin{bmatrix} A_{11} & A_{12} \\ A_{21} & A_{22} \end{bmatrix} \begin{Bmatrix} T \\ O \end{Bmatrix}_1^L \quad (2.4.16)$$

or $\psi_3^R = A_{11}$ (2.4.17)

and $\phi_3^R = A_{21}$ (2.4.18)

Similarly, the transfer matrix for branch B is simply

$$\begin{Bmatrix} S_V \end{Bmatrix}_4^R = [T_m]_4 \begin{Bmatrix} S_V \end{Bmatrix}_4^L \quad (2.4.19)$$

where

$$[T_m]_4 = [B] = \begin{bmatrix} 1 & 1/k_3 \\ -\omega^2 I_4 & 1 - \frac{\omega^2 I_4}{k_3} \end{bmatrix} \quad (2.4.20)$$

and [B] is the overall transfer matrix for branch B. The angular displacement and torque to the right of I' (driving gear) is equal to the angular displacement and torque to the right I'' (driven gear) and is also equal to angular displacement and torque to the left of section 4.

Therefore

$$\psi_3^R = \psi_4^L \quad (2.4.21)$$

$$\phi_4^R = \phi_4^L \quad (2.4.22)$$

Equation (2.4.19) becomes

$$\begin{Bmatrix} \psi \\ \phi \end{Bmatrix}_4^R = \begin{bmatrix} B_{11} & B_{12} \\ B_{21} & B_{22} \end{bmatrix} \begin{Bmatrix} A_{11} \\ A_{21} \end{Bmatrix} \quad (2.4.23)$$

which yields

$$\phi_4^R = B_{21} \cdot A_{11} + B_{22} \cdot A_{21} \tag{2.4.24}$$

The boundary condition at the free end is

$$\phi_4^R = 0 \tag{2.4.25}$$

and substituting in Equation (2.4.25) into (2.4.24) gives

$$0 = B_{21} \cdot A_{11} + B_{22} \cdot A_{21} \tag{2.4.26}$$

The natural frequencies of the system are obtained from Equation (2.4.26) using the condition

$$\phi_1^L = 0 \tag{2.4.27}$$

$$\phi_4^R = 0 \tag{2.4.28}$$

which simply states that no external torque is required to cause the system to oscillate at its natural frequency.

The solution to Equation (2.4.26) subject to the conditions defined in Equations (2.4.27) and (2.4.28) were obtained numerically using the bisection method [23].

The mode shape to the right of each rotor is obtained with the initial state vector and transfer matrix of that section. The mode shape thus obtained is then adjusted to the mode shape of the actual system since the appropriate speed ratios are known.

To evaluate the dynamic torque, a modal analysis of the system was performed as explained in Section (2.3). The modal equations are

$$a_1 \ddot{p}_1 = N I_3^r \omega_4^2 \gamma_0 \sin \omega_4 t \quad (2.4.29)$$

$$a_r \ddot{p}_r + C_r p_r = (N \psi_3^r I_3^r \omega_4^2 - \phi_3^r) \gamma_0 \sin \omega_4 t \quad (\text{for } r=2,3,4) \quad (2.4.30)$$

The steady state solution to Equation (2.4.30) for the off resonant modes is

$$p_r = \frac{(N \psi_3^r I_3^r \omega_4^2 - \phi_3^r)}{a_r (\omega_r^2 - \omega_4^2)} \gamma_0 \sin \omega_4 t \quad (\text{for } r = 2,3) \quad (2.4.31)$$

and for the resonant mode it is

$$p_4 = \frac{(N \psi_3^4 I_3^4 \omega_4^2 - \phi_3^4)}{C_4} Q \gamma_0 \sin \omega_4 t \quad (\text{for } r = 4) \quad (2.4.32)$$

where Q is the dynamic magnification at resonance.

The amplitude of the fluctuating torque on the slower shaft can be obtained, as discussed in Section 2.4.2.

In order to obtain an insight into the interdependence of the mean and fluctuating torque components, results were calculated for a range of mean and fluctuating torque values.

2.4.2 Derivation of Torque Equation

The linear system depicted in Fig. 2.1 comprises the subsystems A and B. Subsystem A contains three discs and subsystem B two discs. The velocity ratio between subsystem A and B is N . Therefore, the linear system under consideration has four degrees of freedom.

If q be the generalized deflection, coordinate, then

$$q = q_1, q_2, q_3, q_4$$

where

$$q_3' = q_3'$$

$$\text{and } q_3'' = Nq_3'$$

The q_3' and q_3'' indicate the generalized deflection for the driving and driven gear respectively.

The system has four principal modes and hence four principal coordinates p , such that

$$\{p = p_1, p_2, p_3, p_4\}$$

Let the system be distorted in the n th mode only such that $p_n = 1$, then the distortion can be expressed by the modal vector

$$\{q\} = \psi^n$$

In the n mode, when the distortion is imposed upon the system, let the torque applied by subsystem A to subsystem B be ϕ_i^n

The equation for the general static distortion is

$$\{q\} = \sum_{n=1}^4 p_n \psi^n \tag{2.4.33}$$

where $\{p_n\}$ is the principal coordinate and $\{\psi^n\}$ the modal vector corresponding to n th mode. The torque applied by subsystem A to subsystem B is

$$\{\phi_i\} = \sum_{n=2}^4 p_n \phi_i^n \tag{2.4.34}$$

since $\phi_i^1 = 0$ corresponding to the rigid body mode.

The governing equation for the free vibration of the complete system is

$$\left. \begin{aligned} a_1 \ddot{p}_1 &= 0 \\ a_n \ddot{p}_n + C_n p_n &= 0 \end{aligned} \right\} \text{ for } n = 2, 3, 4 \quad (2.4.35)$$

where, $[a_n]$ is the inertia coefficient corresponding to $\{p_n\}$ the n th principal coordinate, and $[C_n]$ is the stiffness coefficient corresponding to the $\{p_n\}$.

The equation of kinetic energy associated with the motion in the rigid body mode is

$$\begin{aligned} T &= \frac{1}{2} [I_1 \dot{q}_1^2 + I_2 \dot{q}_2^2 + I_3' \dot{q}_3'^2 + I_3'' \dot{q}_3''^2 + I_4 \dot{q}_4^2] \\ &= \frac{1}{2} [I_1 \dot{q}_1^2 + I_2 \dot{q}_2^2 + (I_3' + I_3'' N^2) \dot{q}_3^2 + I_4 \dot{q}_4^2] \\ &= \frac{1}{2} [a_1] \{\dot{p}_1^2\} \end{aligned} \quad (2.4.36)$$

where

$$I_3 = I_3' + N I_3''$$

the superscripts ' and '' identify the driving and driven gear respectively.

If the angular transmission error be $\gamma(t)$ considering the gear in subsystem A as a reference gear, then at any instant the configuration is defined by the vector

$$\{p_1, p_2, p_3, p_4, \gamma(t)\}$$

where the displacement q of the individual discs is obtained from the relations:

in Subsystem A

$$q_j = \sum_{n=1}^4 p_n \psi_j^n \quad (\text{for } j = 1, 2)$$

$$q_3' = q_3 = \sum_{n=1}^4 p_n \psi_3^n$$

in Subsystem B

$$q_3'' = Nq_3 + \gamma(t)$$

$$= N \sum_{n=1}^4 p_n \psi_3^n + \gamma(t)$$

$$q_j = \sum_{n=1}^4 p_n \psi_j^n \quad (\text{for } j = 4)$$

The kinetic energy in any general distortion of the system is

$$T = \frac{1}{2} \sum_{j \neq i}^4 I_{ij} (\dot{q}_j)^2 + \frac{1}{2} I_i' (\dot{q}_i')^2 + \frac{1}{2} I_i'' (\dot{q}_i'')^2$$

But $\dot{q}_i'' = N\dot{q}_i' + \dot{\gamma}$

Thus,

$$T = \frac{1}{2} \sum_{j=1}^4 I_j \dot{q}_j^2 + \frac{1}{2} I_i'' \dot{\gamma}^2 + I_i'' \dot{\gamma} (N\dot{q}_i')$$

$$= \frac{1}{2} \sum_{n=1}^4 a_n \dot{p}_n^2 + \frac{1}{2} I_i'' \dot{\gamma}^2 + NI_i'' \dot{\gamma}^2 \sum_{n=1}^4 p_n \psi_i^n \quad (2.4.37)$$

To obtain the strain energy, for the distortion $\{p_1, p_2, p_3, p_4, 0\}$, it is first noted that the strain energy for the rigid body mode is zero and consequently $C_1 = 0$. The strain energy for any general distortion is

$$V = \frac{1}{2} \sum_{n=2}^4 C_n p_n^2 \quad (2.4.38)$$

From Equation (2.4.34) the torque exerted by subsystem A on subsystem B is

$$\phi_i^n = \sum_{n=2}^4 p_n \phi_i^n$$

If the distortion due to transmission error

$$\{0, 0, 0, 0, \gamma(t)\}$$

is admitted to the strain energy, the strain energy is increased by

$$\frac{1}{2} C_{ii} [\gamma(t)]^2 + \gamma(t) \sum_{n=2}^4 p_n \phi_i^n$$

where C_{ii} is the torque applied by subsystem A to subsystem B during an imposed static separation

$$q_i'' = \gamma(t) = 1$$

$$\text{while } p_1 = p_2 = p_3 = p_4 = 0$$

Thus the total strain energy becomes

$$V = \frac{1}{2} \sum_{n=2}^4 C_n p_n^2 + \frac{1}{2} C_{ii} [\gamma(t)]^2 + \gamma(t) \sum_{n=2}^4 p_n \phi_i^n \quad (2.4.39)$$

Using T and V in Lagrange's from [23], the equation of motion reduces to

$$a_1 \ddot{p}_1 = -N I_i'' \ddot{\gamma}(t)$$

$$a_n \ddot{p}_n + C_n p_n = -N \psi_i^n I_i'' \ddot{\gamma}(t) - \phi_i^n \gamma(t) \quad (\text{for } n = 2, 3, 4)$$

$$Q_Y = \sum_{n=2}^4 p_n \phi_i^n + N I_i'' \sum_{n=1}^4 \ddot{p}_n \psi_i^n + I_i'' \gamma(t) + C_{ii} \ddot{\gamma}(t) \quad (2.4.40)$$

2.4.3 Force Analysis

Figure 2.6 depicts the nomenclature employed in the force analysis of geared systems. If gear 1 is the driving gear mounted on shaft x and gear 2 is the driven gear mounted on shaft y, then the force exerted by gear 1 against gear 2 is F_{12} . The force of gear 1 against shaft x is F_{1x} where a F_{x1} denotes the force of shaft x against gear 1. Thus the first element is associated with the origin of the force and the second subscript indicates the element where the force is manifested. The superscripts r and t refer to the radial and tangential directions respectively.

If W_t is the transmitted load (force) then

$$W_t = F_{21}^t$$

with $T_{x1} = Q_Y$ the applied fluctuating torque and $d_1 = d$ the diameter of the driving gear, then

$$Q_Y = \frac{d}{2} W_t \quad (2.4.41)$$

The radial component of the force F_{21}^r is small and produces a compressive stress, which is beneficial in fatigue loading.

2.4.4 Stress Analysis

Figure 2.7 shows a spur gear tooth loaded at its tip by a force W_t which acts at a pressure angle α . This force is assumed to be distributed equally across the tooth width b . The force W_t exerts a bending load on the gear tooth. Gear teeth under normal operating conditions

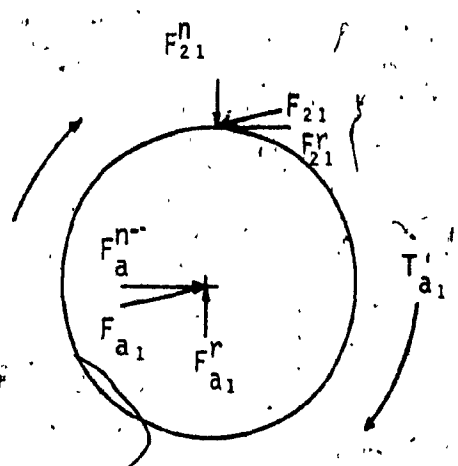
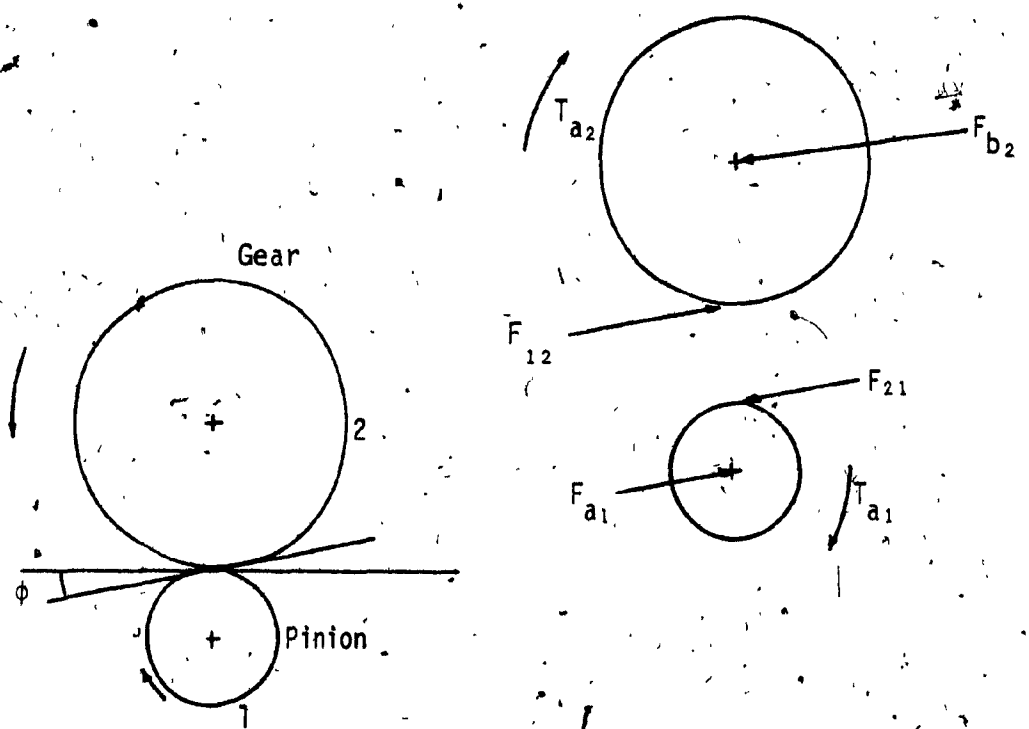


Fig. 2.6: Free Body Diagram of Forces Acting Upon a Simple Gear Train.

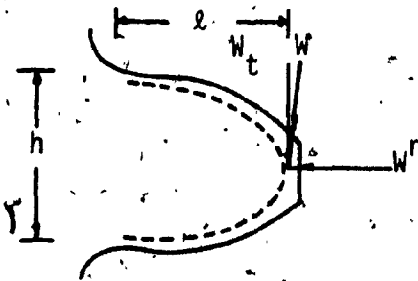
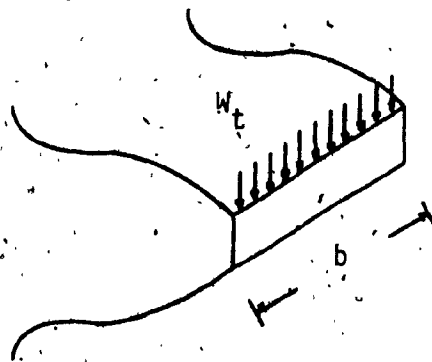


Fig. 2.7: Free Body Diagram of Gear Tooth with Forces Acting on it.

are subjected to transmitted loads W_t as well as, impact loads as successive teeth come into contact. The magnitude of the incremental or impact load is a complex function of several factors such as gear manufacturing accuracy, operating speed, tooth rigidity transmitted torque and the moments of inertia of the mating gears. To account for the presence of impact loads it is assumed that the force W_t at the tip of one tooth accounts for the entire torque carried by the gear. Theoretically, when a tooth is in contact at its tip, the load is shared by at least one other tooth. Because of errors in the tooth profile, this distribution of load does not take place, thereby justifying the conservative assumption that one tooth carries the full load at its tip.

An analysis to determine whether the bending stresses were higher when carrying part of the load at the tip or when carrying all the load nearer the base of the cantilevered tooth, was done by Lewis [24]. Lewis proposed that a parabola be inscribed within the tooth outline (Fig. 2.7). Since the actual tooth cross section is stronger except where the two configurations are tangent, the maximum bending stress is

$$S = \frac{W_t}{b} \frac{.6l}{h^2} \tag{2.4.42}$$

where

S = bending stress of the root of gear tooth

W_t = tangential load

b = width

l = length

h = height

The term $6\ell/h$ is a linear function of the size of the tooth (proportional to h) and the shape of the tooth (ratio of h/ℓ). In terms of diametral pitch P , which is the number of teeth per inch of pitch diameter, and the form or shape factor Y , the bending stress is

$$S = \frac{W_t P}{bY} \quad (2.4.43)$$

2.4.5 Fatigue Loading

Gearing elements are subjected to a wide variety of operating conditions. Only rarely however, are gears subjected to constant loads of the type depicted in Fig. 2.8 throughout their entire service history. Theoretically, under these idealized conditions, gears should have infinite life.

Gears in industrial equipment, experience variable loading conditions as illustrated in Fig. 2.9. These loading conditions result from vibration, fluctuating power or load requirements, non-uniform road surfaces, variation in atmospheric gust patterns, wind loading, wave motion at sea, and repeated temperature changes.

In practice, very rarely a single application of a static load is responsible for failure, but on the other hand, the repeated application of a load of much lesser magnitude, may ultimately cause sudden and catastrophic failure.

Figure 2.10 shows various types of gearing service loads which are encountered in practice. In a number of cases, the variation of stress (or load) with time may be approximated by a sinusoid. Irrespective of the nature of the applied forces the shape of the loading cycle exists. The parameters used to characterize gearing stress histories [25] are

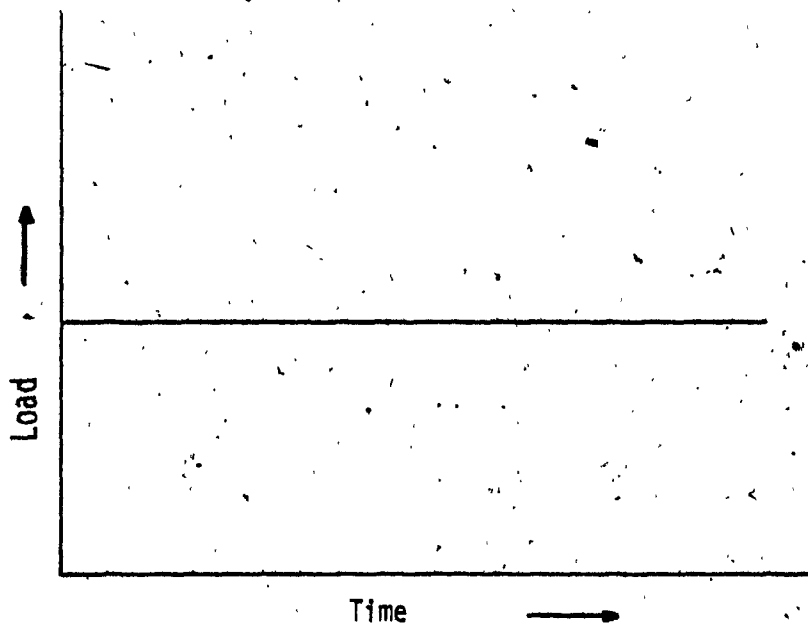


Fig. 2.8: Static Loading.

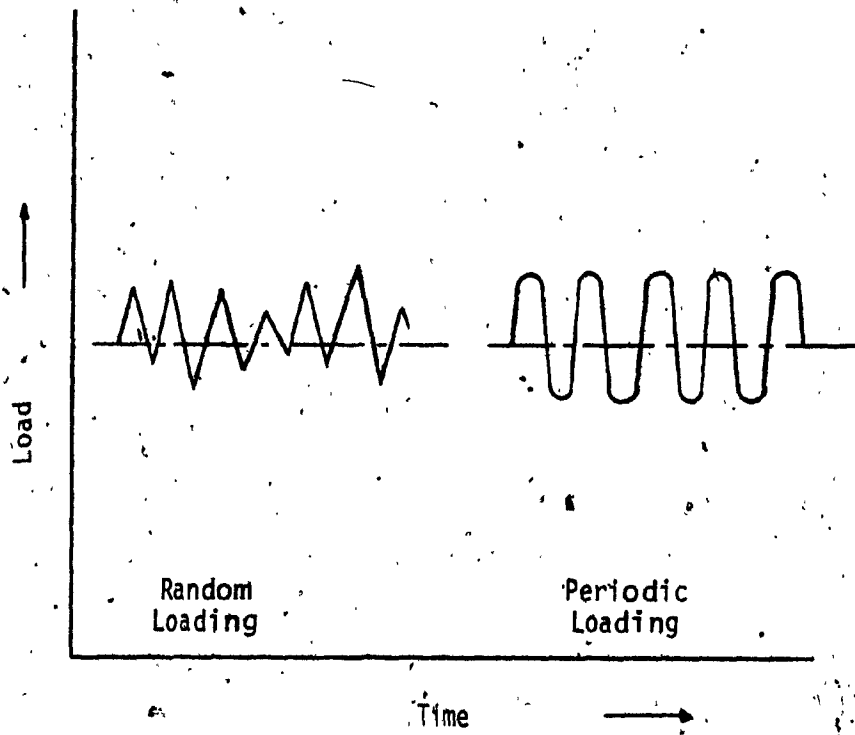
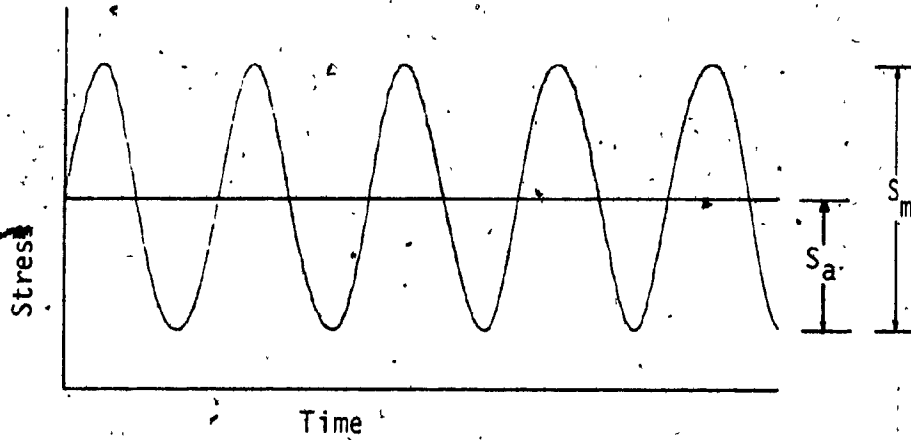
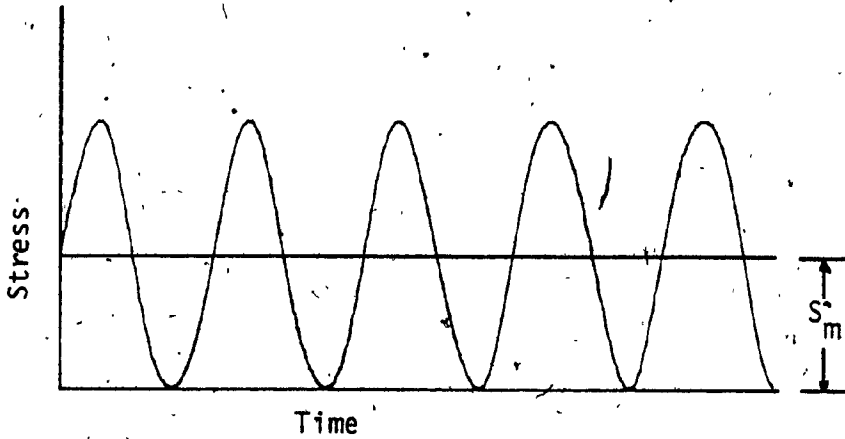


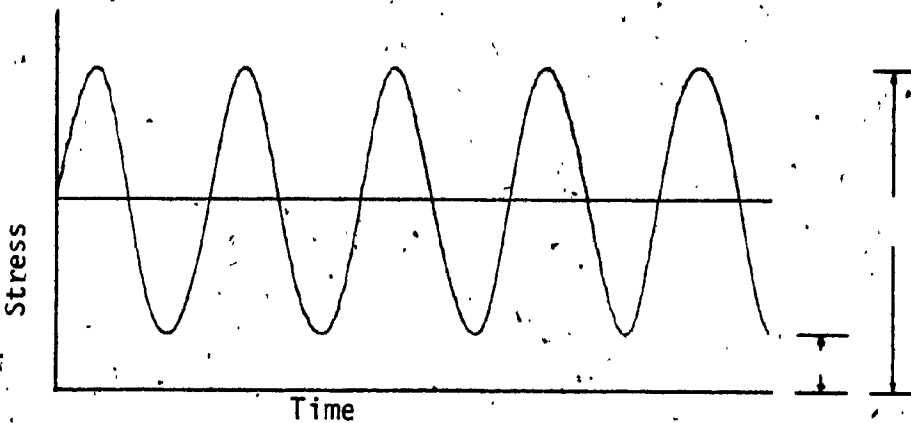
Fig. 2.9: Fatigue Loading



(a) Reversed Stress



(b) Repeated Stress



(c) Fluctuating Stress

Fig. 2.10: Stress Versus Time Relationship.

alternating stress (S_a), stress range (S_r), maximum stress (S_{max}), minimum stress (S_{min}) and mean stress (S_m). The stress cycle can be defined completely if two of the four parameters S_{max} , S_{min} , S_a , S_m are known. Since tensile loading is considered positive and compressive loading negative, it follows that

$$S_m = \frac{S_{max} + S_{min}}{2}$$

$$S_{min} = S_m - S_a$$

$$S_{max} = S_m + S_a$$

$$S_r = 2S_a = S_{max} - S_{min}$$

2.4.6 Fatigue Failure

Material fatigue is a very common engineering problem. It affects each and every component that moves and it also affects stationary objects if the object experiences cyclic forces or deformations. To handle material fatigue, one must have a complete knowledge of the cyclic loading conditions imposed on the element. Secondly, every material has its characteristic fatigue behavior which is frequently dependent on the nature of the applied load. To obtain detailed material fatigue data is a very time consuming process and consequently, our current understanding of material fatigue is incomplete and sketchy.

Gears often fail under the action of repeated or fluctuating stresses even if the maximum fluctuating stress is below the ultimate strength of the material and frequently even below the yield strength. Such failures occur for stress histories which involve the repetition of many stress cycles and are commonly referred to as fatigue failures.

A fatigue failure begins with small surface cracks. At the outset, the crack is so small that it cannot be detected by the naked eye. The crack initiates at a point of discontinuity in the material, such as a change in cross-section, a key way, or a hole. It can also begin at stamp marks or inspection marks, internal cracks, or at irregularities caused by machining. Once the crack has formed, the stress concentration effect is enhanced and the crack progresses more rapidly. Since the stress area decreases in size, the stress increases in magnitude, until the remaining area fails suddenly. Thus a fatigue failure can be recognized by the progressive development of crack and the sudden fracture as shown in Fig. 2.11.

When a material fails statically, the large deflection causes high stresses which exceed the yield strength. Thus static failure gives warning in advance because it is visible whereas fatigue failure gives no warning; it is sudden and complete and thus dangerous.

2.4.7 Fatigue Life with Fluctuating Stress

Failure by fatigue is caused by the repeated application and removal of stress. For a given material, if the intensity of the applied stress is high, the number of stress cycles before failure occurs will be low. The relationship between the fatigue failure stress and the number of applied stress cycles is given by the "fatigue life stress curve" or "S-N curve". The fatigue failure stress decreases exponentially from a relatively high value S_f close to the ultimate strength at about 10^3 stress cycles, down to the endurance stress S_e for an infinite number of stress cycles (Fig. 2.12). Comparing Figs. (2.12a) and (2.12b), it is clear that the log graph emphasizes the knee of the

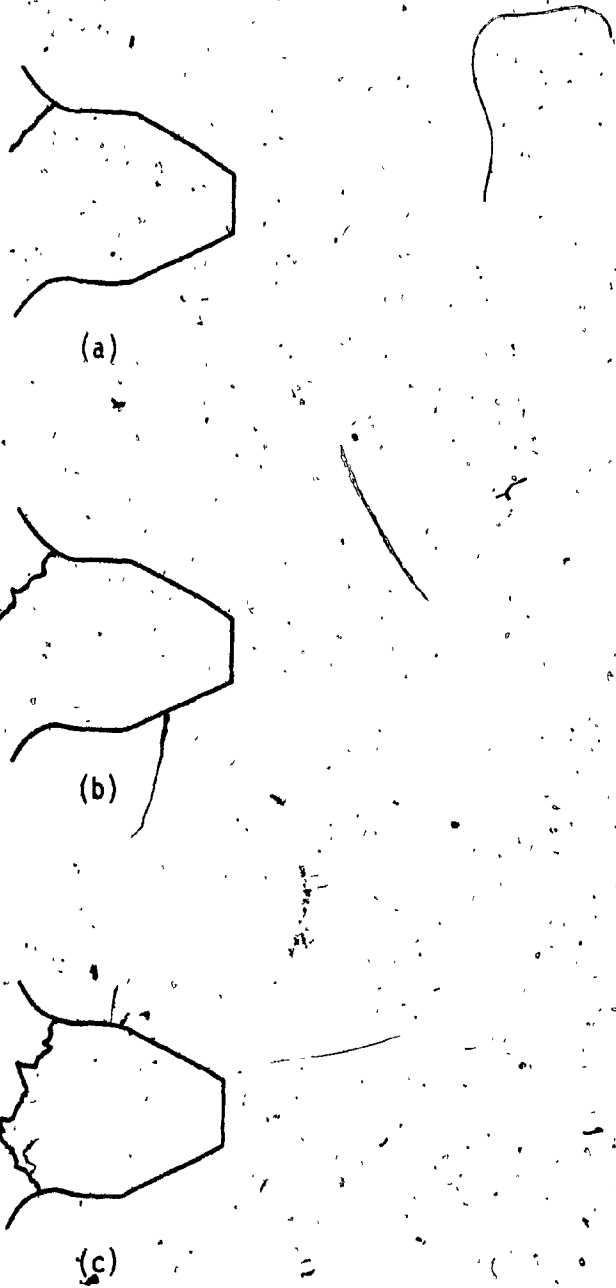
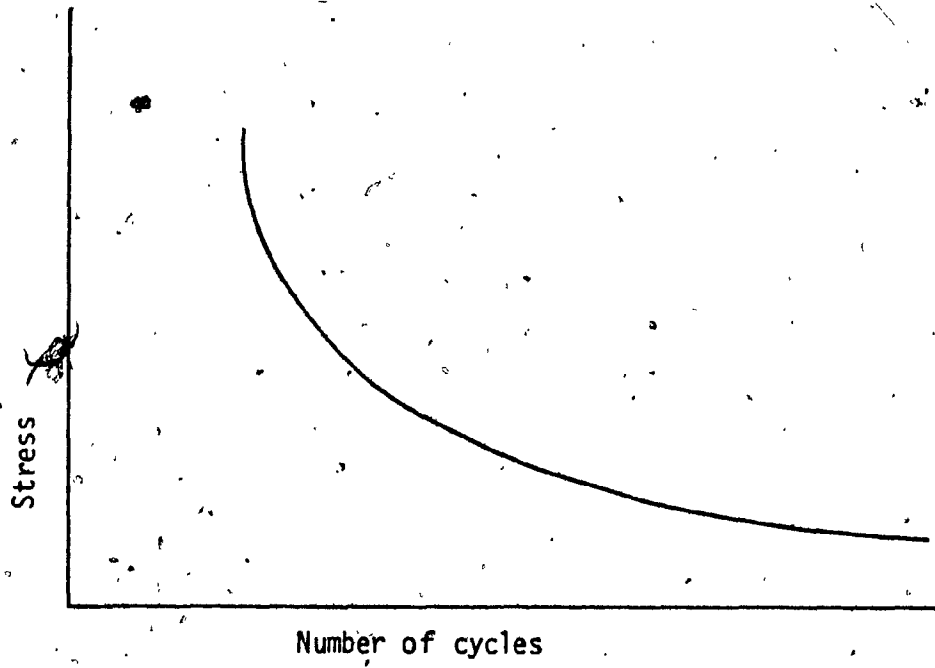


Fig. 2.11: Fatigue Fracture of a Gear Teeth



(a)

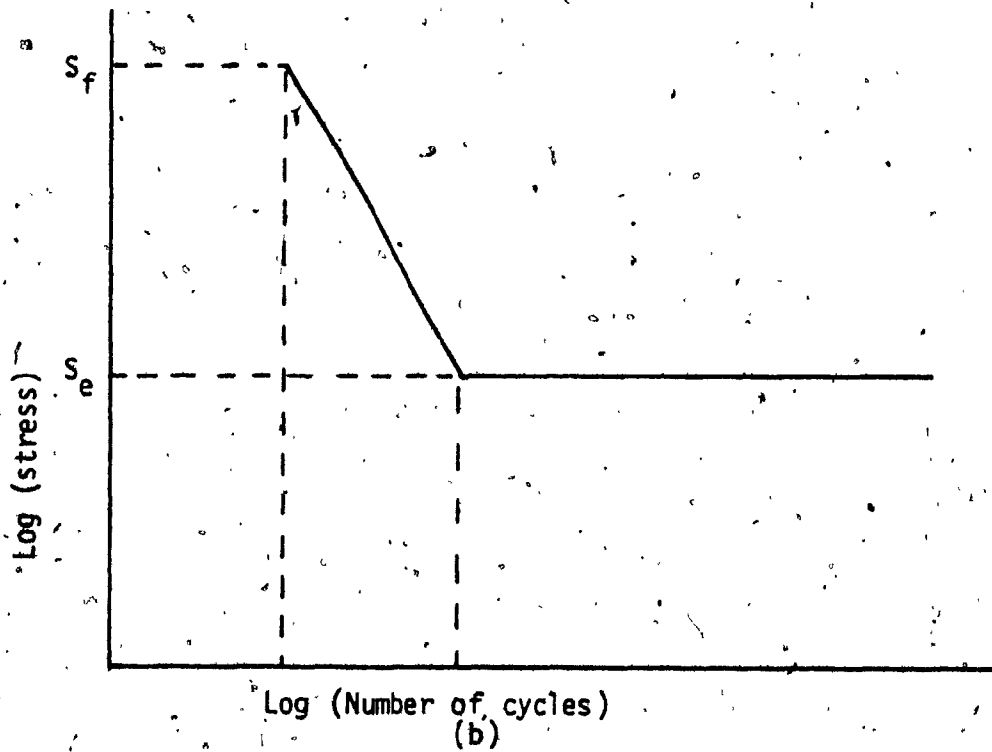


Fig. 2.12: S-N Curve

curve, which might not be apparent if the results were plotted by using the Cartesian coordinates.

The ordinate of the S-N diagram is called the fatigue strength S_f . For steels, a knee occurs in the graph (plotted on log paper), at $N = 10^6$ and beyond this knee, failure will not occur no matter how large the number of cycles is. The strength corresponding to the knee is called the endurance limit S_e or the fatigue limit. For non-ferrous metals and alloys, the knee does not occur and hence these materials do not have an endurance limit.

The mean fatigue life corresponding to any reversible (bending) stress is found from the relation

$$N(S) = \left(\frac{c}{S}\right)^\theta \quad (2.4.44)$$

where N is the mean life in cycles at a stress level S , c is a material constant and θ is the negative reciprocal of slope of the mean S-N curve. It should be emphasized that Equation (2.4.44) is only applicable to reverse-bending stress histories for which the mean stress value is zero [26].

2.4.8 Fatigue Life with Mean and Fluctuating Stress

In the determination of material fatigue life, it has been observed that the mean stress can significantly alter its endurance strength to cyclic loads. In general, the behavior of materials in the presence of mean stresses is such that tensile mean stresses reduce and compressive means increase the life at a given amplitude of loading. For different mean stresses, a group of curves can be plotted with each line corresponding to a different mean stress as shown in Fig. 2.13.

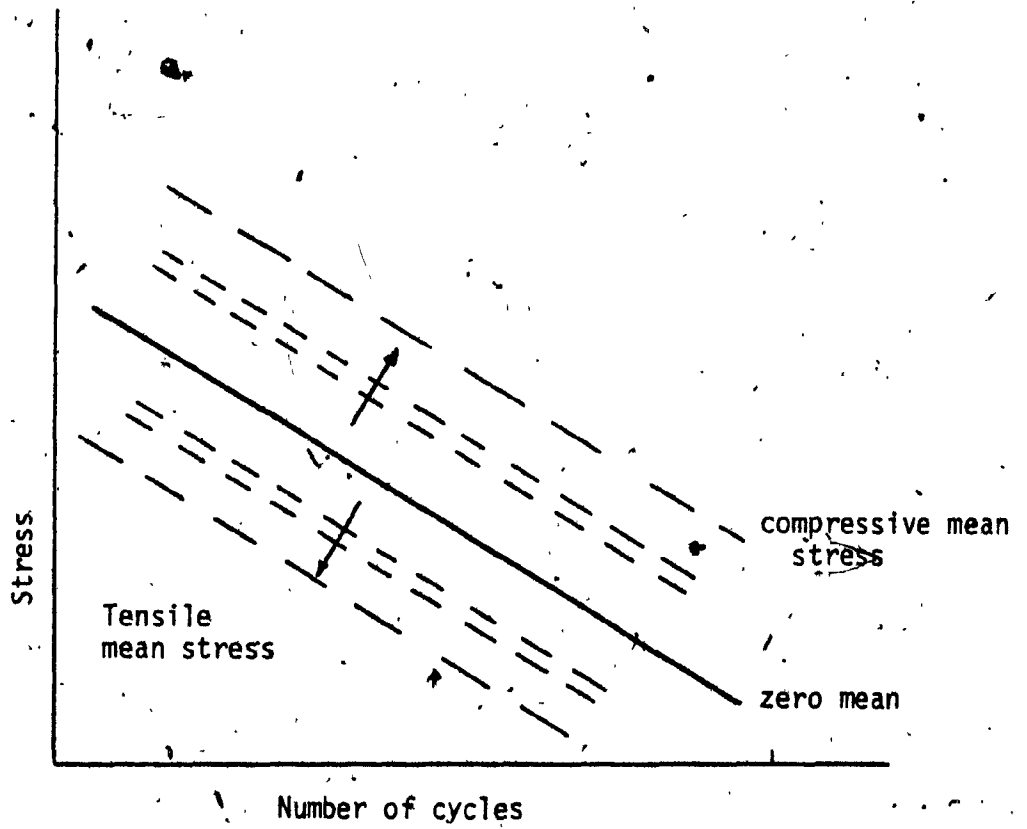


Fig. 2.13: Fatigue Life with Mean Stress

The theory of prediction of fatigue strength as influenced by the mean stresses is not fully developed. Several empirical relations have been proposed and these are adequate for the handling of simple problems. All of these are based on the concept of superimposing an alternating stress on a mean stress. For the combination of these stresses attempts are made to find the limiting values in fatigue life [26].

The superposition of stresses can be described with the help of Fig. 2.14. The limiting value of any combination of stresses is S_f , i.e. the true fracture strength in monotonic tension. According to Fig. 2.14, at zero mean stress, the maximum allowable alternating stress is s_f but when $S_a = S_m = S_f$, the expected life will not be more than one quarter of a cycle. Similarly, when the mean stresses approach S_f the allowable alternating amplitude superimposed on the mean be zero. Thus, for an ideal behavior, when the mean and alternating stresses are present, the fracture strength is

$$S_a + S_m \leq S_f \quad (2.4.45)$$

However, this behavior is only valid if damage did not accumulate from cycle to cycle.

This problem has been approached in a practical way by developing empirical relations. In essence, the adopted approach is similar to the concept of Fig. 2.14 and the most widely used relations are shown in Fig. 2.15.

The ordinate of the diagram is a fully reversed alternating stress S_a for a chosen life span. The limiting maximum mean stress is arbitrarily chosen as either the ultimate strength S_{ut} or the yield strength S_{yt} .

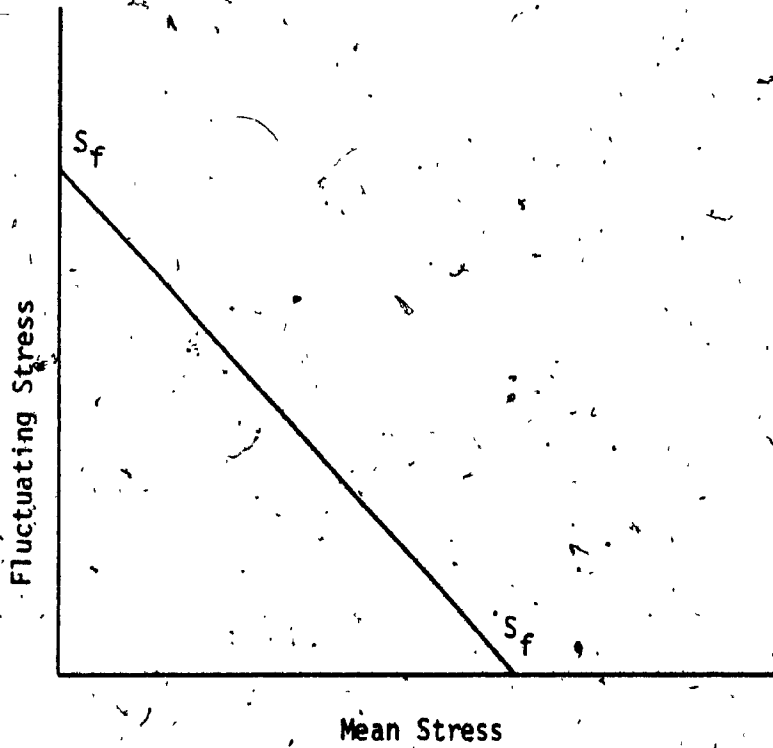


Fig. 2.14: Fatigue Life with Fluctuating and Mean Stress

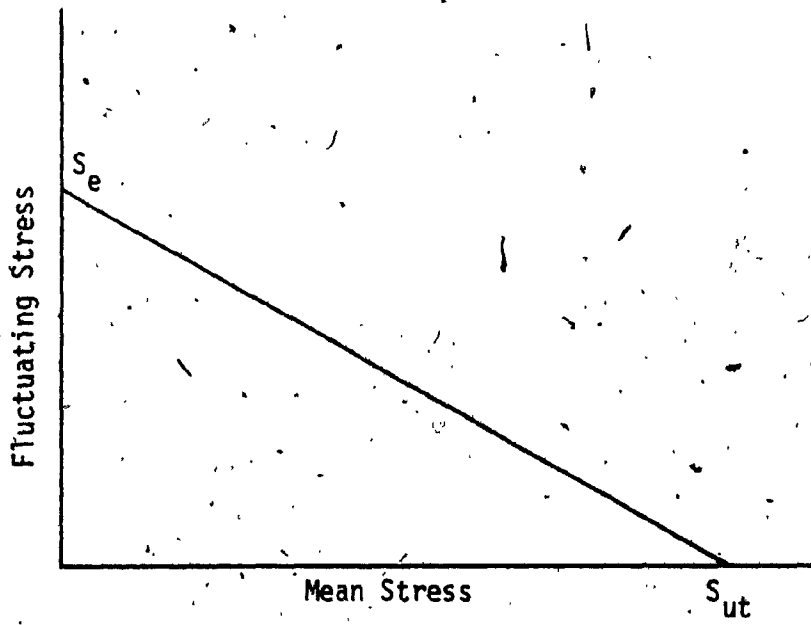


Fig. 2.15: Modified Goodman Diagram

These strengths are below the true fracture strength. The line connecting the selected points on the two axes indicates a combination of mean and superimposed alternating stresses that gives the same endurance as the selected fully reversed amplitude.

Materials also have different responses depending on the number of cycles experienced. To account for cycle-dependent material properties and mean stresses, a concept similar to Fig. 2.16 has been adopted i.e. alternating stress plus the mean stress can never exceed the true cyclic fracture strength. In other words, a change in fatigue life is caused by a mean stress which may be expressed as

$$N(S_f - S_m) = \left(\frac{c}{S_f - S_m} \right)^\theta \quad (2.4.46)$$

It has been suggested [26] that the endurance strength of a material is dependent on the applied steady stress. With the increase in mean stress the endurance strength reduces as shown in Fig. 2.17 and the governing equation is

$$S_a = S_e \left[1 - \frac{S_m}{S_{ut}} \right] \quad (2.4.47)$$

where S_a is new endurance strength.

The bending strength of gear teeth depends upon the type of surface finish, its size in comparison to the rotating beam specimen ($d = 0.30$ in), the ambient temperature etc. In the analysis of the strength of gear teeth, the miscellaneous effect factor (which takes care of all factors mentioned above) has been considered. In the case under investigation, the load acts only upon one of the tooth faces, and hence the tooth is subjected to one way bending only. The strength in one way bending is

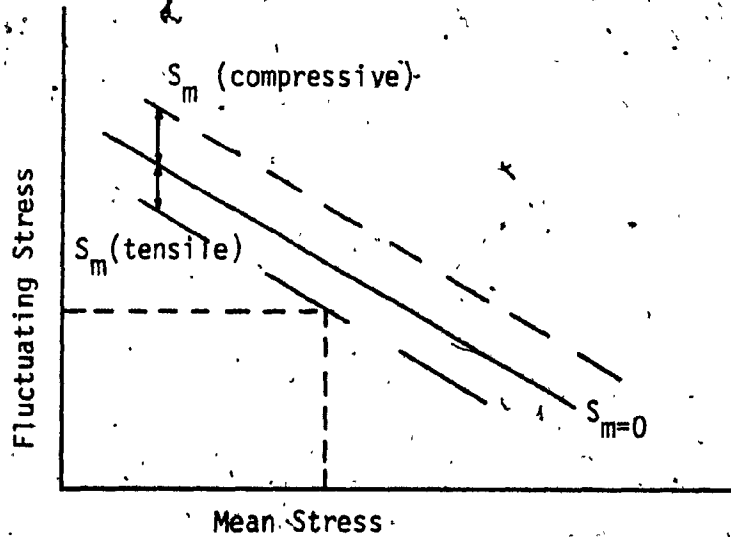


Fig. 2.16: Fatigue Life with Tensile and Compressive Mean Stress

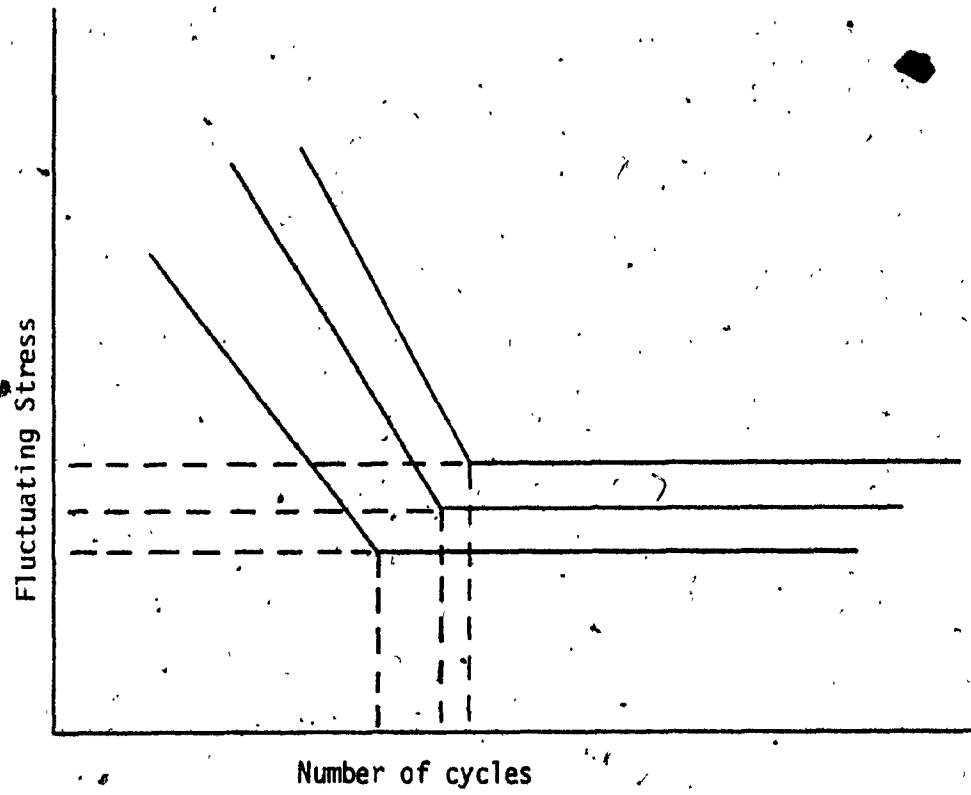


Fig. 2.17: Effect of Mean Stress on Endurance Strength

generally 40 to 50 percent higher than the two way strength S_e . Thus for one way bending $K_f = 1.4$ has been used.

2.4.9 Effect of Various Transmission Errors on the Fatigue Life of Gear Teeth

The gear tooth life has been evaluated for the various values of static transmission error.

It has also been attempted to determine the effect of variable transmission error as an exponentially decaying function of the gear speed. If γ_0 be the static transmission error, λ be slope of the curve, ω the angular velocity and γ_B a constant, then the transmission error is expressed as:

$$\gamma_0 = \gamma_B e^{-\lambda\omega} \quad (2.4.48)$$

By taking several values of γ_B and λ , the fatigue life has been evaluated at different velocities.

2.5 Stochastic Model

2.5.1 Introduction

When the parts of any system undergo motions which fluctuate in time, they are said to be vibrating. The characteristic forms can be noted from the records taken from transducers such as accelerometers or strain gauges. Naturally, in studying such records, one looks for a particular pattern or regularity, so that the variation can be characterized simply. For example, the vibration record can be easily characterized, as being predominantly a simple harmonic motion. A sinusoid can be generally used as an analytical approximation to the

vibration, since it represents most physical situations. A random vibration is one in which no obvious pattern in a vibration record can be noticed.

A more detailed study of randomness involves the belief that apart from the given record, one ought to consider all the other possible records which might have also been produced under the same conditions. If identical experiments are performed a number of times, and the records too are identical (either regular or irregular), then this process can be called deterministic. However, if the conditions, over which the experimenter has control, are kept the same always and the records differ from one another in each case, then the process is known as random. If this is the case, then only one record is not adequate and a statistical description of the totality of all possible records is required. Such random functions are characterized by the fact that a deterministic prediction of their instantaneous value is not possible. A deterministic approach is one in which a sinusoid is characterized by its amplitude as well as its frequency. But in random vibration, characterization by an average amplitude and a decomposition of frequency, can be regarded as adequate. Usually, the rms or root-mean-square value is the average amplitude used. The mean square spectral density indicates the frequency decomposition. If there is no difference in such averages with different values of time then the random process described by the whole ensemble is called stationary.

Thus, a random process is described by the whole ensemble of the possible time histories which might have been the result of the same experiment.

2.5.2 Random Model

It has been noticed that with time, the amplitude fluctuations in gears, undergoes variations. Thus, for each different angular velocity, the fatigue life of gears also changes. It is practically impossible to account for this change in fatigue life through a deterministic model. Only if the load is treated as a random variable can this aspect be considered. In spite of the unpredictability of its outcome, the random process does exhibit some degree of statistical regularity which makes it possible to adopt a statistical approach to the problem [27]. The statistical quantities such as mean and mean square values can be established by averaging and the outcome can be obtained with the help of the system transfer function and subsequently expressed in terms of its probability density function.

2.5.3 System Transfer Function

Frequency response functions give the complex amplitude of responses at one point caused by a unit amplitude of excitation at some other point. These complex frequency response functions are sometimes called system transfer functions. Or in other words, the frequency response function is the ratio of the output to the input under steady state conditions, with the input equal to a harmonic time function of unit amplitude.

Thus, in any linear system, there is a direct relationship between the input and the output. This relationship is true for random fluctuations as well.)

$$\text{Input} \times \text{System Transfer Function} = \text{Output}$$

This function may also be expressed as

$$A(\omega) \times H(\omega) = B(\omega)$$

where $A(\omega)$ and $B(\omega)$ are polynomials. If, only the force solution is taken into consideration, the impedance transform becomes

$$Z(\omega) = \frac{A(\omega)}{B(\omega)}$$

and its reciprocal admittance transform is denoted by

$$H(\omega) = \frac{1}{Z(\omega)}$$

The admittance transform $H(\omega)$ is defined as the ratio in the subsidiary plane of the output over input with all the initial conditions equal to zero.

2.5.4 Narrow Band Random Process

The mean square spectral density of a stationary random process is a partial, though incomplete description of the process. This description is examined for two extreme cases. A wide band spectrum and a narrow band spectrum. For a narrow band normally distributed process, the average frequency of the oscillations, the probability distribution of the envelope and the probability distribution of the peaks are obtained.

The narrow band process depicted in Fig. 2.18 is stationary and random in nature. Its mean square spectral density $S(\omega)$ is useful only in a band or range of frequencies whose width is small in comparison to the magnitude of the center frequency of the band. In samples which represent such a process only a narrow range of frequencies appears. Narrow band processes are typically observed as the response variables where the excitation variables are wide band processes and the systems

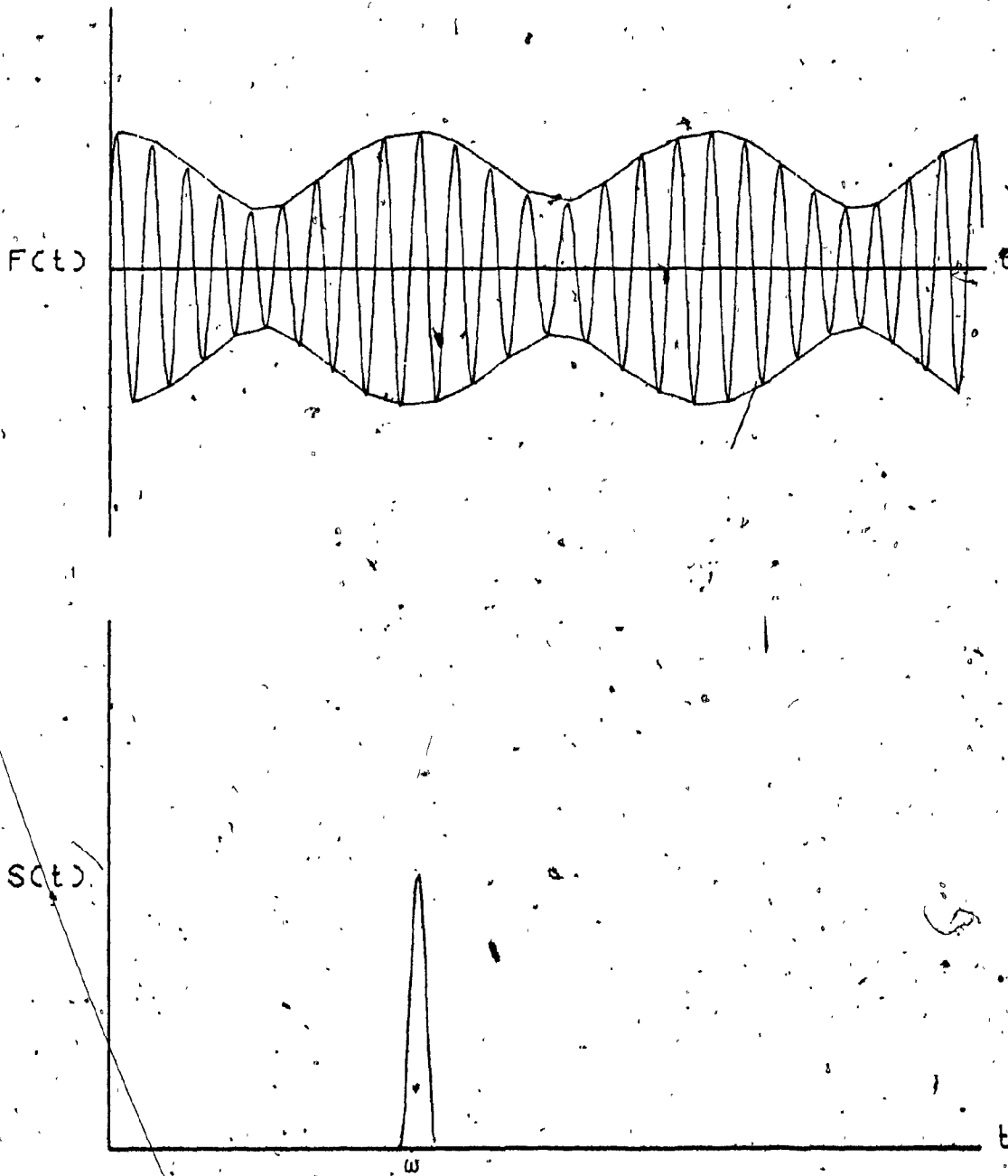


Fig. 2.18: Narrowband Record and its Spectral Density

are strongly resonant vibratory systems. The spectral density function is concentrated around the frequency of the instantaneous variation within the envelope. The spectral density is the contribution of the mean square value in the frequency interval $\Delta\omega$ divided by $\Delta\omega$. Mathematically, it is given as

$$S(\omega) = \lim_{\Delta\omega \rightarrow 0} \frac{\Delta(\bar{x}^2)}{\Delta\omega}$$

$S(\omega)$ is determined by squaring the output taking the average and then dividing by the frequency interval $\Delta\omega$.

2.5.5 Response of Gears to Random Vibration

Identification of an excitation (input) or of a response (output) is possible. The excitation may be either a force history or a motion (i.e. displacement, velocity or acceleration) history. The response may be in the form of either a desired motion history or even a desired stress history. If the excitation is a random process in nature, then the response quantity will be a random process too. For a linear time invariant system, if the excitation is steady state and simple harmonic, then the response is also steady state, simple harmonic motion at the same frequency. The amplitude as well as the phase of the response, are both dependent on the frequency.

Gear vibrations are contained in frequencies which have a continuous distribution over a wide range. If $S(\omega)$ be the spectral density, i.e. $S(\omega)$ be the density of the mean square value in the interval $\Delta\omega$ at the frequency ω then [28]

$$S(\omega) = \frac{Y^2}{2\Delta\omega}$$

(2.5.1)

where, the transmission error $\gamma(t)$ is periodic, and is represented as

$$\gamma(t) = \gamma_0 \sin \omega t \quad (2.5.2)$$

The input spectral density of the displacement excitation is

$$S_X(\omega) = \frac{\gamma_0^2}{2\Delta\omega} \quad (2.5.3)$$

The frequency response function or transfer function $H(\omega)$ modifies the input excitation to yield the output response. Thus,

$$H(\omega) = \frac{\text{Output response}}{\text{Input excitation}}$$

or
$$H(\omega) = \frac{\text{Output stress}}{\text{Input displacement}}$$

$$= \frac{K_G Q_Y(\omega)}{\gamma_0} \quad (2.5.4)$$

where K_G a geometric shape factor [29]. If $S_S(\omega)$ be the spectral density of the response then, the input and response spectral density are related as

$$S_S(\omega) = |H(\omega)|^2 S_X(\omega) \quad (2.5.5)$$

The variance of the first derivative of stress and second derivative of stress with time are

$$\sigma_{\dot{S}}^2 = \int \omega^2 \cdot S_S(\omega) d\omega \quad (2.5.6)$$

$$\sigma_{\ddot{S}}^2 = \int \omega^4 \cdot S_S(\omega) d\omega \quad (2.5.7)$$

where σ is the rms value.

2.5.6 Failure Mechanism in Gears

When any mechanism, i.e. gear, ceases performing its desired function, then it is regarded as having failed. Several criteria have to be fulfilled to ensure the satisfactory performance of the gear. Gears are basically governed by the vibration environment, but other environmental factors such as temperature, pressure, radiation etc. often interact with vibration environment to change the fundamental cause of the failure mechanism.

Classification of failures can be according to the behavior of the gear (tooth) i.e. in the absence of failure due to vibration. The two classifications are (A) reversible and (B) irreversible depending upon whether or not the failure disappears with the removal of the excitation.

Failure of gears due to vibration depends on the level of vibration. The higher the level of vibration, the more probable is the chance of failure. In the case of stationary random vibration the most convenient measures of level are the mean and the mean square. If the mean is zero, there is simply the mean square or the root-mean-square level. The characteristics of a random process are thus indicated to some extent by these parameters. A stationary narrow band, Gaussian process can be completely described with the help of the mean square spectral density.

Accumulation of damage may also be the cause of failure. Depending upon the amplitude of the excursion, a finite amount of damage is produced by each excursion. When the incremental damage accumulated reaches unity, failure occurs.

2.5.7 Fatigue Failure

When a fluctuating stress history acts upon a gear tooth a number of small changes takes place. There is migration of dislocations, localized plastic deformation, microscopic cracks are created and there is slow growth of these cracks. Eventually, if the stress excursions are large enough, there is rapid growth of one of the cracks, and the material ruptures.

The mean S-N curve or fatigue curve makes it easier to understand the fatigue of gears. S is the fixed stress amplitude and N is the number of cycles until fracture. The fatigue curve is not a single curve. To be more precise, it is the mean of the statistical distribution of fatigue lives obtained for given stress amplitudes. To illustrate its application a representative S-N curve for materials is considered. This curve is approximated by a straight line when log S is plotted against log N which means that the S-N curve may be approximated by the equation

$$N S^b = c \quad (2.5.8)$$

where c is a constant dependent on the material.

It is a more difficult problem to predict fatigue failure when the stress is a random process instead of the fixed amplitude fluctuation. According to the Palmgren-Miner hypothesis when n cycles of stress amplitude S have been experienced, the material has "used up" a fraction of its fatigue life equal to n/N where N is the number of cycles at which failure occurs under uniform amplitude S as predicted by the S-N curve. It is assumed that at this stress level, the fractional damage can be added to the corresponding fractional damages of other stress levels to

obtain the total damage experienced. Thus for n_i cycles of stress amplitudes S_i for $i = 1, 2, \dots$ the total cumulative damage fraction is taken as

$$D = \sum_i \frac{n_i}{N_i} \quad (2.5.9)$$

According to the Palmgren-Miner hypothesis when, D reaches the value of unity, fatigue failure occurs. This hypothesis places no restriction with regard to the order of application of the various stress levels. Hence, it is applicable to random processes in which there is a cycle-to cycle change in the stress amplitude. In accordance with this hypothesis, an incremental damage can be ascribed to each cycle. If these damages are accumulated, it leads to a total damage $D(\Delta T)$ for a time interval ΔT . As ΔT is increased the damage $D(\Delta T)$ increases monotonically. At some time ΔT_f , the total damage reaches the value unity and failure occurs.

Using a model developed in [30], the expected damage accumulated in a time interval ΔT_i is found to be

$$E[D(\Delta T_i)] = \Delta T_i \frac{1}{\pi} \left(\frac{\sqrt{2}}{C} \sigma_s \right)^\theta \Gamma \left(\frac{\theta}{2} + 1 \right) \left(\frac{\sigma_s}{\sigma_s'} \right)^{\theta-1} \quad (2.5.10)$$

The time failure i.e. when $E[D(\Delta T_i)] = 1$ may be evaluated from Equation (2.5.10).

Lin [31] showed that for stationary Gaussian processes with zero mean, the expected number of peaks is

$$E[N_p] = \frac{1}{2\pi} \frac{\sigma_s''}{\sigma_s'} \quad (2.5.11)$$

The expected number of peaks is found corresponding to the expected number of cycles. Thus, for complete failure of the tooth the total number of cycles (L) required is

$$L = E[N_p] \Delta T_i \quad (2.5.12)$$

Studies were also conducted to investigate the difference in gearing life, if there is variation in the transmission error or γ . Two separate cases were examined. In case I, the transmission error was independent of the speed of operation and in Case II, the transmission error was dependent on the speed. In the latter, the relationship between the transmission error and the speed of operation was

$$\gamma_o = \gamma_B e^{-\lambda\omega} \quad (2.5.13)$$

CHAPTER 3
RESULTS, CONCLUSIONS AND RECOMMENDATIONS
FOR FUTURE WORK

CHAPTER 3

ANALYSIS OF RESULTS, COMBUSTION AND

RECOMMENDATION FOR FUTURE WORK

3.1 Discussion of Results

In order to have an estimation of the span of life of a gear in a linear branched torsional system in a random loading environment, a number of calculations has been made. Through both deterministic and random approaches at different speeds, an idea of the working torque and useful life of gears was attained. The working torque and life of gears was estimated at different loading conditions by bringing about changes in the static angular transmission error at any particular speed of operation. Apart from these, an estimate of the span of working torque and useful life of gears has been calculated by taking the angular transmission error to be an exponentially decaying function of the speed of operation.

3.1.1 Effect of Error on Torque

Keeping λ constant at 0, γ_B was increased and the resultant value of the torque was observed at various speeds as seen in Figs. 3.1 to 3.4.

When γ_B is 0.00001, it is observed from Fig. 3.1 that initially, with increase in speed from 200 rad/sec there is a gradual increase in torque. Then suddenly a steep rise occurs above 400 rad/sec and the torque reaches its peak value (1600 lb-in) at 600 rad/sec near the second natural frequency. After this, as the speed increases further, a steep decrease in torque is noted upto 800 rad/sec. When speed becomes even greater (above 800 rad/sec) a gradual increase in torque is observed.

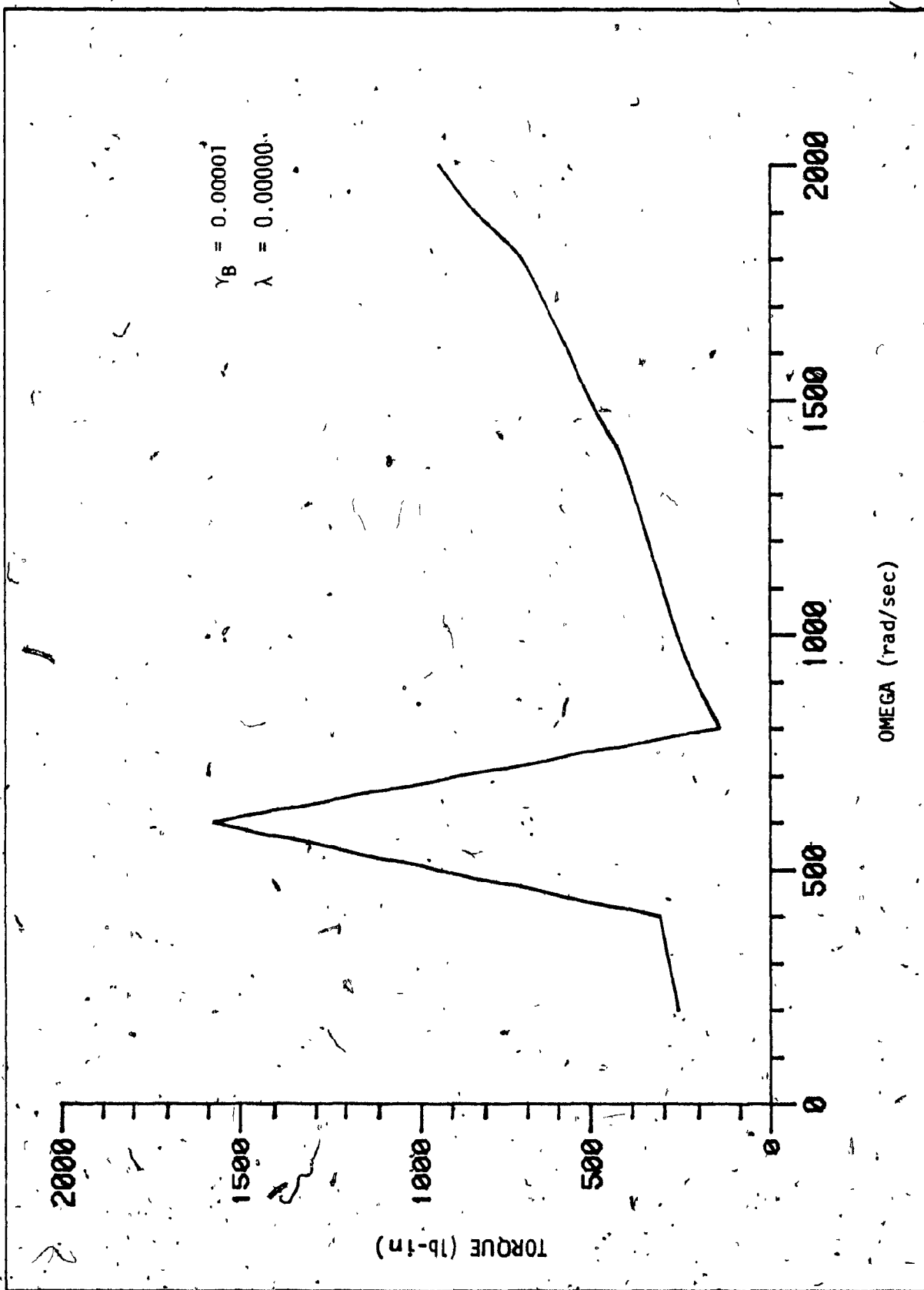


Fig. 3.1: Variation of Torque Versus Speed for $\gamma_B = 0.00001$, and $\lambda = 0$

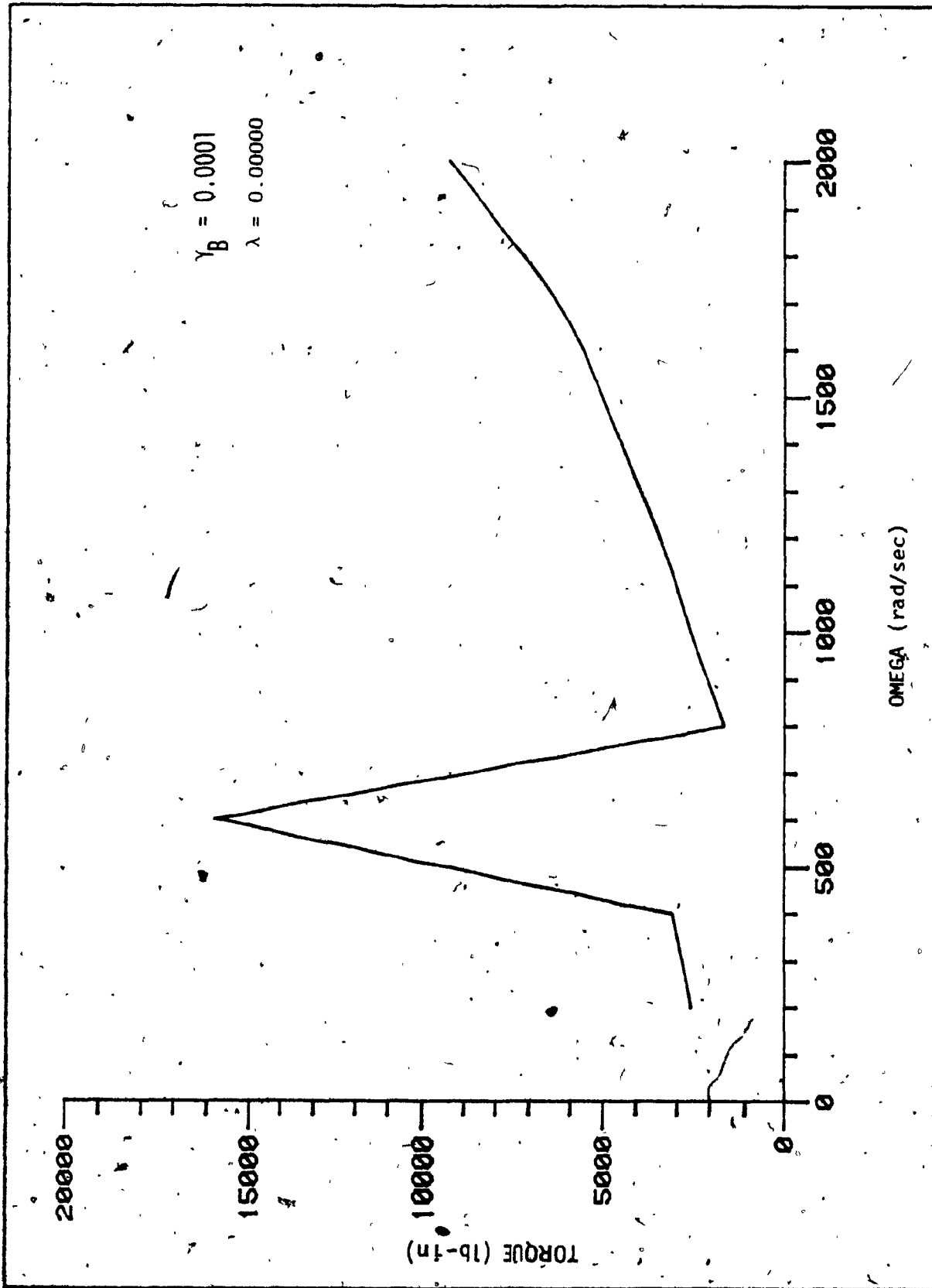


Fig. 3.2: Variation of Torque Versus Speed for $\gamma_B = 0.0001$ and $\lambda = 0$

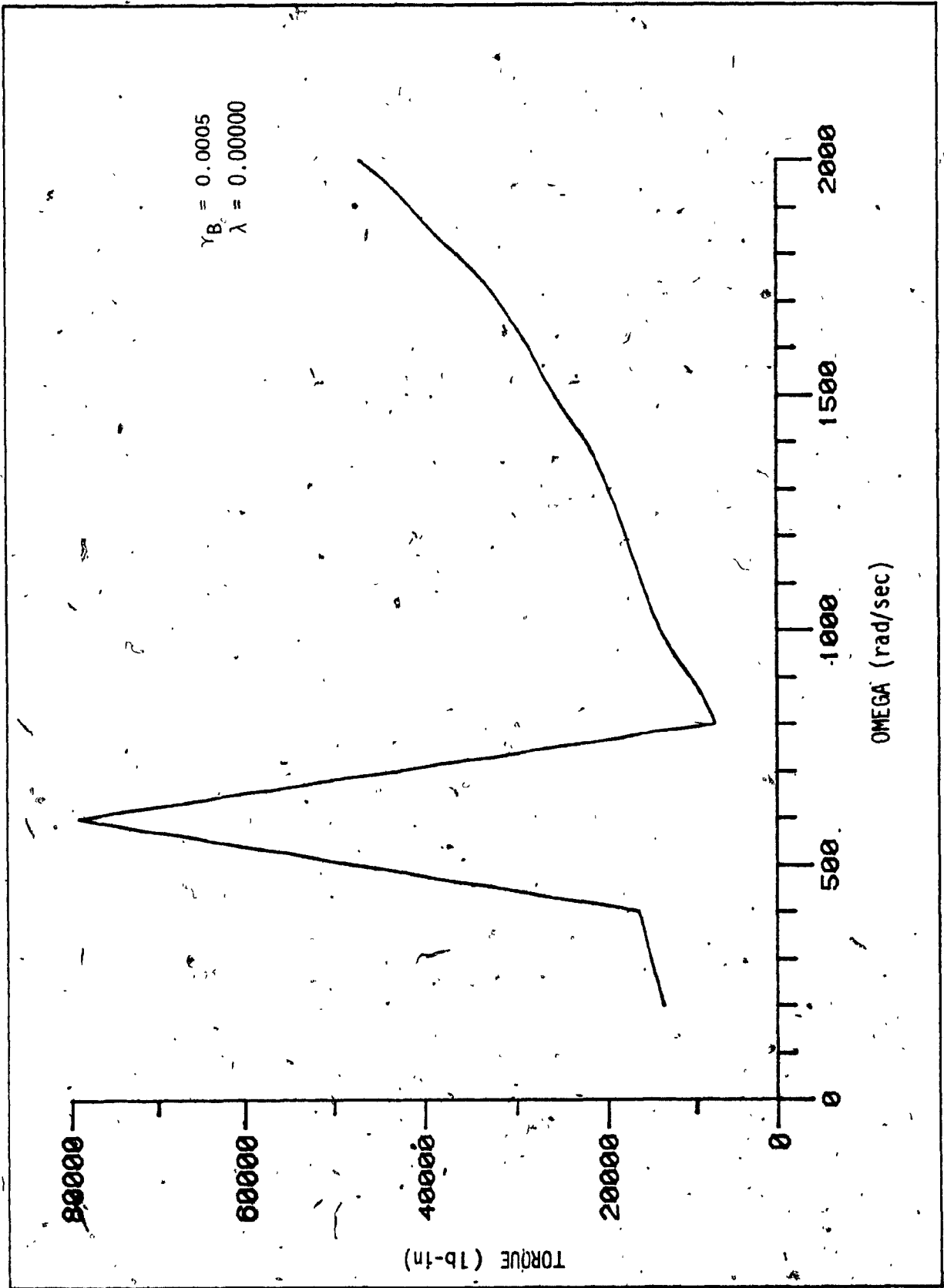


Fig. 3.3: Variation of Torque Versus Speed for $\gamma_B = 0.0005$ and $\lambda = 0$

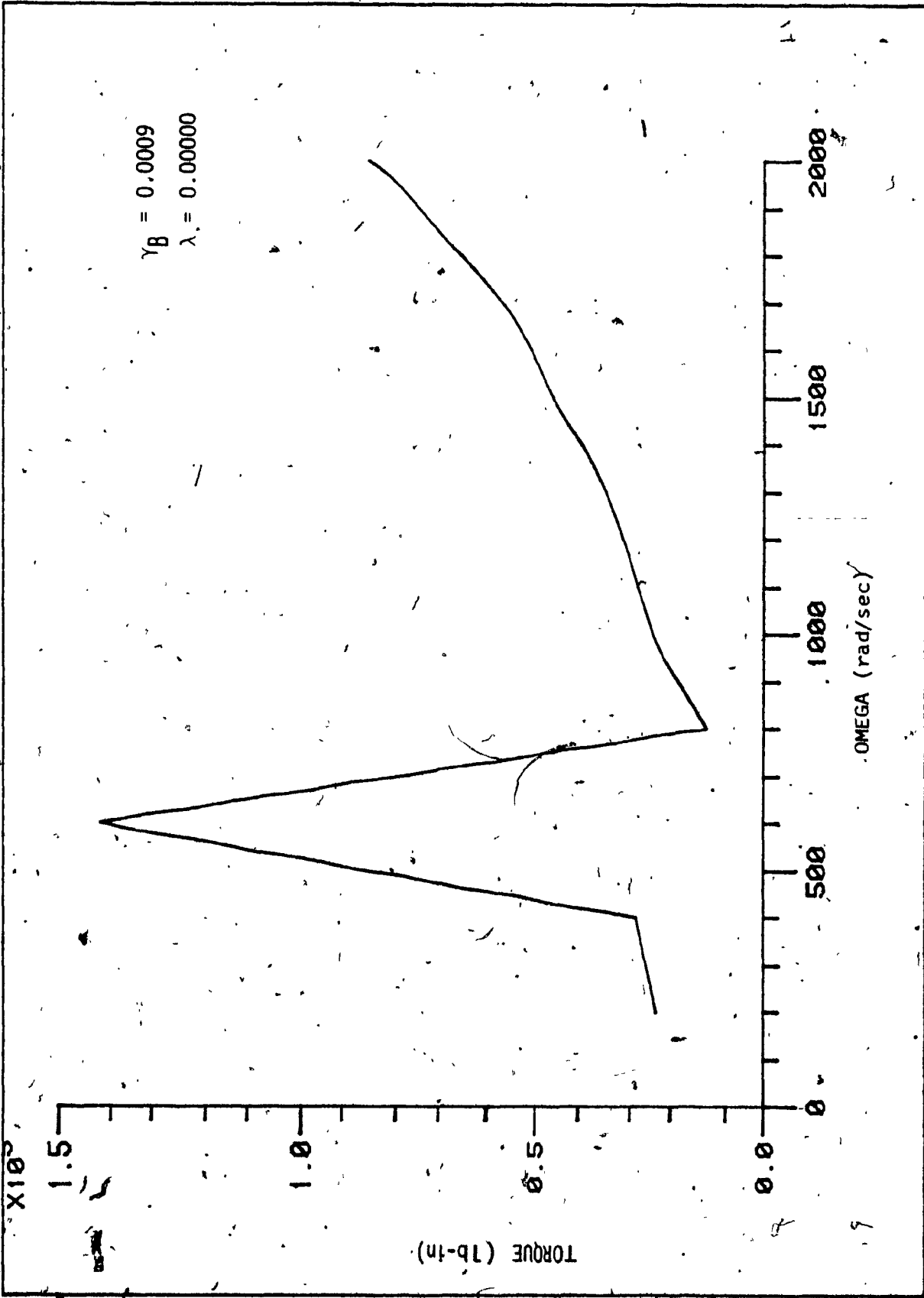


Fig. 3.4: Variation of Torque Versus Speed for $\gamma_B = 0.0009$ and $\lambda = 0$

A similarity in the nature of the curve is observed in Figs. 3.2 to 3.4 when γ_B is 0.0001, 0.0005 and 0.0009 respectively. The peak value of torque obtained for $\gamma_B = 0.0001$ was 16000 lb-in and for $\gamma_B = 0.0005$ it was 80,000 lb-in for $\gamma_B = 0.0009$ it was 150,000 lb-in.

Figure 3.5 shows the variation of torque with speed for $\gamma_B = 0.00001$ and $\lambda = 0.00008$. From 200 rad/sec to 400 rad/sec a steady but slow rise is observed in the corresponding torque. There is an abrupt and steep rise in torque when the rotational speed increases from 400 rad/sec to 600 rad/sec, followed by an equally abrupt fall from 600 rad/sec to 800 rad/sec. Thus the peak value of torque is approximately 1500 lb-in at 600 rad/sec near the second natural frequency. Above 800 rad/sec, there is once again a gradual and steady rise in the value of torque corresponding to the increase in speeds. Figs. 3.6 to 3.8 exhibit the same nature of the curve, γ_B being 0.0001, 0.0005 and 0.0009 respectively. The peak value of torque is approximately 1500 lb-in, 15000 lb-in, 75000 lb-in and 140,000 lb-in as in evident form Figs. 3.5 to 3.8 at 600 rad/sec.

In the third set of calculations shown in Figs. 3.9 to 3.12, λ is kept constant at 0.0007 while the values of γ_B are 0.00001, 0.0001, 0.0005 and 0.0009 respectively. As seen in all four figures from 200 rad/sec there is a slow rise up to 400 rad/sec, much slower than in the previous case. Again there is a steep and sudden increase in the value of torque from 400 rad/sec to 600 rad/sec. The peak values of torque in Figs. 3.9 to 3.12 are 1000 lb-in, 10000 lb-in, 50000 lb-in and 90000 lb-in respectively at 600 rad/sec near the second natural frequency. A sudden decrease in the value of torque is now noticed with the increase in speed to 800 rad/sec and torque reaches its minimum

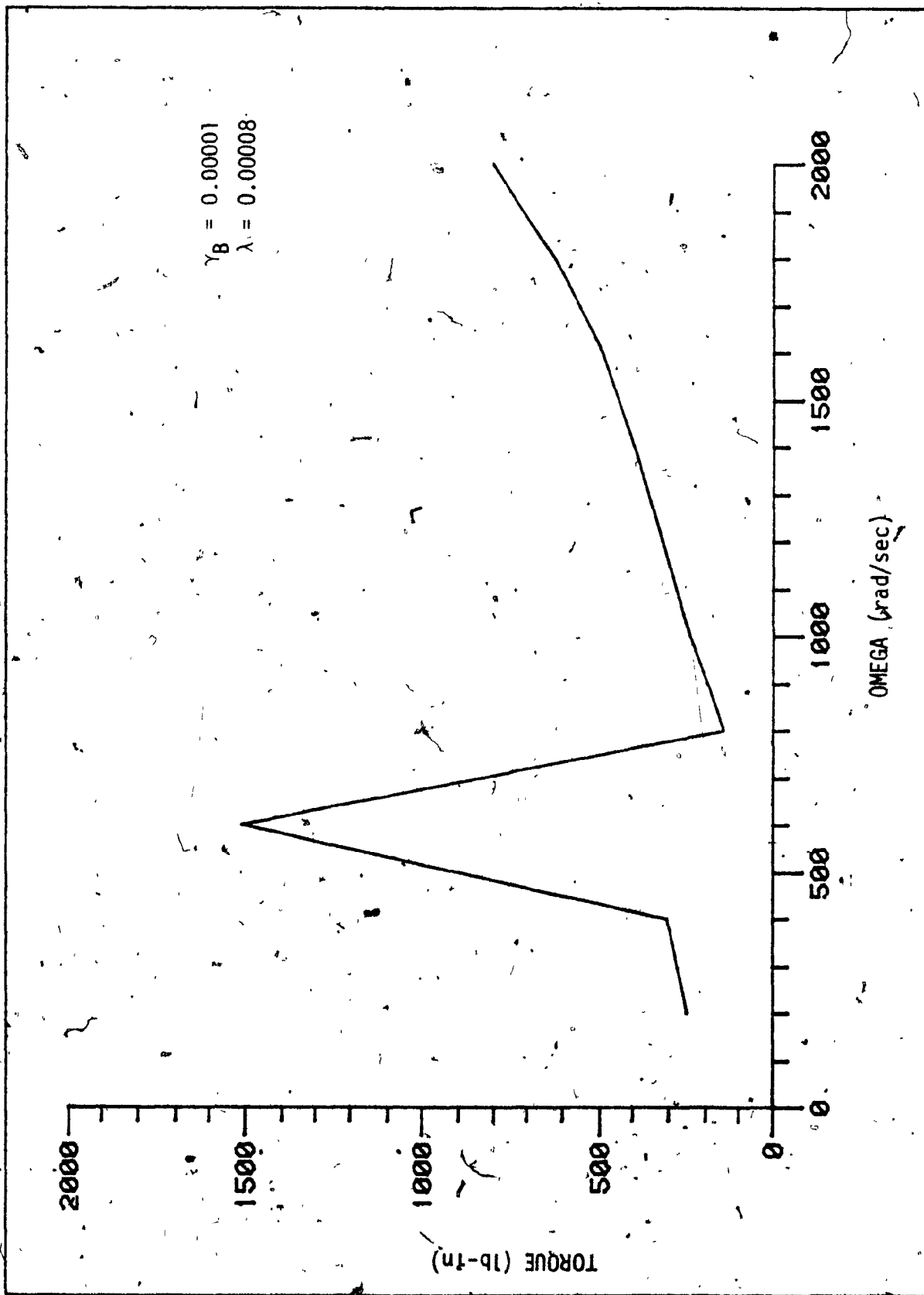


Fig. 3.5: Variation of Torque Versus Speed for $\gamma_B = 0.00001$ and $\lambda = 0.00008$

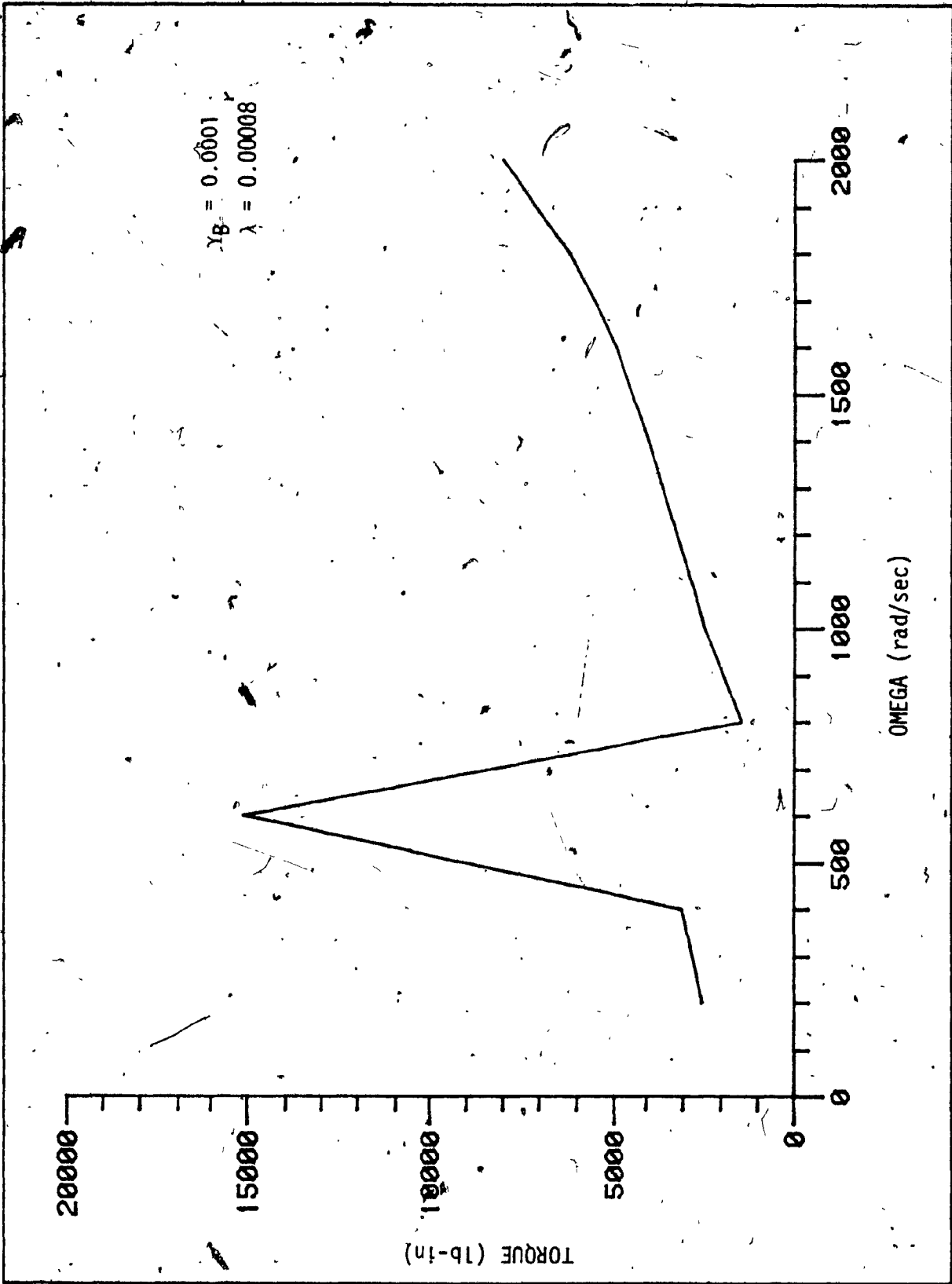


Fig. 3.6: Variation of Torque Versus Speed for $\gamma_B = 0.0001$ and $\lambda = 0.00008$

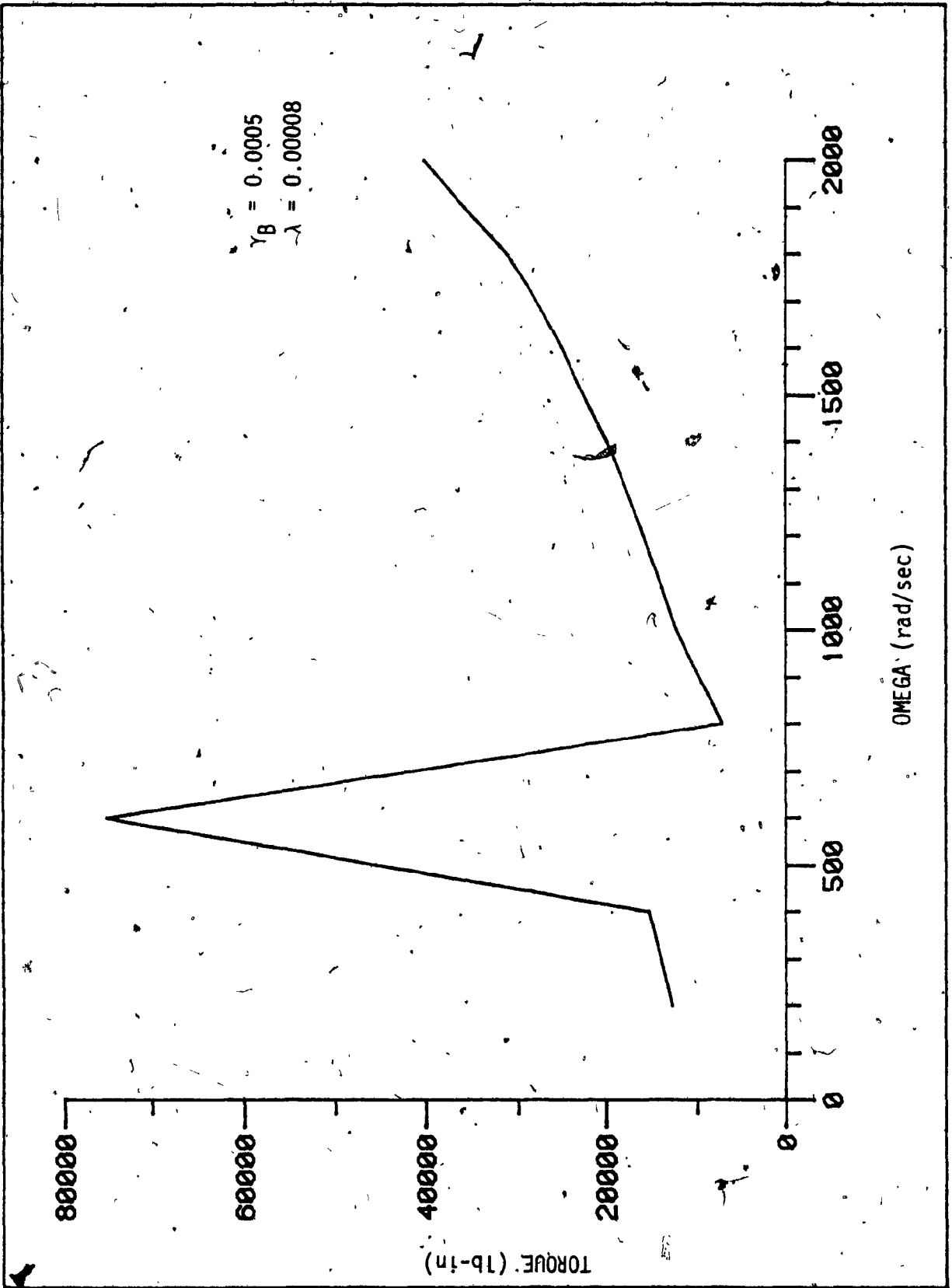


Fig. 3.7: Variation of Torque Versus Speed for $\gamma_B = 0.0005$ and $\lambda = 0.00008$

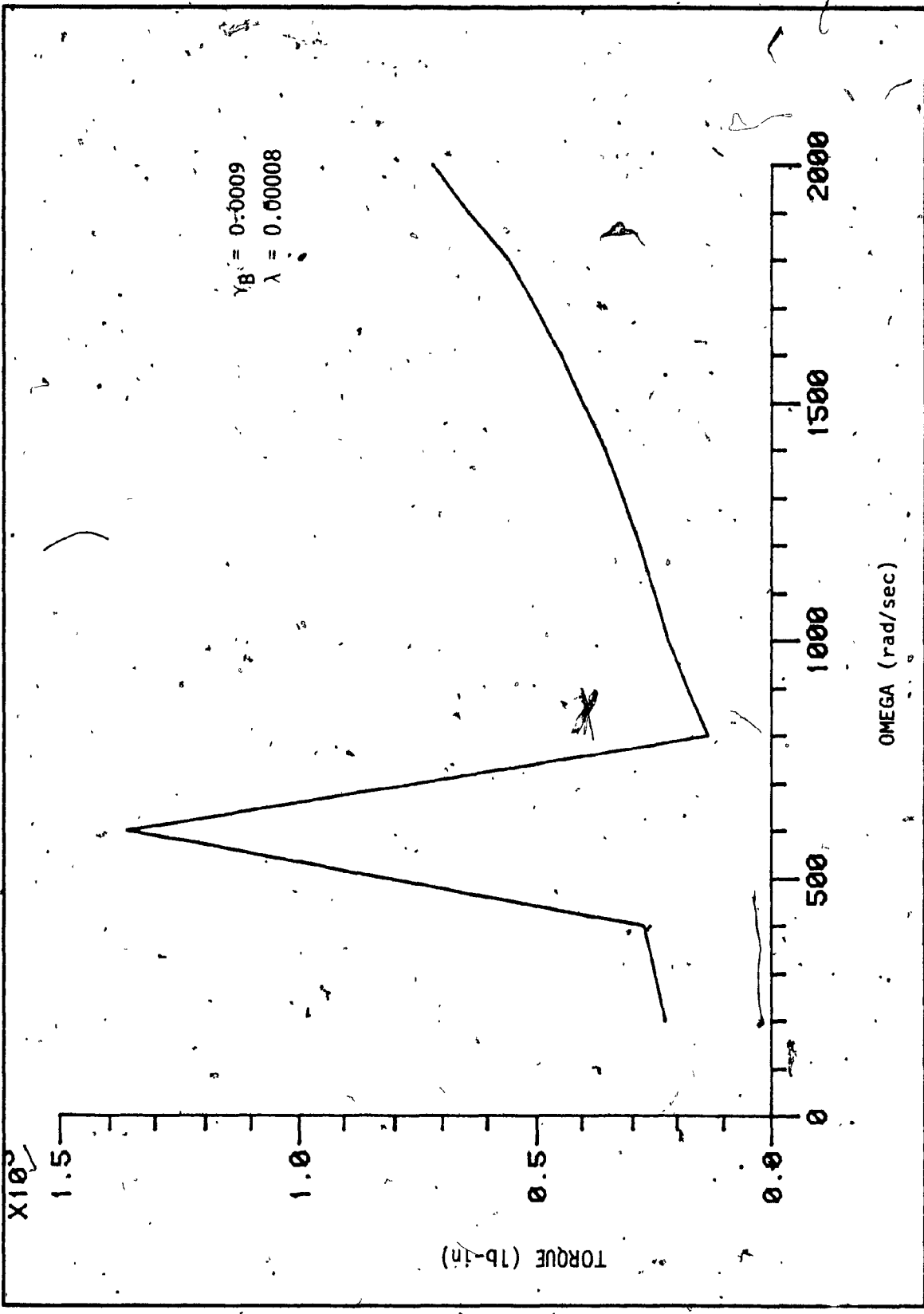


Fig. 3.8: Variation of Torque Versus Speed for $\gamma_B = 0.0009$ and $\lambda = 0.00008$

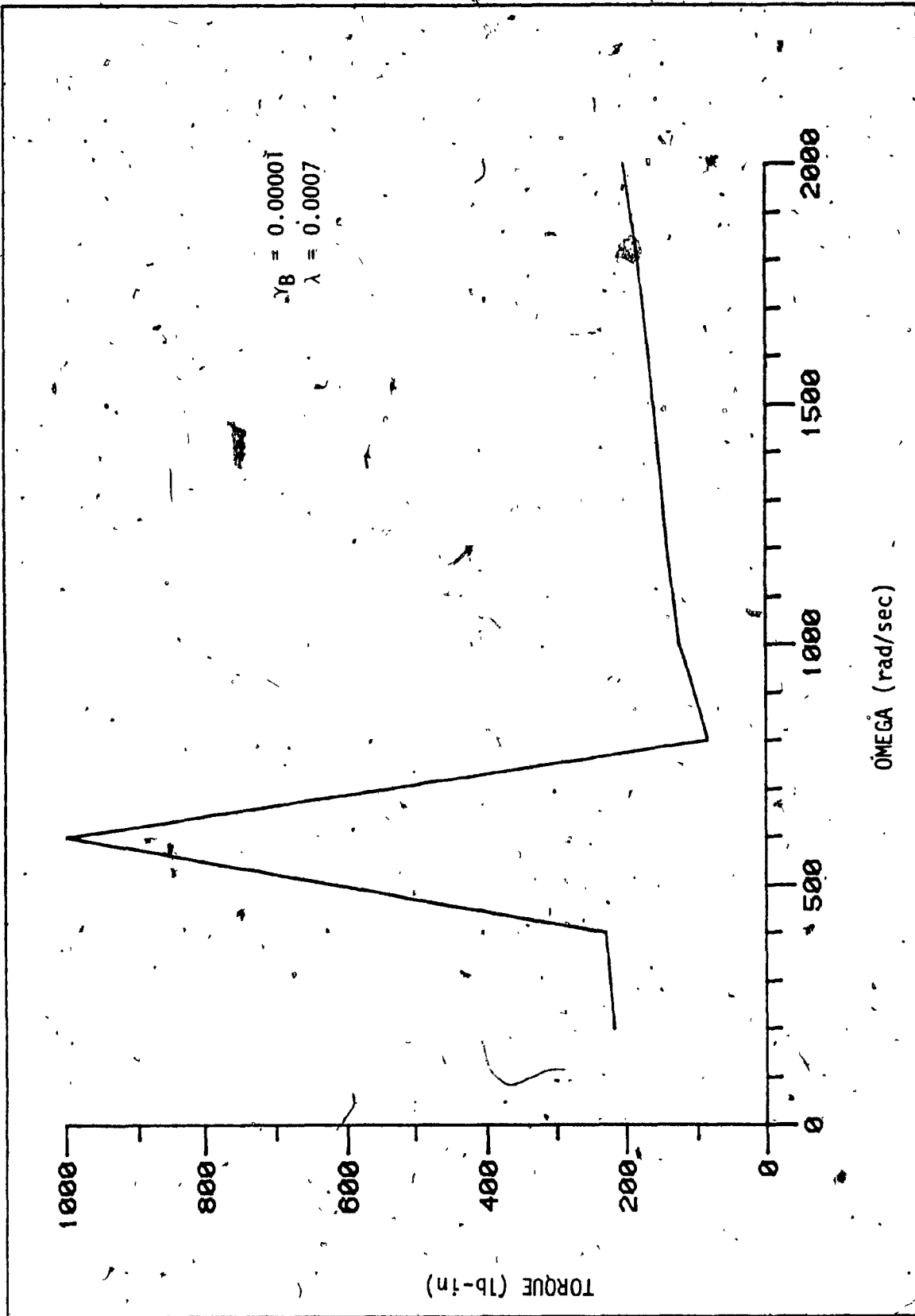


Fig. 3.9: Variation of Torque Versus Speed for $\gamma_B = 0.00001$ and $\lambda = 0.0007$

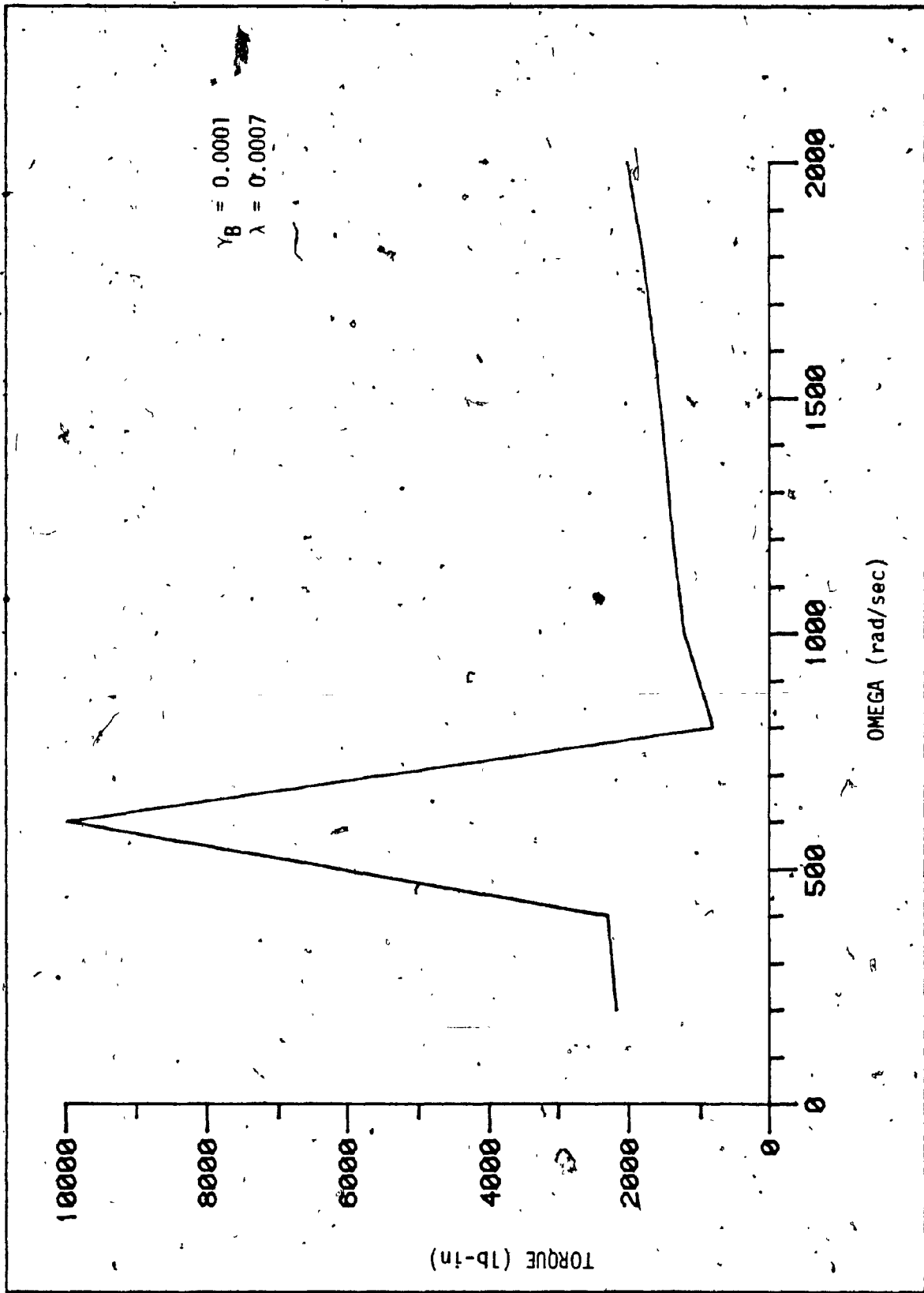


Fig. 3.10: Variation of Torque Versus Speed for $\gamma_B = 0.0001$ and $\lambda = 0.0007$

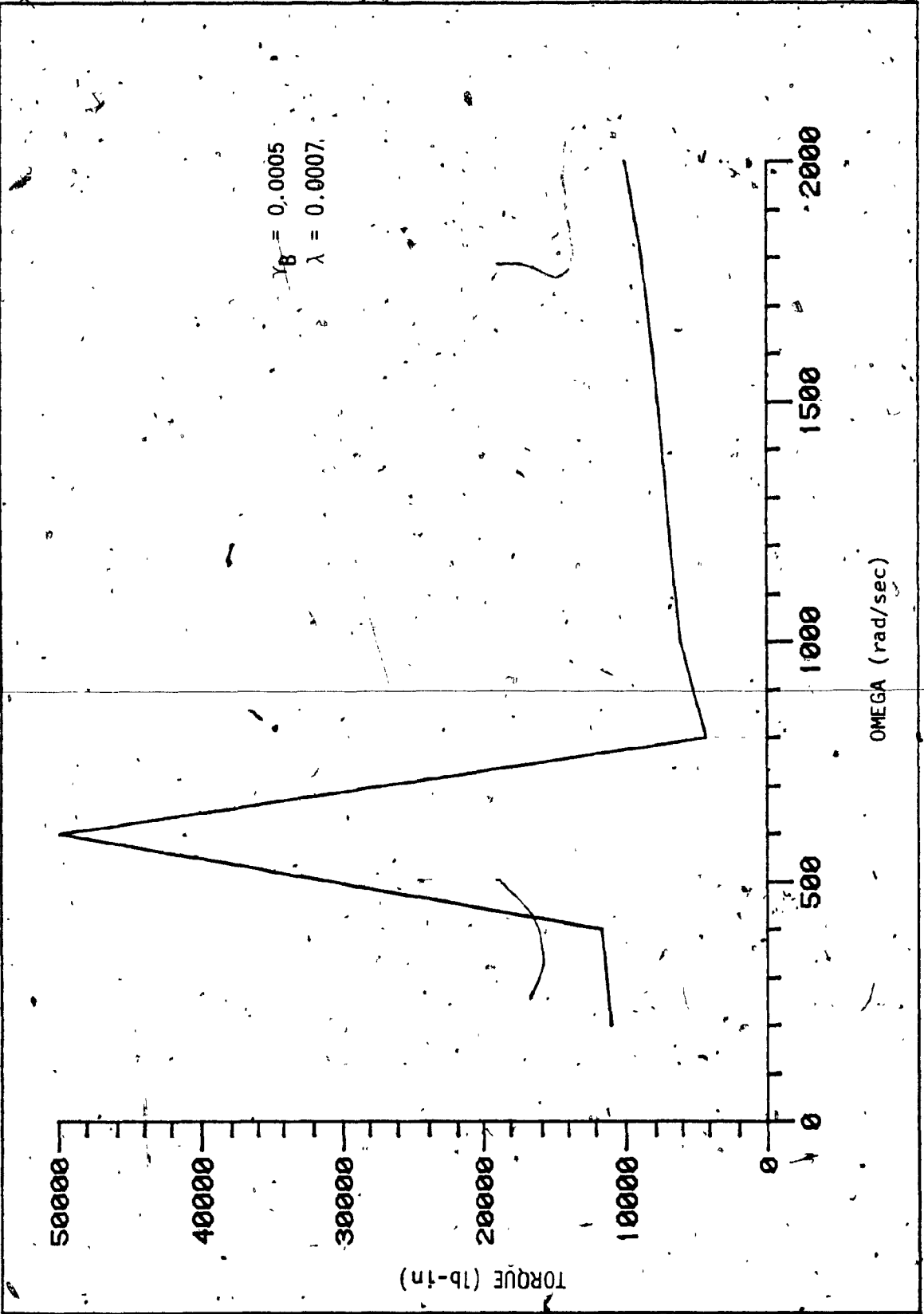


Fig. 3.11: Variation of Torque Versus Speed for $\gamma_B = 0.0005$ and $\lambda = 0.0007$

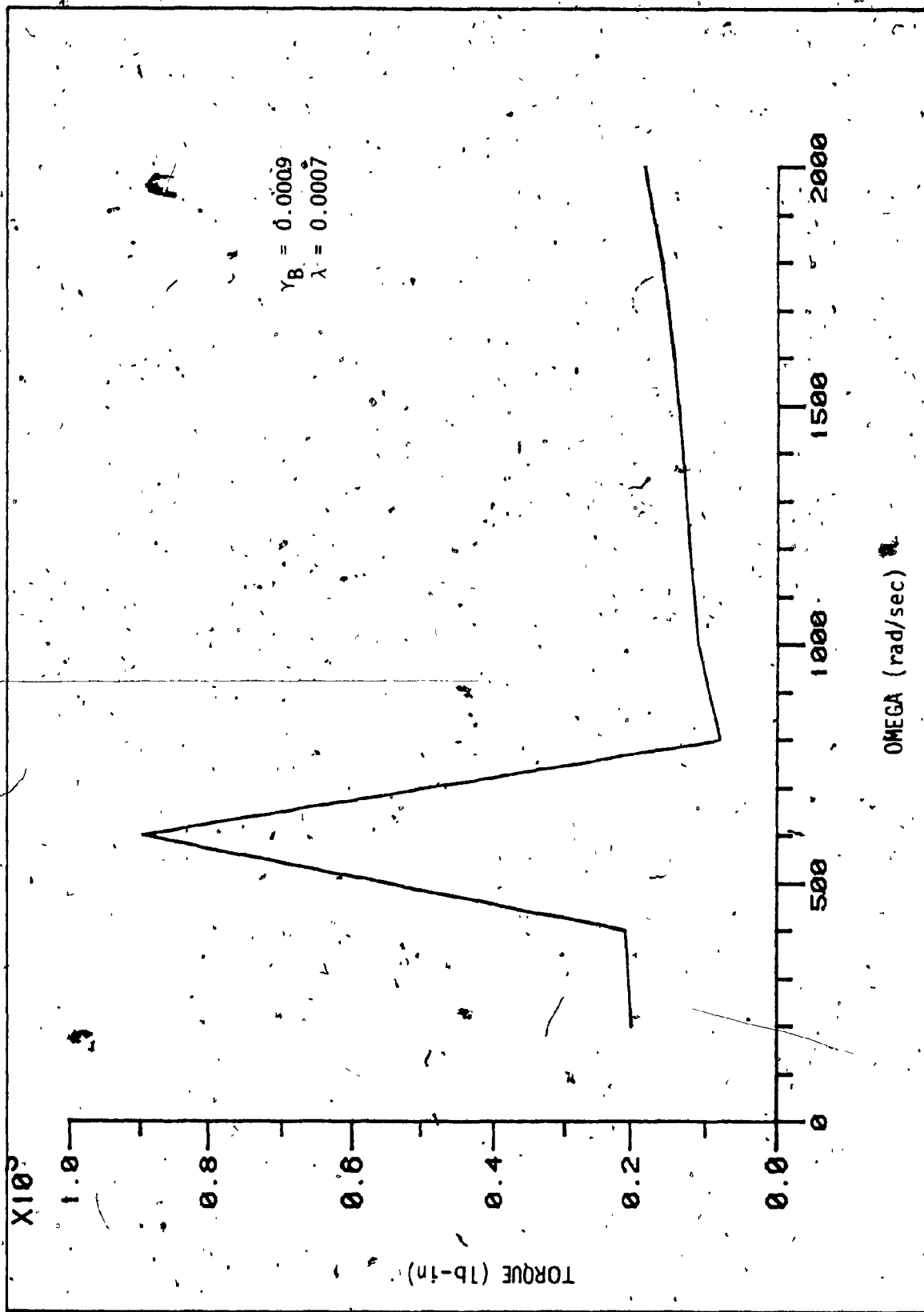


Fig. 3.12: Variation of Torque Versus Speed for $Y_B = 0.0009$ and $\lambda = 0.0007$

value at this speed, in all four figures. Following this abrupt decrease, there is a gradual increase in the value of torque when speed further increases past 800 rad/sec. But this increase is very slow, far slower than in the previous cases.

Hence, from observations of all the four cases, one may conclude that the value of torque is in direct proportion to the increase in error (λ_B). If the error (λ_B) increases there is a corresponding increase in the value of torque.

It is also observed that by keeping the error (γ_B) constant and increasing the values of λ , there is a corresponding decrease in the value of torque e.g. in the set of Figs. 3.1, 3.5 and 3.9, γ_B is constant at 0.00001, while λ increases from 0, to 0.00008 to 0.0007 respectively. A corresponding decrease in the peak torque can be noticed in these three figures from 1600 lb-in to 1500 lb-in to 1000 lb-in respectively. The same characteristics hold for the other values of error in the three remaining sets of Figs. 3.2, 3.6, 3.10 and 3.3, 3.7, 3.11 and 3.4, 3.8, 3.12. The values of error (γ_B) in these three sets is 0.0001, 0.0005 and 0.0009 respectively.

Thus, from the three cases described earlier, two salient points emerge, namely;

- 1) increase in error leads to a proportional increase in torque,
- 2) increase in the value of λ leads to a decrease in torque.

3.1.2 Effect of Error on Working Life of Gears

An estimate of the effect of the error γ on the working life of gears has been attempted through both the deterministic and random approaches. In the deterministic approach results were obtained for zero

mean load, for steady or mean load equal to the fluctuating load and lastly, for mean load equal to twice the fluctuating load.

Keeping λ constant at 0, four figures have been taken into consideration - 3.13 to 3.16 where γ_B varies, being 0.00001, 0.0001, 0.0005 and 0.0009 respectively. In Fig. 3.13 gearing life is observed to be minimum at 600 rad/sec near the second natural frequency, and maximum at 800 rad/sec between the second and third natural frequencies. The mean load does not have a significant effect on the working life. At all the frequencies, random life is less than the deterministic life. In Fig. 3.14 it is clear that at 600 rad/sec the working life of gear is a minimum for all values of mean load. A marked change is evident in Fig. 3.15 where the gear fails near the second natural frequency. However, the working life of the gear is maximum at 800 rad/sec between the second and third natural frequencies. It is also noted that at higher frequencies, the mean load has a significant effect on working life. When the mean load is equal to the fluctuating load, the gear will fail near 1700 rad/sec. If mean load is twice the fluctuating load, the gear will fail near 1300 rad/sec. In Fig. 3.16 whatever the working load, the gear fails before the second natural frequency. On higher speeds, it can be observed that its life is maximum at 800 rad/sec. The gear will fail at approximately 900 rad/sec when the mean load is twice the fluctuating load, at 1300 rad/sec when mean load is equal to fluctuating load; and at approximately 1800 rad/sec, even in the absence of the mean load, by the dynamic load produced by the gearing error. By random approach, the gear will fail at approximately 1600 rad/sec.

In the four Figs. 3.17 to 3.20, λ is constant at 0.00008 with values of γ_B of 0.00001, 0.0001, 0.0005 and 0.0008 respectively. The

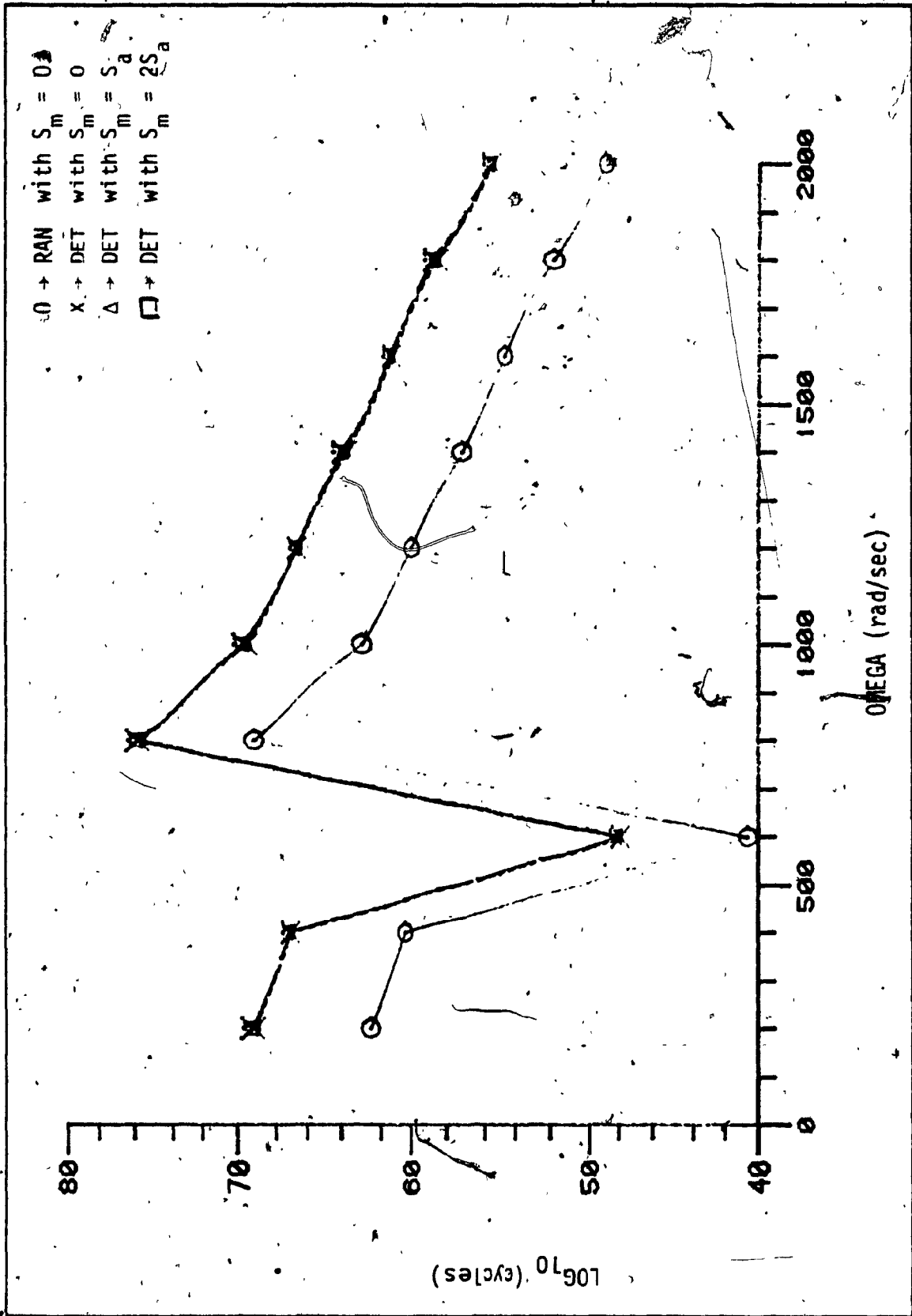


Fig. 3.13: Variation of Life Versus Speed for $\gamma_B = 0.00001$ and $\lambda = 0$.

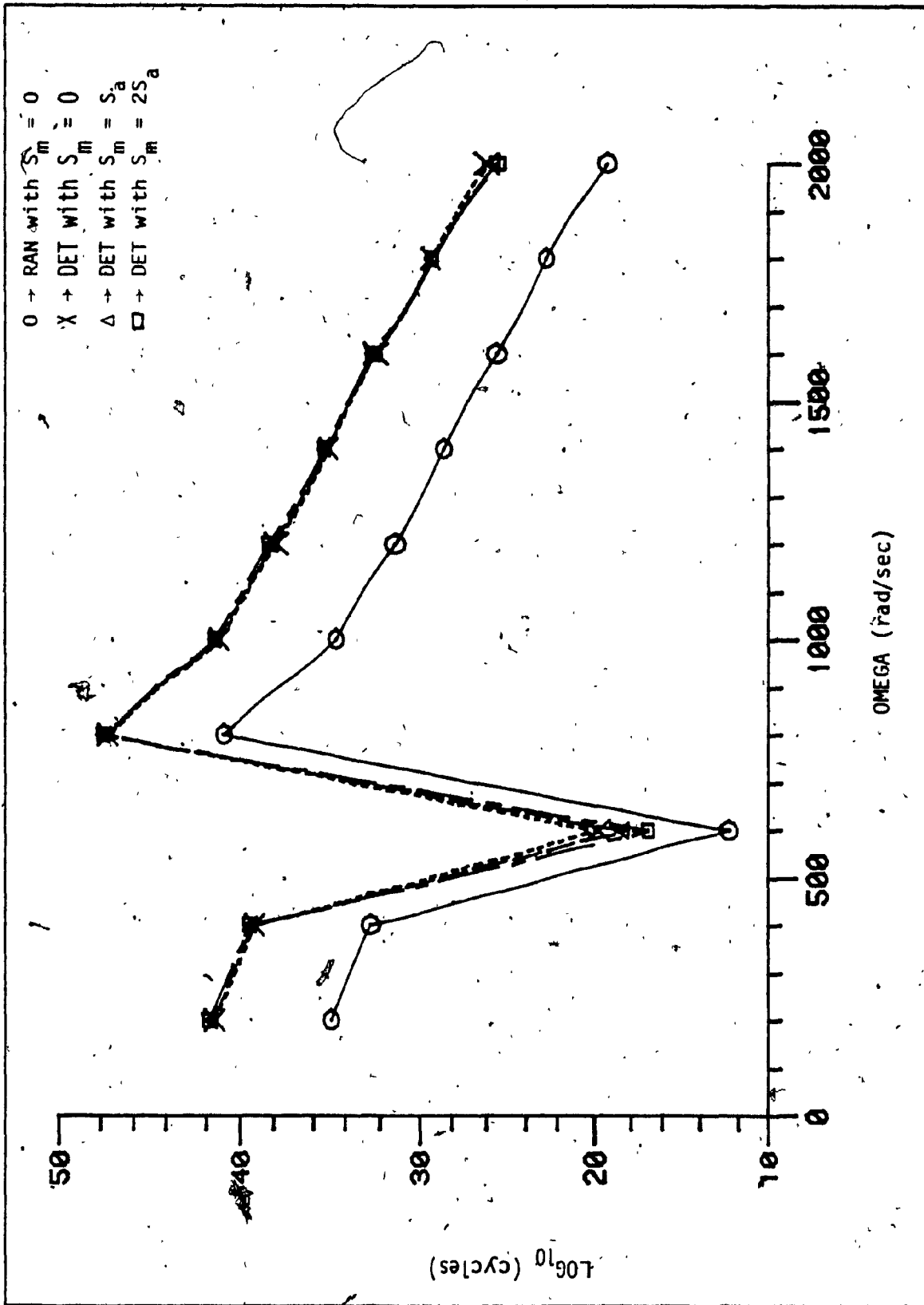


Fig. 3.14: Variation of Life Versus Speed for $\gamma_B = 0.0001$ and $\lambda = 0$

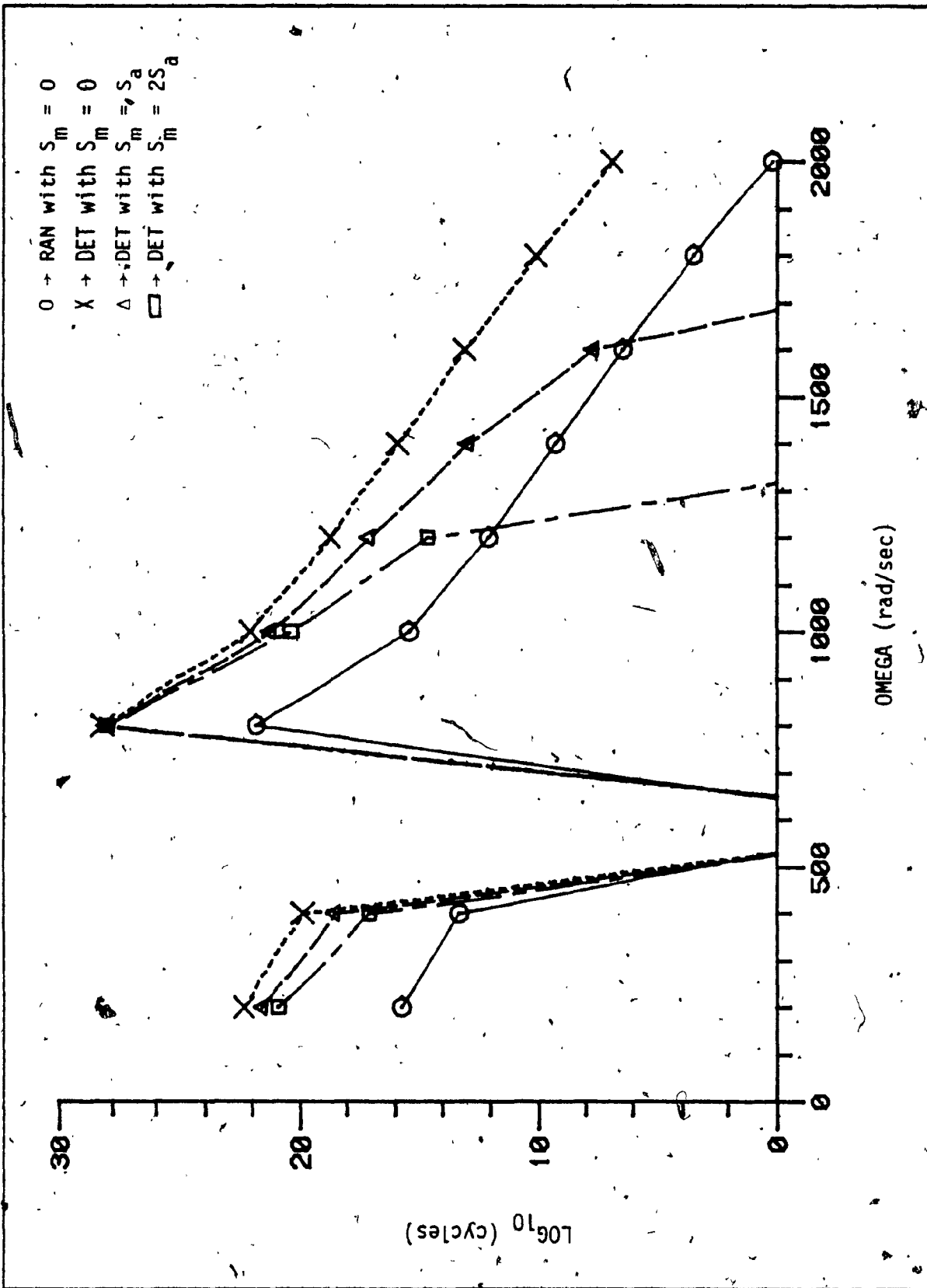


Fig. 3.15: Variation of Life Versus Speed for $\gamma_B = 0.0005$ and $\lambda = 0$

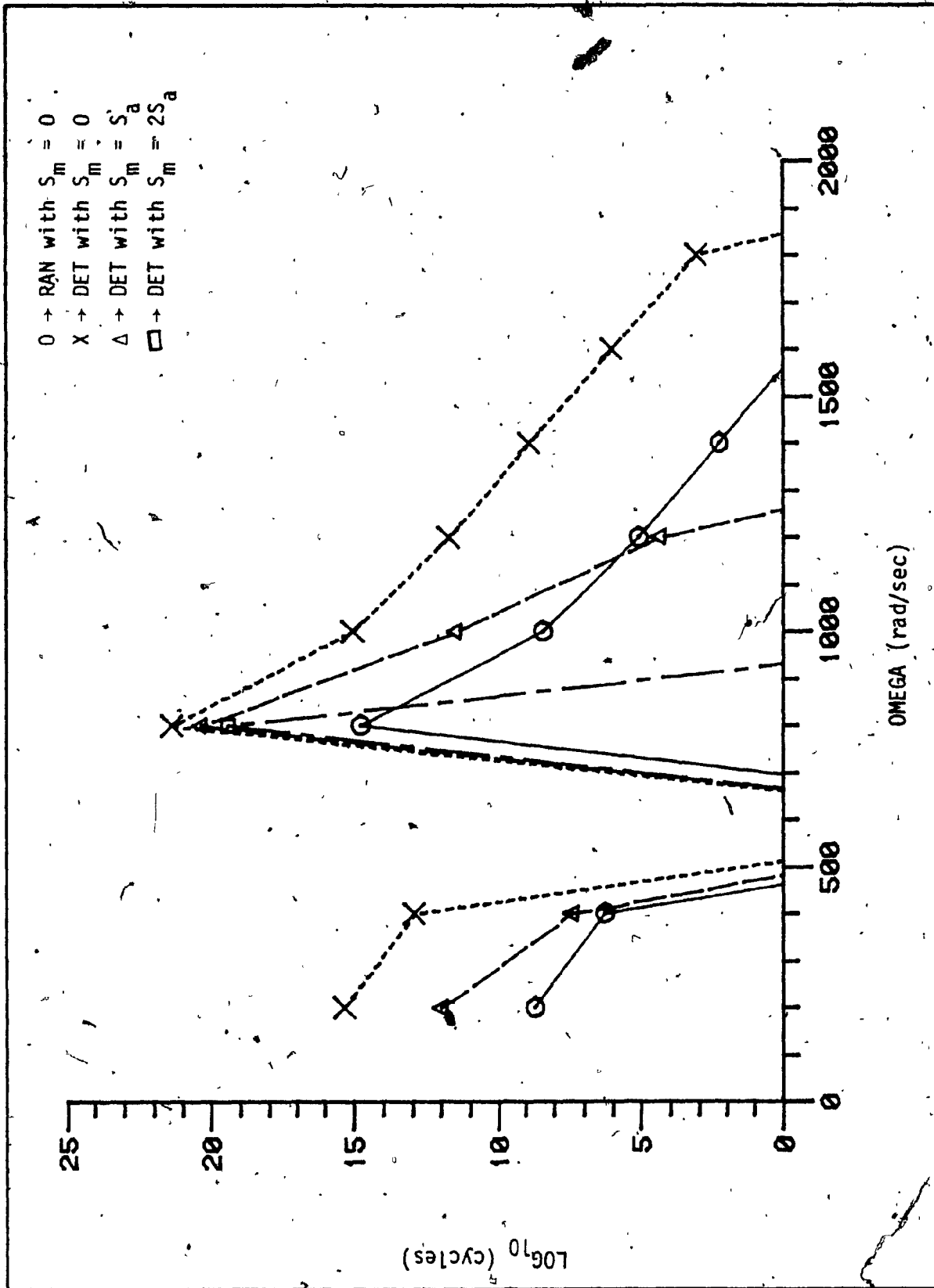


Fig. 3.16: Variation of Life Versus Speed for $\gamma_B = 0.0009$ and $\lambda = 0$

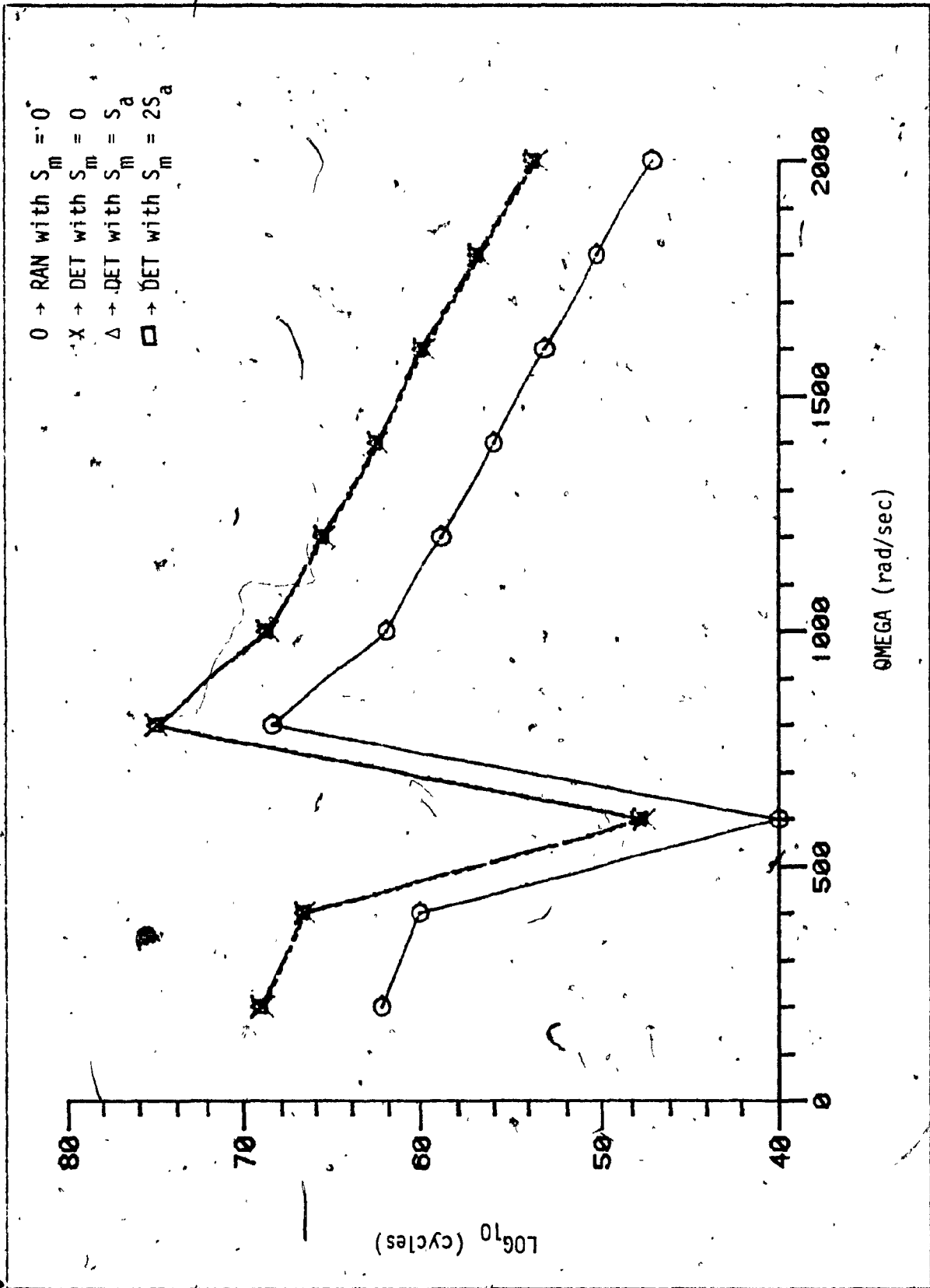


Fig. 3.17: Variation of Life Versus Speed for $\gamma_B = 0.00001$ and $\lambda = 0.00008$

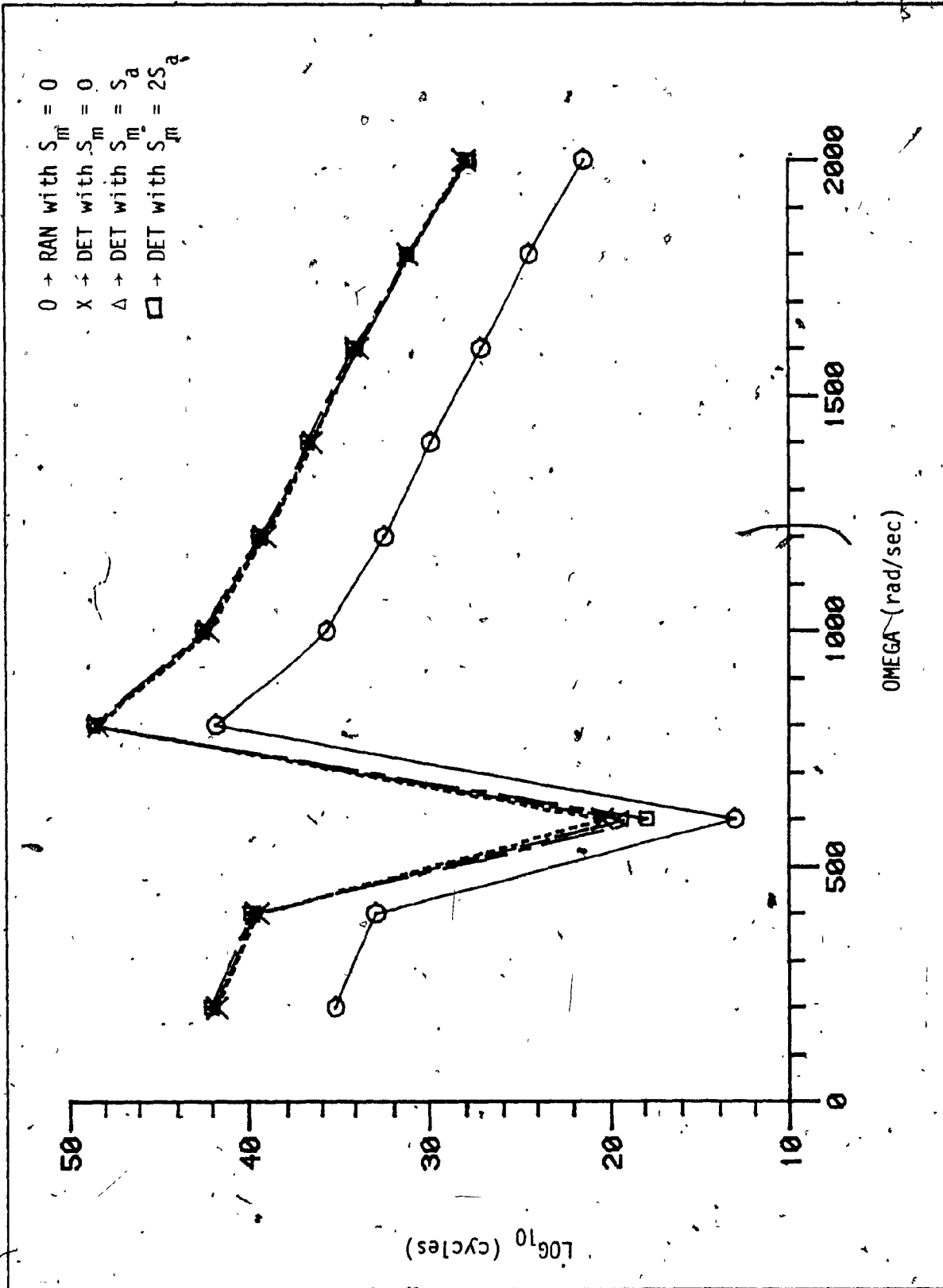


Fig. 3.18: Variation of Life Versus Speed for $\gamma_B = 0.0001$ and $\lambda = 0.00008$

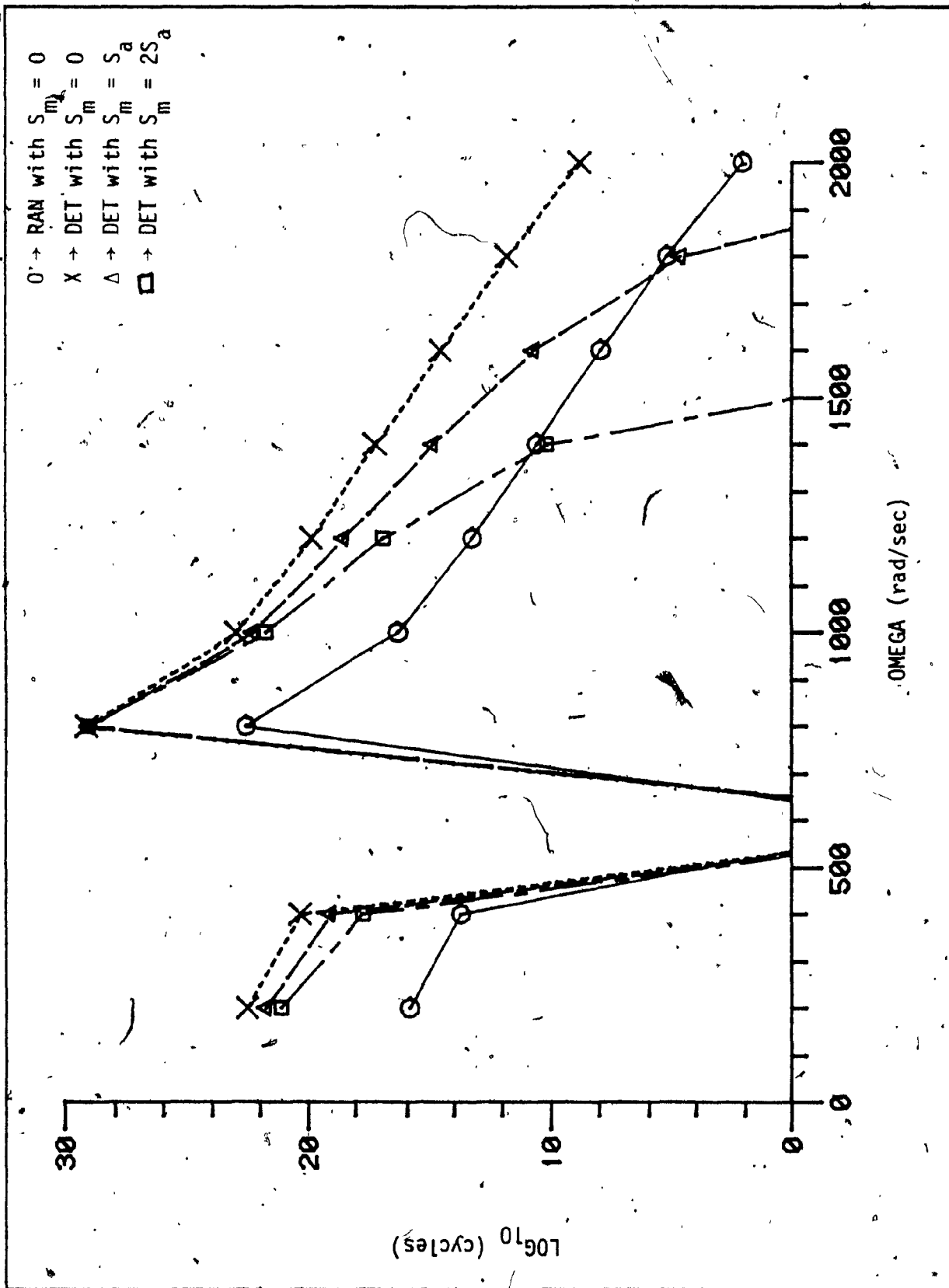


Fig. 3.19: Variation of Life Versus Speed for $\gamma_B = 0.0005$ and $\lambda = 0.00008$

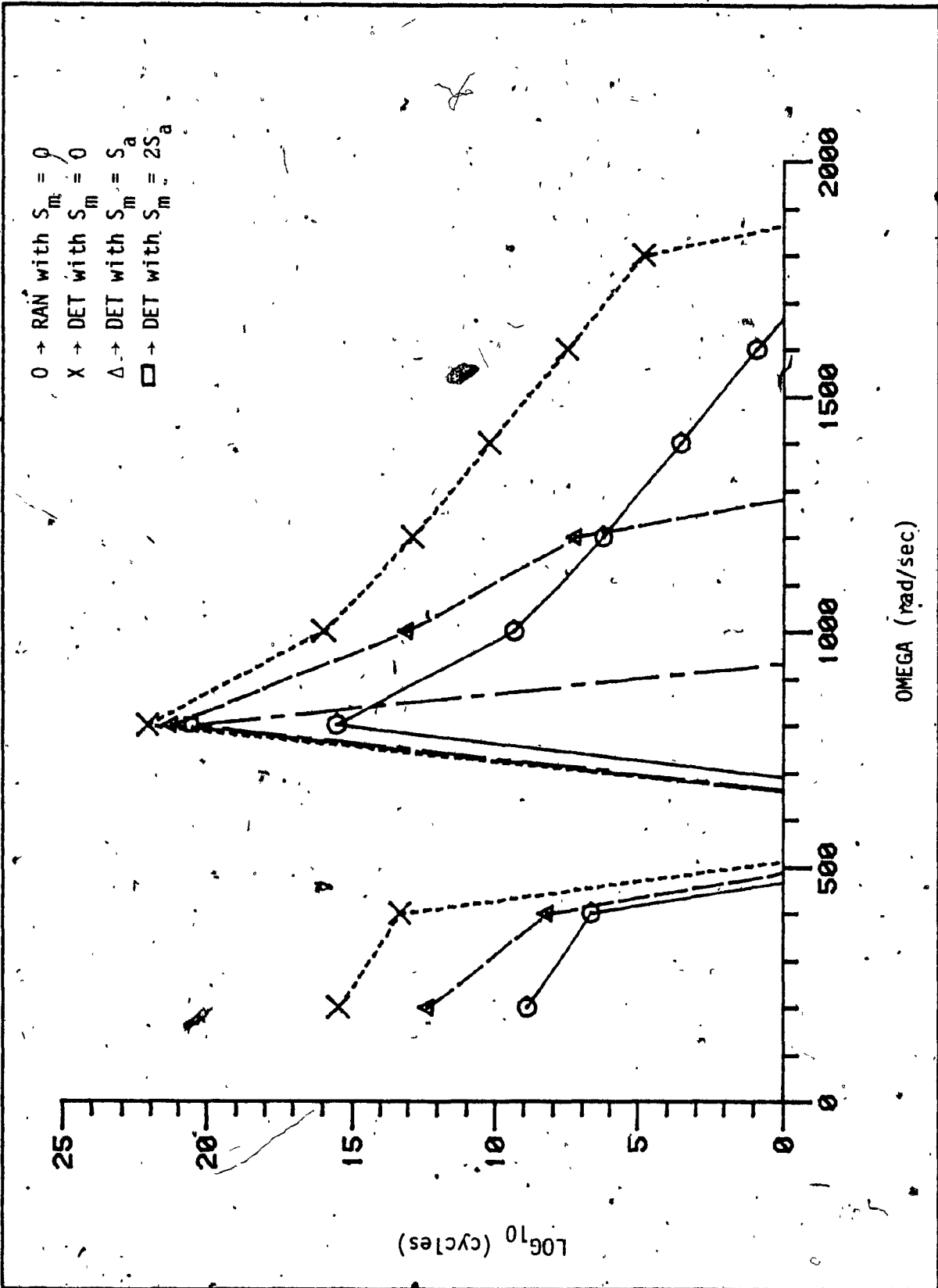


Fig. 3.20: Variation of Life Versus Speed for $\gamma_B = 0.0009$ and $\lambda = 0.00008$

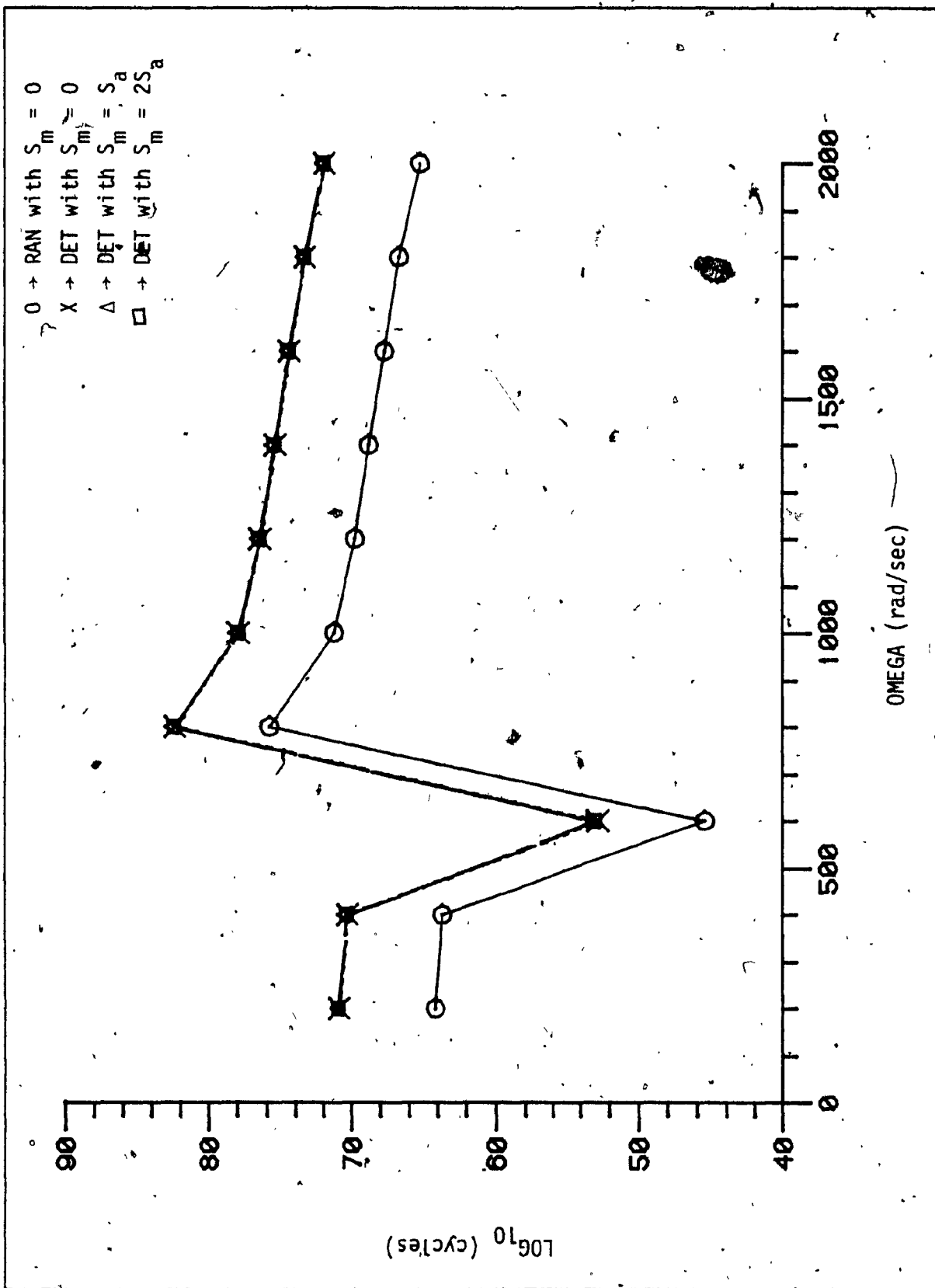


Fig. 3.21: Variation of Life Versus Speed for $\gamma_B = 0.00001$ and $\lambda = 0.0007$

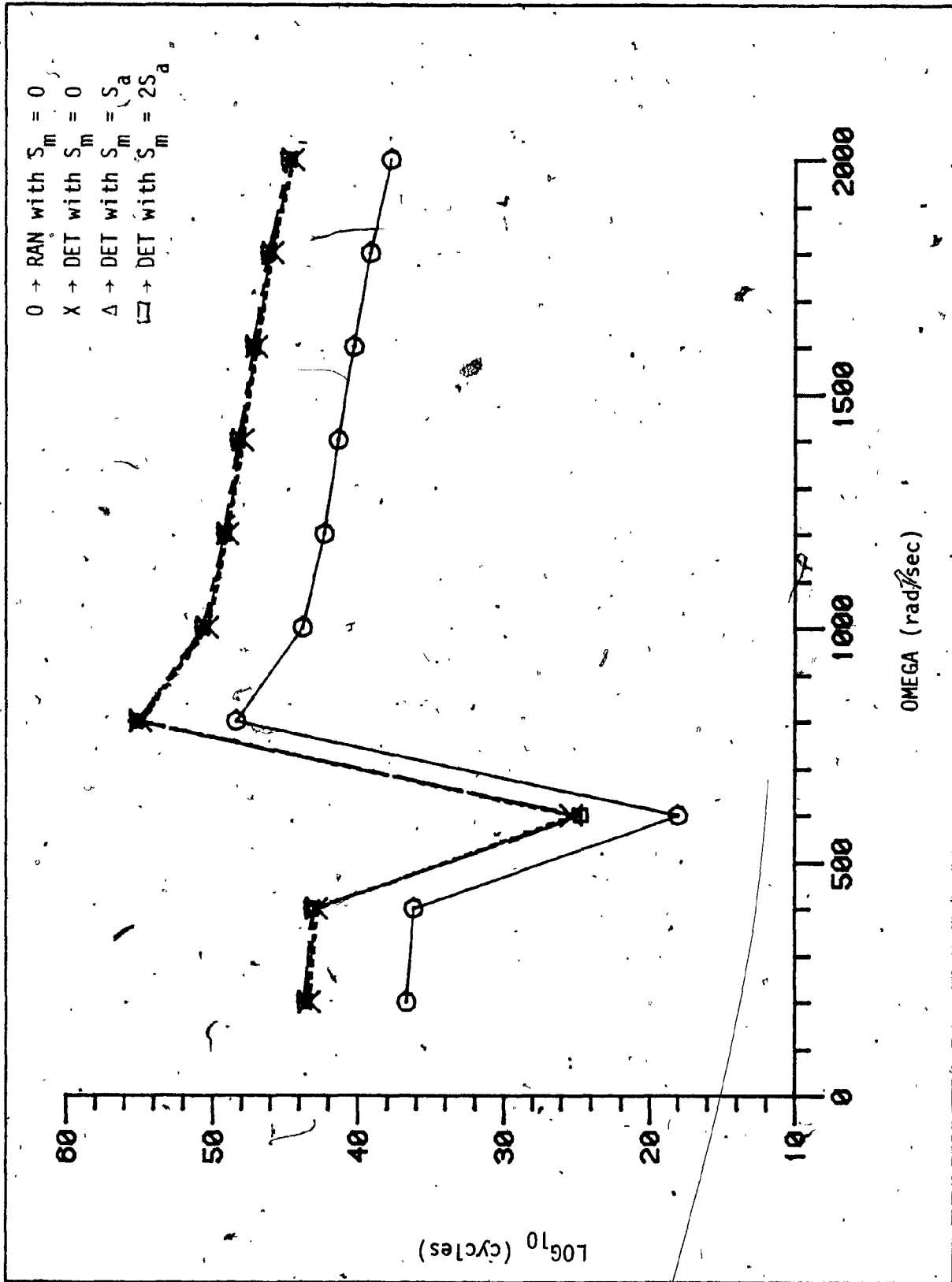


Fig. 3.22: Variation of Life Versus Speed for $\gamma_B = 0.0001$ and $\lambda = 0.0007$

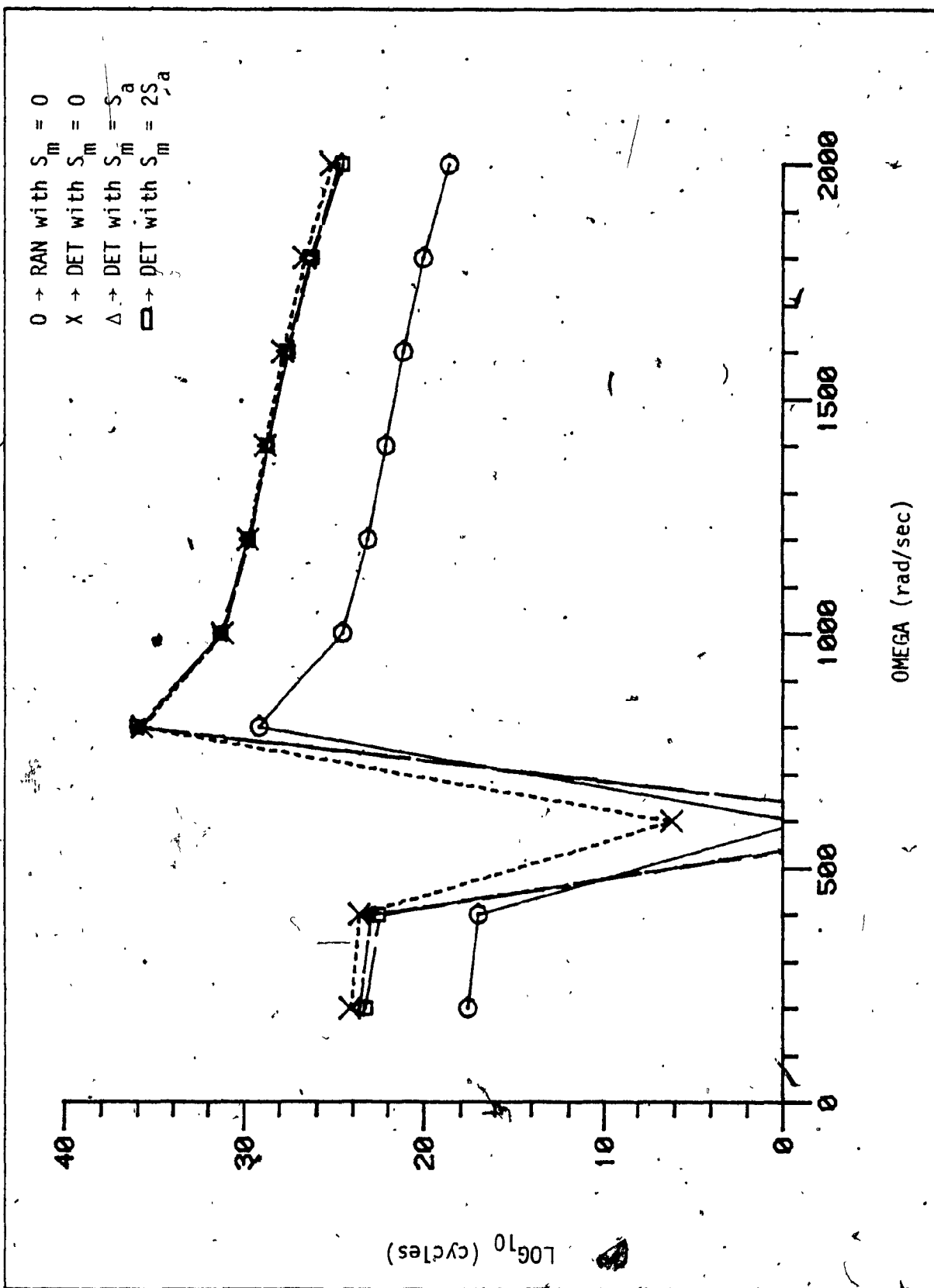


Fig. 3.23: Variation of Life Versus Speed for $\gamma_B = 0.0005$ and $\lambda = 0.0007$

life of gears in Figs. 3.17 and 3.18 is minimum at 600 rad/sec, near the second natural frequency and maximum at 800 rad/sec between second and third natural frequencies. The effect of the mean load on gearing life is significant in Fig. 3.18 at 600 rad/sec. Figure 3.19 shows that the gear fails near 600 rad/sec. Again its life becomes maximum at 800 rad/sec.

Above 1000 rad/sec, the higher the ratio of mean load to the fluctuating load, the lower is the frequency at which failure takes place. For example, when this ratio is 2, failure occurs at 1500 rad/sec. Similarly, when this ratio is 1, the failure frequency increases to 1850 rad/sec. These frequencies for the other two cases, are above 2000 rad/sec.

In Fig. 3.20, failure in all four cases, takes place below the second natural frequency. In the higher frequency range, the nature of the curves is similar to the earlier case, except that the gear fails at a lower frequency. According to the random approach, the gear will fail at approximately 500 rad/sec or at 1700 rad/sec, and the life of the gear will be maximum at 800 rad/sec.

In Figs. 3.21 to 3.24, λ is constant at 0.0007 and the values of γ_B are 0.00001, 0.0001, 0.0005 and 0.0009 respectively. From Figs. 3.21 and 3.22, it can be deduced that the mean load does not have a significant effect but the random life is less than the deterministic life, at all frequencies. The minimum life of gears is at 600 rad/sec near the second natural frequency and the maximum at 800 rad/sec between the second and third natural frequencies, in both these figures. Figure 3.23 shows that the effect of the mean load is more prominent at low frequencies than at higher frequencies. At about 600 rad/sec, it is observed that

the gear fails in the presence of steady load. When calculations are made employing the random approach, the life of the gear is less than that given by the deterministic approach.

Lastly, Fig. 3.24 clearly shows that the gear fails at 600 rad/sec and life is greatly influenced by the presence of a steady load which is evident in the region 200 rad/sec to 500 rad/sec and also maximum at 800 rad/sec, between the second and third natural frequencies.

Thus, from a detailed study of the different cases presented, it is apparent that the working or useful life of a gear is minimum (if not zero) at 600 rad/sec near the second natural frequency and maximum at 800 rad/sec, between the second and third natural frequency. Further, gearing error and mean load have a significant effect on gearing life. The higher the error or mean load, the lesser becomes the useful life of gears, causing complete breakdown in some cases. Lastly, with increase in the value of the decay constant λ , there is a substantial increase in the working life of gears especially at higher frequencies.

3.2. Conclusion

This study outlines a method for estimating the useful working life of a gear subjected to a dynamic loading environment, which includes manufacturing and assembly errors as well as fluctuations in the transmitted torque. The static transmission error has been considered as periodic as well as, an exponentially decaying function of speed.

The conclusions drawn, based on the results obtained are:

- 1) The dynamic torque increases with an increase in operating speed thus reducing the working life, for a given error. This appears to be valid at all frequencies of vibration except at the natural

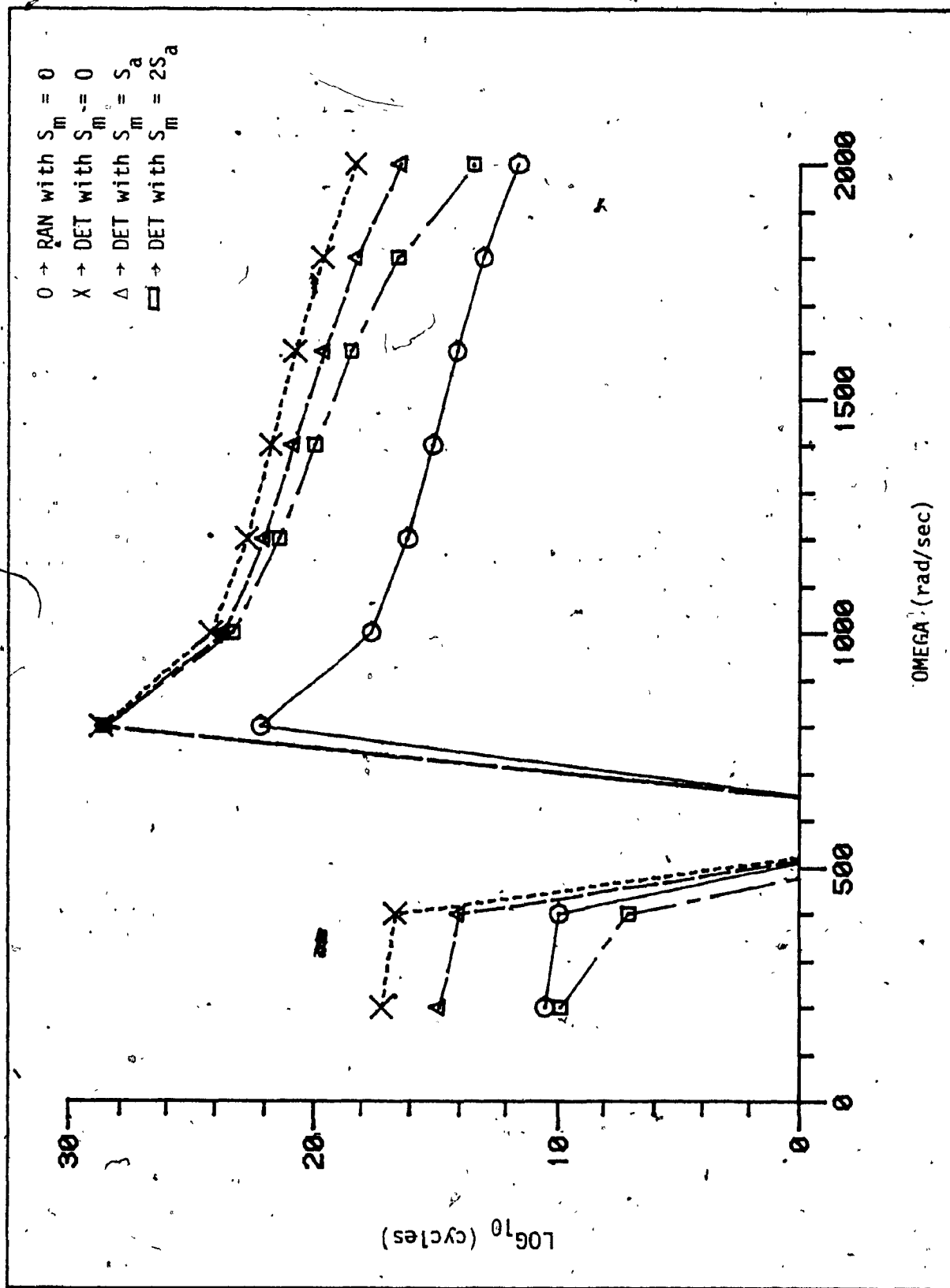


Fig. 3.24: Variation of Life Versus Speed for $\gamma_B = 0.00009$ and $\lambda = 0.0007$

frequencies, where it is observed that initially life decreases steeply and after reaching a particular value (in some cases failure may occur) increases rapidly.

2) Failure of gears may occur at the second natural frequency of the system. If not, a maximum life is reached between the second and third natural frequencies of the system.

3) The dynamic torque increases with an increase in gearing error resulting in a decrease of the working life of gears. This is valid at all operating speeds.

4) An increase in the static and/or fluctuating torque decreases the life of gears.

3.3 Recommendation for Future Work

The following items are proposed as a list of suggestions for the extension of the analytical work presented in this thesis:

1) In an operating machinery where gears are a prime element, the load is transmitted through gear trains. At high velocity of operation, the gear teeth do not remain rigid and thus, there is loss of contact between gear teeth. The separation of teeth causes an oil film to fill the space which makes the system nonlinear. This should be considered in dealing with the geared system.

2) All operating machinery are inherently provided with some damping. Hence in any practical case damping should be considered.

3) In a geared system, often gears fail due to surface wear. Thus surface failure of gear teeth under steady and dynamic loading conditions should be considered.

4) The present work can be extended to torsional systems having branches at different stations with different velocity ratios.

5) Investigate the implementation of this work in the development of health monitoring programs for equipment where primary failures are attributed to gears.

REFERENCES

REFERENCES

1. Dudley, Darle W., "The Evolution of Gear Art", American Gear Manufacturers Associations, Washington, D.C., 1969, pp. 5.
2. Ibid 1, pp. 18.
3. Ibid 1, pp. 36.
4. Ibid 1, pp. 48.
5. Ibid 1, pp. 49.
6. Ibid 1, pp. 50.
7. Ibid 1, pp. 51.
8. Ibid 1, pp. 52.
9. Ibid 1, pp. 66.
10. Tuplin, W.A., "Gear Tooth Stresses at High Speed", Proceedings of The Institution of Mechanical Engineers, 1950, Vol. 163, pp. 162-167.
11. Tuplin, W.A., "Dynamic Load on Gear Teeth", Machine Design, 1953, Vol. 25, pp. 203-211.
12. Mahalingam, S., and Bishop, R.E.D., "Dynamic Loading of Gear Teeth", 1974, Journal of Sound and Vibration, Vol. 36(2), pp. 179-189.
13. Bishop, R.E.D., "Note on a Torsional Failure Caused by Gear Inaccuracy", 1962, Journal of Mechanical Engineering Science, Vol. 4, No. 2, pp. 188-189.
14. Yates, H.G., "Prediction and Measurement of Vibration in Marine Geared-Shaft System", Institution of Mechanical Engineers, April 1955.
15. Johnson, D.C., and Bishop, R.E.D., "A Note on the Excitation of Vibrating System by Gearing Errors", Journal of the Royal Aeronautical Society, June 1955, Vol. 59, pp. 434-435.
16. Johnson, D.C., "The Excitation of Resonant Vibration by Gear Tooth Meshing Effects", 1958, Proceedings of International Conference on Gearing, pp. 18023.
17. Ibid 12, pp. 181.
18. Xistris, G.D., D.Sc. Thesis, Ecole Polytechnique, Montreal, Department of Mechanical Engineering, 1978.
19. Maten, S., "Vibration Velocity Measuring Program", ASME Paper No. 70-PEM-27, March 1970.

20. Glen, C.A.W. and Watson, D.C., "Vibration Analysis as a Maintenance Tool in the Canadian Navy", Transactions of the Institute of the Marine Engineers, Canadian Division, Supplement No. 32, June 1968.
21. Xistris, G.D., "Vibration Monitoring of a 750 k.w. Gas Turbine Generator", SAE Paper No. 730-932, October 1973.
22. Greenwood, Donald T., "Classical Dynamics", Prentice Hall, Inc. Englewood Cliffs, N.J., 1977.
23. Hornbeck, Robert, W., "Numerical Method", Quantum Publishers, Inc., 257 Park Avenue South, New York, N.Y., 10010.
24. Juvinall, R.C., "Stress, Strain and Strength", McGraw Hill Book Company, New York, 1967.
25. Sandor, B.I., "Cyclic Stress and Strain", The University of Wisconsin Press, Wisconsin, 1972.
26. Deiter, G.E., "Mechanical Metallurgy", McGraw Hill Book Company, New York, N.Y.
27. Crandall, S.H. and Mark, W.D., "Random Vibration in Mechanical Systems", Academic Press, Inc., New York, 1969.
28. Thomson, William T., "Theory of Vibration with Applications", Prentice-Hall Inc., Englewood Cliffs, New Jersey, 1972.
29. Osgood, C.C., "Fatigue Design", Wiley, New York, 1970.
30. Ibid 18.
31. Lin, Y.K., "Probabalistic Theory of Structural Dynamics", McGraw Hill, 1957.

APPENDIX
COMPUTER PROGRAMME

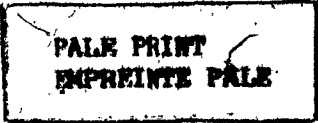
```
PROGRAM GSR(INPUT,OUTPUT,TAPE60=INPUT,TAPE61=OUTPUT,TAPE10,  
1 TAPE11,TAPE12,TAPE15)  
COMMON HE,HC,A,B,MA,ME,MC,AJE,AJ1,A21,E21,E22,C21,C22  
COMMON TN,PD,FACE,FFX,SARF,SIZE,TIME  
COMMON QMEGA,SIGS,SIGSL,SIGSID,AAAF  
COMMON AJ(7),AK(6),RA(2,2,8),CMG(7),ACT(4,4),STRESS(800)  
COMMON SUT(5),GTH(5),SLOPE(5),CCNST(5),GAMMAE(4),ALAMDA(4)  
COMMON ALIFE(80),RANLIFE(80),RANTIME(80)  
COMMON IL,IGE,ILAM  
DIMENSION AM(4,4)  
EXTERNAL FCN  
CALL HPLATA  
CALL JUMP  
K=1  
W1=0.0  
DC 100 J=1,30000  
W2=K1+0.1  
WTOL=0.1  
FTOL=0.01  
NLIM=100  
I=1  
CALL ROOT (FCN,W1,W2,W,WTOL,FTOL,NLIM,I)  
C WRITE(61,20) I  
C 20 FORMAT(5X,15.5X)  
I2=-2  
IF(I.EC.I2) GO TO 200  
CMG(K)=K  
WRITE(61,50) CMG(K)  
50 FORMAT(5X,"CMG(K)=",F10.3,5X)  
K=K+1  
200 W1=K1+0.1  
100 CONTINUE  
CALL AMODE(AM,E)  
NN=4  
DC 110 I=1,NN  
110 WRITE(61,300) (AM(I,J),J=1,NN)  
300 FORMAT(10X,7F17.7)  
PRINT*,"CALCULATION OF MODE SHAPE FOR ACTUAL SYSTEM"  
DC 220 I=1,NN  
220 WRITE (61,300) (ACT(I,J),J=1,NN)  
CALL GTRDYS  
CALL GTLIFE  
CALL RANDOM  
STOP  
END
```

```

FUNCTION . FCN(W)
COMMON RB,RC,N,P,NA,NE,NC,AJE,AJC,A11,A21,E21,E22,C21,C22
COMMON TN,PE,PFCL,PFY,SARF,SIZF,TEMP
COMMON OMEGA,SIGS,SIGSD,SLGSDD,APAA
COMMON AJ(7),AK(6),RA(2,2,8),OMG(7),ACT(4,4),STRESS(800)
COMMON SUT(5),GTH(5),SLCPE(5),CONST(5),GAMMA(4),ALAMDA(4)
COMMON ALIFE(80),RANLIFE(80),RANTIME(80)
COMMON IM,IGE,ILAM
RA(1,1,1)=1.0
RA(1,2,1)=0.0
RA(2,1,1)=(-W**2)*AJ(1)
RA(2,2,1)=1.0
DO 10 L=2,N
LL=L-1
RA(1,1,L)=1.0
RA(1,2,L)=1.0/AK(LL)
RA(2,1,L)=(-W**2)*AJ(L)
RA(2,2,L)=1.0-(W**2)*AJ(L)/AK(LL)
85 FORMAT(5X,F15.3,5X,F15.3,5X)
10 CONTINUE
IA=1
IS=(NA+NE+NC)+1
IP=(NA+NI+NC)*4+1
I1=1
IA2=4+I1
IAL=(NA*4)-3
DO 20 IA1=1A2,IAL,4
CALL RMMRVF(RA,RA,RA,2,2,2,IA1,I1,IP)
CALL SWITCH(RA(1,1,IA),RA(1,1,IS),2,2)
20 CONTINUE
A11=RA(1,1,IA)
A21=RA(2,1,IA)
IE=NA+1
GO TO 67
I1 =NA*4+1
IE2=4+I1
IEL=(NA+NE)*4-3
DO 30 IE1=IE2,IEL,4
CALL RMMRVF(RA,RA,RA,2,2,2,IE1,I1,IP)
CALL SWITCH(RA(1,1,IE),RA(1,1,IS),2,2)
30 CONTINUE
67 E21=RA(2,1,IE)
E22=RA(2,2,IE)
GO TO 167
IC=(NA+NE)+1
IW=(NA+NE)*4+1
IC2=4+I1
ICL=(NA+NE+NC)*4-3
DO 40 IC1=IC2,ICL,4
CALL RMMRVF(RA,RA,RA,2,2,2,IC1,I1,IP)
CALLSWITCE(RA(1,1,IC),RA(1,1,IS),2,2)
40 CONTINUE
C21=RA(2,1,IC)
C22=RA(2,2,IC)
167 FCN=A11*E21+L22*A21
166 CONTINUE
RETURN
END

```

```
SUBROUTINE RPDATA
COMMON RE,RC,N,M,NA,NE,NC,AJB,AJC,A11,A21,E21,E22,C21,C22
COMMON TN,PD,FACE,FFY,SARF,SIZE,TEMP
COMMON OMEGA,SIGS,SIGSD,SIGSLD,AAAF
COMMON AJ(7),AK(6),RA(2,2,6),CMG(7),ACT(4,4),STRESS(800)
COMMON SUT(5),GTH(5),SLOPE(5),CONST(5),GAMMAE(4),ALAMDA(4)
COMMON ALIFE(80),RANLIFE(80),RANTIME(80)
COMMON IM,IGE,ILAM
READ(60,*)N,M,RE,RC,NA,NE,NC,AJB,AJC
READ(60,*)(AJ(I),I=1,N)
READ(60,*)(AK(I),I=1,N)
PRINT*,"N,M,RE,RC,NA,NE,NC,AJB,AJC"
WRITE(61,105)N,M,RE,RC,NA,NE;NC,AJB,AJC
105 FORMAT(5X,2I5,2F10.3,3I5,2F20.4)
PRINT*,"AJ(I)="
WRITE(61,115)(AJ(I),I=1,N)
115 FORMAT(5X,F10.3,5X)
PRINT*,"AK(I)="
WRITE(61,125)(AK(I),I=1,N)
125 FORMAT(5X,E10.3,5X)
READ(60,*)TN,PD,FACE,FFY,SARF,SIZE,TEMP
PRINT*,"TN,PD,FACE,FFY,SARF,SIZE,TEMP"
WRITE(61,135)TN,PD,FACE,FFY,SARF,SIZE,TEMP
135 FORMAT(5X,8F10.5,5X)
READ(60,*)(GAMMAE(IGE),IGE=1,4)
READ(60,*)(ALAMDA(ILAM),ILAM=1,4)
READ(60,*)(SUT(IM),IM=1,5)
READ(60,*)(GTH(IM),IM=1,5)
PRINT*,"GAMMAE="
WRITE(61,135)(GAMMAE(IGE),IGE=1,4)
PRINT*,"ALAMDA="
WRITE(61,135)(ALAMDA(ILAM),ILAM=1,4)
PRINT*,"SUT="
WRITE(61,135)(SUT(IM),IM=1,5)
PRINT*,"GTH="
WRITE(61,135)(GTH(IM),IM=1,5)
RETURN
END
```



```
SUBROUTINE JUMP
COMMON RE,RC,N,M,NA,NE,NC,AJE,AJC,A11,A21,E21,F22,C21,C22
COMMON TN,PD,FACE,PFY,SAHF,SIZE,TEPF
COMMON OMEGA,SIGS,SIGSD,SIGSDD,AAAA
COMMON AJ(7),AK(6),RA(2,2,8),ONG(7),ACT(4,4),STRESS(800)
COMMON SUT(5),GTH(5),SLOPE(5),CONST(5),GAMMAE(4),ALAMDA(4)
COMMON ALIFE(80),RANLIFE(80),RANTIME(80)
COMMON IM,IGF,ILAM
NE1=NA+1
NEL=NA+NE
DO 10 I=NE1,NEL
II=I-1
AJ(I)=AJ(I)*(RE**2)
AK(I)=0.8*(10.**6)
AK(II)=AK(II)*(RE**2)
10 CONTINUE
NC1=NA+NE+1
NCL=NA+NE+NC
DO 20 I=NC1,NCL
II=I-1
AJ(I)=AJ(I)*(RC**2)
AK(II)=AK(II)*(RC**2)
20 CONTINUE
AJ(NA)=AJ(NA)+AJE*(RE**2)+AJC*(RC**2)
WRITE(6,125) AJ(NA)
125 FORMAT(5X,"AJ LAST IN EA =",F15.3,5X)
PRINT*,"JUMP STARTS"
WRITE(6,135)(AJ(I),I=1,N)
135 FORMAT(5X,F15.3,5X)
WRITE(6,145)(AK(II),II=1,N)
145 RORMAT(5X,F15.3,5X)
PRINT*,"END OF JUMP"
RETURN
END
```

```

SUBROUTINE ROOT (FCN,W1,W2,W,WTOL,FTOL,NLIM,I)
LOGICAL PRINT
PRINT = .TRUE.
IF (I.NE.0) PRINT = .FALSE.
F1=FCN(W1)
F2=FCN(W2)
IF (F1*F2 .GT.0) GO TO 50
DO 20 J=1,NLIM
W=(W1+W2)/2.
FR=FCN(W)
WEHR=ABS(W1-W2)/2.
IF (.NOT.PRINT) GO TO 5
C 105 FORMAT (1H0,13HAT ITERATION ,14,5H W = ,E12.5,
1 9H F(W) = ,E12.5)
5 IF (WEHR.LE.WTOL) GO TO 60
IF (ABS(FR).LE.FTOL) GO TO 70
IF (FR*F1.LT.0) GO TO 10
W1=W
F1=FR
GO TO 20
10 W2=W
F2=FR
20 CONTINUE
I= -1
C WRITE (61,115) NLIM,W,FR
115 FORMAT (1H0,26HTOLERANCE NOT MET AFTER ,14,
1 15H ITERATIONS W = ,E12.5,12H AND F(W) = ,E12.5)
RETURN
50 I= -2
C WRITE(61,125)
125 FORMAT (1H0,5X,"FUNCTION HAS SAME SIGN AT W1 AND W2 ")
RETURN
60 I=1
C WRITE(61,135) J,W,FR
135 FORMAT (1H0,19HW TOLERANCE MET IN ,14,18H ITERATIONS W=
1 ,E12.5, 8H F(W) = ,E12.5)
RETURN
70 I=2
C WRITE(61,145) J,W,FR
145 FORMAT (1H0,19HF TOLERANCE MET IN ,14,18H ITERATIONS,W=
1 ,E12.5, 8H F(W) = ,E12.5)
RETURN
END
```



```
SUBROUTINE SWITCH(A,B,II,JJ)  
DIMENSION A(1),B(1)  
IC=0  
DO 10 J=1,II  
DO 10 J=1,JJ  
IC=IC+1  
10 A(IC)=B(IC)  
RETURN  
END
```

```
SUBROUTINE AMODE(AM,E)
COMMON HE,RC,N,M,NA,NB,NC,AJB,AJC,A11,A21,E21,E22,C21,C22
COMMON TN,PD,FACE,FFY,SARF,SIZE,TEMP
COMMON OMEGA,SIGS,SIGSD,SIGSDD,AAAA
COMMON AJ(7),AK(6),RA(2,2,8),OMG(7),ACT(4,4),STRESS(800)
COMMON SUT(5),GTH(5),SLOPE(5),CONST(5),GAMMA(4),ALANDA(4)
COMMON ALIFE(80),FANLIFE(80),RANLIME(80)
COMMON IM,IGB,ILAM
DIMENSION AN(4,4)
DIMENSION AN(2,1),A1(2,1)
DO 150 KK=1,4
W=OMG(KK)
AN(1,1)=1.0
AN(2,1)=0.0
RA(1,1,1)=1.0
RA(1,2,1)=0.0
RA(2,1,1)=(-W**2)*AJ(1)
RA(2,2,1)=1.0
CALL RMRVF(RA,AF,A1,2,2,1,1,1,1)
AM(3,KK)=A1(1,1)
ACT(1,KK)=A1(1,1)
DO 10 L=2,N
LL=L-1
RA(1,1,L)=1.0
RA(1,2,L)=1.0/AK(LL)
RA(2,1,L)=(-W**2)*AJ(L)
RA(2,2,L)=1.0-(W**2)*AJ(L)/AK(LL)
10 CONTINUE
IA=1
IS=(NA+NL+NC)+1
IP=(NA+NB+NC)*4+1
I1=1
IA2=4+I1
IAL=(NA*4)-3
DO 20 IA1=IA2,IAL,4
CALL RMRVF(RA,RA,RA,2,2,2,IA1,I1,IP)
CALL SWITCH(RA(1,1,IA),RA(1,1,IS),2,2)
IF(IA1.EQ.9) GO TO 39
CALL RMRVF(RA,A1,AN,2,2,1,5,1,1)
AM(2,KK)=AN(1,1)
ACT(2,KK)=AN(1,1)
IF(KK.EQ.1) ACT(2,KK)=1.000000
IF(IA1.EQ.5) GO TO 20
39 CONTINUE
CALL RMRVF(RA,AN,A1,2,2,1,9,1,1)
AM(3,KK)=A1(1,1)
ACT(3,KK)=A1(1,1)
IF(KK.EQ.1) ACT(3,KK)=1.000000
20 CONTINUE
105 FORMAT(5X,E15.3,5X,E15.3,5X)
```

```
105 FORMAT (5X,E15.3,5X,E15.3,5X)
    A11=RA(1,1,1A)
    A21=KA(2,1,1A)
    IE=NA+1
    GO TO 120
    I1 =NA*4+1
    IE2=4+I1
    IEL=(NA+NE)*4-3
    DO 30 IE1=IE2,IEI,4
    CALL RMRVF (KA,RA,RA,2,2,2,IE1,I1,IP)
    CALL SWITCH (KA(1,1,1),RA(1,1,IS),2,2)
30 CONTINUE
120 E21=RA(2,1,4)
    E22=KA(2,2,4)
    GO TO 159
    IC=(NA+NI)+1
    I1 =(NA+NE ) *4+1
    IC2=4+I1
    ICL=(NA+NE+NC)*4-3
    DO 40 IC1=IC2,ICL,4
    CALL RMRVF (KA,RA,RA,2,2,2,IC1,I1,IP)
    CALL SWITCH (KA(1,1,1),RA(1,1,IS),2,2)
40 CONTINUE
    C21=RA(2,1,1)
    C22=KA(2,2,1)
159 TOE=A21
    TOC=A21-TOF
    AN(1,1)=A11
    AN(2,1)=TOE
    CALL RMRVF(KA,AN,A1,2,2,1,13,1,1)
    AM(4,KK)=A1(1,1)
    ACT(4,KK)=A1(1,1)*RE
    GO TO 150
    CALL RMRVF(KA,A1,AN,2,2,1,17,1,1)
    AM(5,KK)=AN(1,1)
    A1(1,1)=A11
    A1(2,1)=TOC
    CALL RMRVF(KA,A1,AN,2,2,1,21,1,1)
    AM(6,KK)=AN(1,1)
    CALL RMRVF(KA,AN,A1,2,2,1,25,1,1)
    AM(7,KK)=A1(1,1)
150 CONTINUE
    RETURN
```

PALE PRINT
EMPREINTE PALE

SUBROUTINE GTRDYS

```
COMMON RE,RC,N,M,NA,NE,NC,AJE,AJC,A11,A21,B21,E22,C21,C22
COMMON TN,PD,FACE,FFY,SARF,SIZF,TEMP
COMMON OMEGA,SIGS,SIGSD,SIGSDD,AAAA
COMMON AJ(7),AK(6),HA(2,2,8),OMG(7),ACT(4,4),STRESS(800)
COMMON SUT(5),GTH(5),SLOPE(5),CONST(5),GAMMA(4),ALAMDA(4)
COMMON ALIFE(80),RANLIFE(80),RANTIME(80)
COMMON IL,IQE,ILAM
DIMENSION P(4),AI(1,4),ASY(4,4),AOMS(4),
1 TQ(4),ASYS(4,4),ASY3(4),
1 AAR(1,4),FY3(4),ASY4(4)
```

IS=1

DO 22 IM=1,1

IF(IM.EC.2)GO TO 117

DO 23 IQE=1,4

DO 24 ILAM=1,4

CCCC WRITE(61,8)IM,IQE,ILAM

8 FGMAT(5X,"IM=",5X,I4,5X,"IQE=",5X,I4,5X,"ILAM=",5X,I4)

OMEGA=200.0

DO 21 IK=1,10

AI(1,1)=0.6

AI(1,2)=10.0

AI(1,3)=0.167

AI(1,4)=2.0

AI3PP=0.6

ASY(1,1)=ACT(1,1)

ASY(2,1)=ACT(2,1)

ASY(3,1)=ACT(3,1)

ASY(4,1)=ACT(4,1)

ASY(1,2)=ACT(1,2)

ASY(2,2)=ACT(2,2)

ASY(3,2)=ACT(3,2)

ASY(4,2)=ACT(4,2)

ASY(1,3)=ACT(1,3)

ASY(2,3)=ACT(2,3)

ASY(3,3)=ACT(3,3)

ASY(4,3)=ACT(4,3)

ASY(1,4)=ACT(1,4)

ASY(2,4)=ACT(2,4)

ASY(3,4)=ACT(3,4)

ASY(4,4)=ACT(4,4)

AOMS(1)=OMG(1)**2

AOMS(2)=OMG(2)**2

AOMS(3)=OMG(3)**2

AOMS(4)=OMG(4)**2

DO 10 J=1,4

DO 10 I=1,4

10 ASYS(1,J)=ASY(I,J)*ASY(I,J)

DO 20 J=1,4

AAR(1,J)=0.0

DO 20 K=1,4

20 AAR(1,J)=AAR(1,J)+AI(1,K)*ASYS(K,J)

A1=AAR(1,1)

A2=AAR(1,2)



```

A3=AA(1,3)
A4=AA(1,4)
C1=A1*AOMS(1)
C2=A2*ACMS(2)
C3=A3*ACMS(3)
C4=A4*ACMS(4)
A14=2.0
AN=0.33333
ASY3(1)=ASY(3,1)
ASY3(2)=ASY(3,2)
ASY3(3)=ASY(3,3)
ASY3(4)=ASY(3,4)
ASY4(1)=ASY(4,1)
ASY4(2)=ASY(4,2)
ASY4(3)=ASY(4,3)
ASY4(4)=ASY(4,4)
DO 40 I=1,4
40 FY3(I)=(-ACMS(I)*(A13PP*(AN)*ASY3(I)+A14*ASY4(I)))
C=30.0
P1DD=(AN*A13PP*(OMEGA**2))/A1
AP1=P1DD/(OMEGA**2)
131 FORMAT (5X,"AP1=",5X,F45.20,5X)
DO 999 I=2,4
OMGUP=OMG(I)*(1.+1./(2.*Q))
OMGL=OMG(I)*(1.-1./(2.*Q))
IF (OMEGA .GT. OMGL .AND. OMEGA .LT.OMGUP) GO
1 TO 910
P(I)=(AN*ASY3(I)*A13PP*(OMEGA**2)-FY3(I))/
1 (AA(1,I)*((OMG(I)**2)-(OMEGA**2)))
GO TO 920
910 P(I)=(AN*ASY3(I)*A13PP*(OMEGA**2)-FY3(I))*Q/
1 (AA(1,I)*ACMS(I))
920 CONTINUE
999 CCNTINUE
TC(1)=P(2)*FY3(2)+P(3)*FY3(3)+P(4)*FY3(4)
E1=P1DD*ASY3(1)
E2=ACMS(2)*P(2)*ASY3(2)
E3=ACMS(3)*P(3)*ASY3(3)
E4=ACMS(4)*P(4)*ASY3(4)
TQ(2)=(E1-E2-E3-E4)*AN*A13PP
TQ(3)=(-A13PP*OMEGA**2)
AK3=800000.0
TC(4)=AK3
FTC=TC(1)+TC(2)+TQ(3)+TQ(4)
DP=TN/PD
GAMMAG=GAMMAE(IGL)*EXP(-ALAMDA(ILAM)*OMEGA)
FPSFTQ=FTC*0.225*39.4*GAMMAO
AFPSFTQ=ABS(FPSFTQ)
WTAN=AFPSFTQ/(PD/2)
165 FORMAT (5X,"WTAN IN POUNDS=",F25.9,5X)
STRESS(1S)=WTAN*DB/(FACE*FFY )
IS=IS+1
OMEGA=OMEGA+200.0
21 CONTINUE
24 CONTINUE
23 CCNTINUE
22 CONTINUE
117 CONTINUE
RETURN
END

```



```
SUBROUTINE GTLIFE
COMMON RE,RC,N,M,NA,NE,NC,AJE,AJC,A11,A21,E21,E22,C21,G22
COMMON TN,PD,FACE,FFY,SARF,SIZE,TEMP
COMMON OMEGA,SIGS,SIGSD,SIGSDD,AAAA
COMMON AJ(7),AK(6),RA(2,2,L),OMG(7),ACT(4,4),STRESS(800)
COMMON SUT(5),GTH(5),SLOPE(5),CONST(5),GAMMAL(4),ALAMDA(4)
COMMON ALIFE(80),RANLIFE(80),RARTIME(80)
COMMON IM,IGE,ILAM
DIMENSION RY(10),RX(10),RH(10)
DIMENSION SMEAN(800)
IS=1
DO 22 IM=1,1
IF(IM.EQ.2)GO TO 117
DO 23 IGE=1,4
DO 24 ILAM=1,4
IR=1
OMEGA=200.0
DO 21 I=1,10
WRITE(61,91)IM,IGE,ILAM,IR,IS
91 FORMAT(5X,"IM=",2X,I4,5X,"IGE=",2X,I4,5X,"ILAM=",2X,I4,2I4,5X)
SF=0.9*SUT(IM)
WRITE(61,910)SUT(IM)
910 FORMAT(5X,"SUT=",F10.2)
AMP=1.4
SE=AMP*0.5*SUT(IM)
SMEAN(IS)=0*ABS(STRESS(IS))/1000.0
WRITE(61,92)SMEAN(IS)
92 FORMAT(5X,"SMEAN(IS) IN KPSI =",2X,F15.5)
SFM=SF-SMEAN(IS)
WRITE(61,922)SFM
922 FORMAT(5X,"SFM=(",5X,F10.5)
SEN=SE*(1-(SMEAN(IS)/SUT(IM)))
WRITE(61,93)SEN
93 FORMAT(5X,"SEN IN KPSI =",5X,F10.3)
IF(SFM.LE.SEN)GO TO 19
IF(SMEAN(IS).GE.SUT(IM))GO TO 19
SLOPE(IM)=3.0/(ALOG10(SFM)-ALOG10(SEN))
ALOG10K=3.0+SLOPE(IM)*ALOG10(SFM)
CONST(IM)=10**ALOG10K
ASTRESS=STRESS(IS)/1000.0
```

```
DYS=ABS(ASTRESS)
IF (DYS.GE.SFM) GO TO 19
ALIFE(IS)=CONST(IM)/(DYS**SLOPE(IM))
PRINT*,"IGE,ILAM,I"
WRITE(61,166)IGE,ILAM,I
166 FORMAT (10X,3I9)
WRITE(61,121) ALIFE(IS),STRESS(IS),OMEGA
WRITE(10,*)ALIFE(IS),OMEGA
121 FORMAT (5X,"ALIFE IN CYCLES=",5X,2E21.10," STRESS PSI",F8.2)
RY(IR)=ALOG10(ALIFE(IS))
RX(IR)=ALOG10(OMEGA)
GO TO 100
19 ALIFE(IS)=0.1
WRITE(61,121)ALIFE(IS),STRESS(IS),OMEGA
WRITE(10,*)ALIFE(IS),OMEGA
100 IR=IR+1
IS=IS+1
OMEGA=OMEGA+200,0
21 CONTINUE
24 CONTINUE
23 CONTINUE
22 CONTINUE
117 CONTINUE
RETURN
END
```

SUBROUTINE RANDOM

```

COMMON RE,RC,N,M,NA,NE,NC,AJE,AJC,A11,A21,E21,E22,C21,C22
COMMON TN,PE,FACE,FFY,SAHF,SIZE,TEMP
COMMON OMEGA,SIGS,SIGSD,SIGSDD,AAAA
COMMON AJ(7),AK(6),RA(2,2,8),OMG(7),ACT(4,4),STRESS(800)
COMMON SUT(5),GTH(5),SLOPE(5),CONST(5),GAMMAE(4),ALANDA(4)
COMMON ALIFE(80),RANLIFE(80),RANTIME(80)
COMMON IM,ICE,ILAM
DIMENSION RY(10),RX(10),RRLIFE(10),RRH(10)

PRINT*,"##### RANDOM STARTS #####"
IK1=1
DO 24 IM=1,5
IF(1E.EC.2) GO TO 107
DO 23 IGH=1,4
DO 22 ILAM=1,4
IS= 1
OMEGA=200.0
DO 21 IW=1,10
AAAA=OMEGA-10.0
91 FORMAT(5X,"AAAA=",5X,F15.5,5X,"EEEE=",5X,F15.5,5X)
CALL INTEC
81 FORMAT(5X,"IM=",2X,I4,5X,"IGH=",2X,I4,5X,"ILAM=",2X,I4,5X,2I4)
IK1=IK1+1
ENP=SIGSLL/(2*3.1414*SIGSD)
R=1.0
TH=SLOPE(IM)
ALLL=TH-1.0
PI=3.1415

ATH=(1.414**TH)*GTH(IM)*(R**ALLL)/PI
ED=1.0
ASD=((SIGSD/1000.0)**TH)/CONST(IM)
ASR=(SIGSD/SIGSD)**ALLL
RANT=ED/(ATH*ASD*ASR)
RANLIFE(IS)=ENP*RANT
121 FORMAT(5X,"RANTIME(IS) IN SEC =",5X,E45.5)
WRITE(61,131)RANLIFE(IS),OMEGA
131 FORMAT("RANLIFE=",E15.5,5X,"OMEGA=",F6.1,5X)
WRITE(15,*)RANLIFE(IS),OMEGA
29 FORMAT(5X,E15.5,3X)
IS=IS+1
OMEGA=OMEGA+200.0
21 CONTINUE
22 CONTINUE
23 CONTINUE
24 CONTINUE
107 CONTINUE
RETURN
END

```

PALE PRINT
EMPREINTE PALE


```

SUBROUTINE      INTEG
COMMON RE,RC,R,E,NA,NE,NC,AJB,AJC,A11,A21,E21,(B22,C21,C22
COMMON TN,PD,FACE,FFI,SARF,SIZE,TEMP
COMMON OMEGA,SIGS,SIGSE,SIGSDD,AAAA
COMMON AJ(7),AK(6),KA(2,2,8),OMG(7),ACT(4,4),STRESS(800)
COMMON SUT(5),GTE(5),SLOPE(5),CONST(5),GAMMAE(4),ALAMDA(4)
COMMON ALIFE(80),RANLIFE(80),RANTIME(80)
COMMON IN,IGH,ILAM
DIMENSION P(4),A1(1,4),ASY(4,4),AOMS(4),TC(4),
1          ASYS(4,4),ASY3(4),AAR(1,4),FY3(4),ASY4(4)

```

```

SUM1=0.0
SUM2=0.0
SUM3=0.0
BOMEGA=AAAA
DO 125 JJ=1,10
A1(1,1)=0.6
A1(1,2)=10.0
A1(1,3)=0.167
A1(1,4)=2.0
A13PP=0.6
ASY(1,1)=ACT(1,1)
ASY(2,1)=ACT(2,1)
ASY(3,1)=ACT(3,1)
ASY(4,1)=ACT(4,1)
ASY(1,2)=ACT(1,2)
ASY(2,2)=ACT(2,2)
ASY(3,2)=ACT(3,2)
ASY(4,2)=ACT(4,2)
ASY(1,3)=ACT(1,3)
ASY(2,3)=ACT(2,3)
ASY(3,3)=ACT(3,3)
ASY(4,3)=ACT(4,3)
ASY(1,4)=ACT(1,4)
ASY(2,4)=ACT(2,4)
ASY(3,4)=ACT(3,4)
ASY(4,4)=ACT(4,4)
AOMS(1)=OMG(1)**2
AOMS(2)=OMG(2)**2
AOMS(3)=OMG(3)**2
AOMS(4)=OMG(4)**2
DO 10 J=1,4
DO 10 I=1,4
10 ASYS(I,J)=ASY(I,J)*ASY(I,J)
DO 20 J=1,4
AAR(1,J)=0.0
DO 20 K=1,4
20 AAR(1,J)=AAR(1,J)+A1(1,K)*ASYS(K,J)
A1=AAR(1,1)
A2=AAR(1,2)
A3=AAR(1,3)
A4=AAR(1,4)
C1=A1*AOMS(1)
C2=A2*AOMS(2)
C3=A3*AOMS(3)
C4=A4*AOMS(4)

```

```

A14=2.0
AN=0.33333
ASY3(1)=ASY(3,1)
ASY3(2)=ASY(3,2)
ASY3(3)=ASY(3,3)
ASY3(4)=ASY(3,4)
ASY4(1)=ASY(4,1)
ASY4(2)=ASY(4,2)
ASY4(3)=ASY(4,3)
ASY4(4)=ASY(4,4)
DC 40 1=1,4
40 FY3(1)=(-ACMS(1)*(A13PP*(AN)*ASY3(1)+A14*ASY4(1)))
C=30.0
P1DD=(AN*A13PP*(EOMEGA**2))/A1
AP1=P1DD/(EOMEGA**2)
DO 999 1=2,4
CMGUP=CMG(1)*(1,+1./(2.*Q))
CMGL =CMG(1)*(1,-1./(2.*Q))
IF (EOMEGA .GT. CMGL .AND. EOMEGA .LT.CMGUP) GO
1 TC 910.
P(1)=(AN*ASY3(1)*A13PP*(EOMEGA**2)-FY3(1))/
1 (AAK(1,1)*((CMG(1)**2)-(EOMEGA**2)))
GO TC 920
910 P(1)=(AN*ASY3(1)*A13PP*(EOMEGA**2)-FY3(1))*C/
1 (AAK(1,1)*ACMS(I))
920 CONTINUE
999 CONTINUE
TC(1)=P(2)*FY3(2)+P(3)*FY3(3)+P(4)*FY3(4)
E1= P1DD*ASY3(1)
E2= ACMS(2)*P(2)*ASY3(2)
E3= ACMS(3)*P(3)*ASY3(3)
E4= ACMS(4)*P(4)*ASY3(4)
TC(2)=(E1-E2-E3-E4)*AN*A13PP
TC(3)=(-A13PP*EOMEGA**2)
AK3=800000.0
TC(4)=AK3
FTC=TC(1)+TC(2)+TC(3)+TC(4)
150 FORMAT (5X,"FTC=",5X,F30.9,5X,"NEWTON METER",5X)
DP=TN/PD
GAMMAO=GAMMAE(IGB)*EXP(-ALANDA(ILAN)*EOMEGA)
113 FORMAT(5X,"GAMMAO=",5X,F15.10,5X)
FPSFTC=FTC*0.225*39.4*GAMMAO
AFPSFTC=ABS(FPSFTC)
WTAN=AFPSFTC/(PD/2.0)
AKKK=2*TN/(PD*PD*FACE*FFY*SARF*SIZE*TEMP)
114 FORMAT(5X,"AFPSFTC=",5X,E10.2,5X,"AKKK=",5X,E10.2)
TF=((AKKK*AFPSFTC)/GAMMAO)
F1=(EOMEGA**2)*(TF**2)*(GAMMAO**2)/2.0
F2=(EOMEGA**4)*(TF**2)*(GAMMAO**2)/2.0
F3=(TF**2)*(GAMMAO**2)/2.0
SUM1=SUM1+F1
SUM2=SUM2+F2
SUM3=SUM3+F3
EOMEGA=EOMEGA+2.0
125 CONTINUE
SIGSD=SQRT(SUM1/10.)
SIGSDD=SQRT(SUM2/10.)
SIGS=SQRT(SUM3/10.)
RETURN
END

```

